SIAM Review
Vol. 54, No. 1, pp. 52–118

Modeling Growth in Biological Materials*

Gareth Wyn Jones†
S. Jonathan Chapman‡

Abstract. The biomechanical modeling of growing tissues has recently become an area of intense interest. In particular, the interplay between growth patterns and mechanical stress is of great importance, with possible applications to arterial mechanics, embryo morphogenesis, tumor development, and bone remodeling. This review aims to give an overview of the theories that have been used to model these phenomena, categorized according to whether the tissue is considered as a continuum object or a collection of cells. Among the continuum models discussed is the deformation gradient decomposition method, which allows a residual stress field to develop from an incompatible growth field. The cell-based models are further subdivided into cellular automata, center-dynamics, and vertex-dynamics models. Of these the second two are considered in more detail, especially with regard to their treatment of cell–cell interactions and cell division. The review concludes by assessing the prospects for reconciliation between these two fundamentally different approaches to tissue growth, and by identifying possible avenues for further research.

Key words. tissue modeling, growth, elasticity, agent-based modeling, multiscale modeling

AMS subject classifications. 74B20, 74L15, 92C10, 92C17

DOI. 10.1137/080731785

1. Introduction.

The study of growth in living organisms has been a fruitful area of research for many centuries. As early as the sixteenth century the scientist Galileo realized that the growth of a body must be limited by its form [15]. In the words of D'Arcy Thompson, in his influential work *On Growth and Form* [250], "if we tried building ships, palaces or temples of enormous size, yards, beams and bolts would cease to hold together; nor can Nature grow a tree nor construct an animal beyond a certain size, while retaining the proportions and employing the materials which suffice in the case of a smaller structure." Thompson made great contributions to the field of biological growth, applying physical principles to the shape and size of all kinds of living structures. The second half of the twentieth century saw a great increase in research on biological growth, drawing on scientific advances in fields as diverse as evolution, genetics, biochemistry, and mechanics.

The modern understanding of biology holds that the form and size of an organism (or parts of an organism) are determined not only by genetic factors but also by

*Received by the editors July 31, 2008; accepted for publication (in revised form) November 15, 2010; published electronically February 8, 2012. This work was supported through funding from the Engineering and Physical Sciences Research Council as part of the "New Frontiers in the Mathematics of Solids" (OxMOS) program EP/D048400/1.
http://www.siam.org/journals/sirev/54-1/73178.html

†School of Engineering and Applied Sciences, Harvard University, 29 Oxford Street, Cambridge, MA 02138 (gareth.wyn@gmail.com).
‡Oxford Centre for Industrial and Applied Mathematics, Mathematical Institute, 24–29 St Giles', Oxford, OX1 3LB, United Kingdom (chapman@maths.ox.ac.uk).

environmental effects. One such environmental factor is the concentration of chemicals in the developing tissue. Most obviously, a tissue requires nutrients in order to grow, and a low concentration of nutrients would therefore inhibit growth. This is certainly true of tumors, as was experimentally established as far back as 1917 [82]. Today, it is widely known that tumor spheroids cultured in vitro fail to grow past a certain radius, due to a necrotic core caused by a lack of nutrients diffusing to the center [221]. Aside from nutrients, concentrations of certain chemicals known as morphogens have a strong effect on the rate of tissue growth [200], and have been extensively studied, especially in embryonic development.

Disease and injury are further factors that can have an effect on the growth rate of tissues. Humans have a modest ability to regrow tissue in response to injury, for instance, in skin tissue. Some other organisms have a much more impressive capability; most notably, some starfish are able to regenerate severed arms [174]. Uninjured organs can also grow to compensate for injury: a study in which one of a rabbit's lungs was removed showed that the remaining lung had grown to compensate [53]. One hypothesis for this is that the remaining lung was placed under greater mechanical stress, thus promoting growth.

That mechanical stress or strain has an effect on tissue growth is common knowledge to the legions of athletes who increase their muscle mass through physical exercise. It has also been demonstrated experimentally time and again. One of the most researched areas is in the study of stress-dependent changes in bone structure, or *bone remodeling* [111, 198]. A commonly cited fact is that tennis players have significant differences between the properties of the bones in their playing and nonplaying arms, with the bone mineral content, bone strength, and cross-sectional area of bone all higher in the playing arm [119]. To cite a small selection of the literature, studies have demonstrated the effect on bone growth of the surrounding tissue [44], weightlessness due to space flight [112], immobilization in plaster casts [156], and physical exercise [158, 204].

Bones are not the only tissue where development is affected by mechanics. Early experiments [276, 86] showed that many of the properties of invasive tumors can be shown to be purely mechanical phenomena. Since then there have been several investigations into the effect of stress fields on the growth of tumors. The results appear contradictory: in [125, 37] the researchers showed that elevated levels of stress inhibit the tumor's development, but in [211, 143] it is shown that tumor growth may be promoted by elevated tissue tension. These results likely indicate that the exact response of a tumor is a combination of many factors, any of which may be dominant, depending on the microenvironment of the component cells.

Muscle tissue can also gain mass when its workload is increased [110, 245] and atrophies when subjected to long periods of disuse [126]. This also holds for the heart muscle, where abnormally high loading leaves the muscle significantly thicker—a process known as cardiac hypertrophy [118, 94]. A similar hypertrophic effect can be seen in arteries as a result of hypertension (high blood pressure) [271]. Other tissues where development is affected by mechanical loading are cartilage [117], the airway [48, 177], and the endothelial lining of blood vessels [202].

In the same way that growth can be affected by mechanical strains and chemical concentrations, these mechanical and chemical fields can themselves be affected by the growth process. For tissues which can be modeled as elastic solids over the typical timescale of growth, *residual stress* may emerge if parts of a tissue grow at a faster rate than others. The term residual stress is taken from the metallurgical literature, where plastic flow in a metallic body often results in a residual stress field that remains when

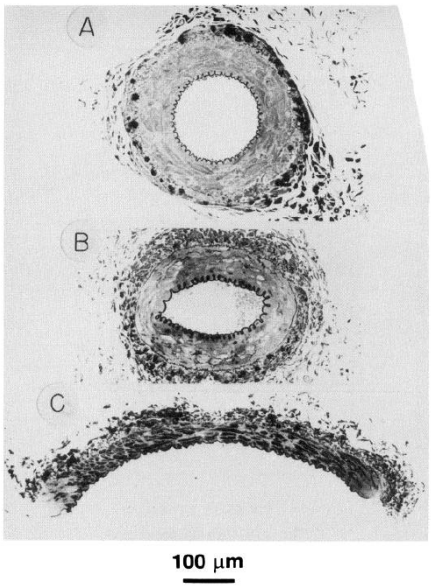

Fig. 1.1 *Cross sections of a rat artery* (A) *in its naturally pressurized state;* (B) *unloaded;* (C) *unstressed and cut along a radial line. Figure reproduced from* [100] *with permission.*

external loads are removed. The idea that this phenomenon occurs in the tissues of growing organisms was widely discussed by botanists in the nineteenth century [214]. For instance, Julius Sachs, in his *Text-book of Botany* [225], stated that "[growth] itself must cause states of tension in the layers of a cell-wall or of the tissue of which an organ is composed, if the layers, although firmly united to one another, grow unequally."

This effect can easily be seen in a kitchen-table experiment with a stick of rhubarb [257]. If the outer layers are removed carefully with a peeler and placed next to the inner pith, they are found to have noticeably shrunk, indicating that the peel was in a state of tension in the original structure, whereas the pith (which has elongated) was in compression. The relief of these stresses allows the plant to gain a "stress-free" state.

Much of the current interest in residual stresses in animals comes from the experiments of Fung and coworkers. Consider an artery that is sliced into sections by cuts made perpendicular to its length, with the resulting annular samples cut along a radial line. It is found [96] that, over time, the sections open up, clearly displaying that residual stress has been relieved, as shown in Figure 1.1. The amount of stress in the arteries can be characterized by the opening angle, which is the angle subtended by the two lines drawn from the center of the section to the ends of the opened artery. This was an important finding, because computations in the absence of residual stress had shown that heart tissue and arteries, when pressurized by blood flowing inside them, have a nonuniform stress profile across the wall, with a high stress at the inner surface [50]. Thus, if the tissue contained no residual stress, its yield stress would have to be high enough to accommodate the stress at the inner surface. Fung did not approve of this implication [97] and suspected that the assumption of zero residual stress in the unloaded state was incorrect. This was borne out by the experiments described above, which were carried out by Fung and coworkers, and independently by Vaishnav and Vossoughi [255]. On including residual stress in the model, the stress

Fig. 1.2 *A logged tree which has cracked due to the release of growth stresses. Picture taken from* [43].

profile across the pressurized artery wall becomes largely uniform, providing a physiological "purpose" to the residual stress: to avoid the buildup of high stresses in the artery, and thus the need for a high-yield stress. The results have been corroborated and extended [146]; in particular, it has been shown that active contraction by smooth muscle cells plays a similar role to residual stress.

Residual stresses have also been observed in developing amphibian embryos [19]. They are also important in tumor mechanics, where, due to the fact that the exterior of the tumor receives more nutrient than the interior, its growth is inhomogeneous—leading (again, if the tumor is modeled elastically) to residual stress fields. Many researchers have taken this idea further and hypothesized that the resulting elevated stress may be sufficient to cause collapse of blood vessels [155, 277]. Some experimental evidence exists for this notion; see [207] for an overview of an experiment in which relief of compressive stress causes the opening of collapsed vessels. However, further study is necessary before this intriguing and plausible idea can be regarded as a physiological fact.

A stress field due to differential growth—as noted by Sachs—also occurs in plants, where it is often referred to as *growth stress*. The effects can be seen most clearly in trees [14, 43], making it an important problem for the logging industry. Not only can logs crack (as shown in Figure 1.2) due to the relieving of growth stresses, thus losing much of their value, but difficulties can arise in the sawing process as the compressed internal part of the log expands, trapping the blade of the saw.

Another instance of growth-determined stress in plant biology is found in the branches of trees. If these were formed of a homogeneous material, they would sag under the influence of gravity. To counter this, trees produce in their branches a type of

wood known as "reaction wood" [272, 273, 83]. This wood can take two forms: In gymnosperms (which include conifers) the wood forms on the underside of branches and induces a compressive stress, bending the branch upwards. Conversely, in angiosperms (flowering trees) the wood forms on the upper side of branches, inducing a tensile stress which also has the effect of bending the branch upwards. In this case the state of stress of the branch does not appear to significantly affect the production of reaction wood; the governing factor appears to be the direction of the gravitational field [272].

For tissues which do not behave elastically over the growth timescale—such as cell ensembles (see section 2.5)—inhomogeneous growth does not lead to residual stress, since these stresses are immediately dissipated by altering the composition of the tissue, or by allowing parts of the tissue to flow relative to one another. The mechanical properties of the tissue are thus a significant factor in determining its response to growth.

We have established that the stress field applied to a growing body can alter its pattern of growth, and that the growth process itself can alter the stress field in the body. Therefore the stress field in a body can act as a regulator of its growth, through a feedback mechanism. This is postulated to be a key mechanism in embryonic [201] and tissue [229] development, and indeed mechanical stress has also been shown to be a fundamental factor in the development of organs in embryos, from eyes [51, 52], to the brain [70] and the heart [247]. On a smaller scale, mechanical compression of *Drosophila* embryos can induce the expression of certain morphogenetic genes, indicating that shape changes can occur as a result of previously induced strains in the embryo [89].

The concept of a feedback mechanism has been postulated in some of the other models that we have mentioned above. Fung hypothesized [97] that the residual stresses in the arterial wall arise as a result of increased stress, which the cells sense and respond to by generating more tissue, thus lowering the stress. In addition, while the main cause of reaction wood in trees is the direction of gravity, recent evidence has shown that, at least in gymnosperms, the stress field in the branch may be a secondary effect [83]. Feedback mechanisms can also occur through the other epigenetic factors mentioned previously; for instance, growth due to morphogen concentration may give rise to stress fields, and the distribution of morphogen concentration in a tissue may be changed by tissue deformation [200]. A full description of tissue growth must include all relevant factors, whether they be mechanical stresses, morphogens, or nutrient fields.

The remainder of this article is devoted to describing various mathematical models that attempt to explain or predict the interplay between growth and stress. Mathematics has a long history of being able to describe aspects of biological and physiological processes analytically [197]. Over the last century it has provided theoretical explanations for such diverse phenomena as pattern formation in animals and intercellular signaling due to ion currents. One of the areas in which a great deal of research is being done is in developing mathematical models for cancer development [39]. This includes models for the growth of tumors [221, 8], but, in general, these models do not yet place an emphasis on the effect of mechanical stress.

The study of the mechanical properties of biological tissues, or *biomechanics*, is a relatively well developed discipline. The recent textbook by Cowin and Doty [60] gives a flavor of the field, as do the three classic texts by Fung [98, 99, 96]. Hard tissues such as bone can be modeled effectively by (anisotropic) linear elasticity, but softer elastic tissues such as blood vessels undergo large deformations and can only be adequately modeled by appealing to nonlinear elasticity models. Other tissues such

as epithelial monolayers or tumors may undergo permanent deformations and as such require viscous or plastic effects to be included in the model. Biomechanical modeling of tissues is by no means complete, and many open problems remain, as recently documented by Humphrey [145]. These include issues relating to cell mechanics, tissue engineering, muscle mechanics, and, indeed, the biomechanics of growth and remodeling, the subject of our review.

The biomechanics of growing tissues was explored in detail in an excellent review by Taber [245], which should be recommended reading for anybody interested in this field. We also note the recent articles by Cowin [58], Garikipati [105], and Ambrosi et al. [3]. Taber considered the three processes of *growth* (change of mass), *remodeling* (change of property), and *morphogenesis* (change of shape). In this review we choose to concentrate on the first two, notwithstanding the fact that stress changes in the embryo can lead to morphogenesis, as discussed earlier. Although remodeling was given the broad definition of a change in some property of the tissue, it has been mostly applied to models of changing directions of anisotropy in tissues as a response to stress stimuli, notably in bone tissue and arteries. As an effect at the level of a single cell, growth and remodeling may be considered to be manifestations of the same process in that cells alter their surroundings by addition or removal of material; the difference between the two is that in remodeling the net change of mass is unimportant in experiments and neglected in models. However, there do exist cases where the two processes go hand in hand: in the remodeling of bone tissue, while the emphasis is often on the changing anisotropy of the material, the density of the material may also vary, corresponding to growth or atrophy via a change in mass.

The large-scale behavior of tissues is, fundamentally, governed by the tissue microstructure. Thus a comprehensive understanding of the growth properties of tissues must rely upon the properties of the cells and the extracellular matrix. In this report, we will first review in section 2 the properties of cells, especially their mechanical properties—partly governed by the cytoskeleton mechanics—and the cell cycle, which governs the rate of division of cells (an essential consideration for growth of epithelial tissues and carcinomas, which consist mostly of cells).

In section 3 we review the modeling of growth in biological tissues, as seen from a macroscale perspective. We begin by discussing how tissue is modeled macroscopically, with a focus on the application of finite elasticity to the problem. Subsequently we present a simplified version of the deformation gradient decomposition method with examples of applications, including a toy problem of circumferential growth in an artery. Finally in this section we consider other elastic models that have been applied to the problem of growth, including theories that treat the tissue as being a mixture of several phases, and a discussion of models applied to the problem of bone remodeling.

In section 4 we consider a different approach to modeling growth in tissues, namely those which consider the individual cells as their fundamental units. We split these into three main types: the cellular automaton model, which is simple but is unable to express realistically the forces experienced by each cell; the off-lattice models, which allow the cells to move in space subject to forces acting on them; and the vertex dynamics models, which model the tissue as a polygonal (or polyhedral) tessellation of cells and where the tissue deforms by specifying the positions of the cell vertices at each time step, subject to the forces exerted by each cell. Of these we consider the second and third in greater detail.

We thus have two classes of models, which take different approaches to the problem of tissue growth. The earlier elastic models are phenomenological, in that they

describe the deformation or growth process, where the effect of stress on growth or vice versa is postulated rather than derived from the cell behavior itself. The second, cell-based, model type takes a keener interest in the way that cells respond to stress (even if rather simplified) but the large-scale response of the tissue is due to an aggregate response of hundreds of cells rather than by some constitutive law.

Ideally, one would apply the principle of homogenization theory to the microscopic model and obtain a constitutive law for the tissue that is grounded in the best understanding of the micromechanics of the cells. This is an exceedingly challenging task. Thus, in section 5, we consider a simpler goal: that of ascertaining how the growth rate of a tissue might depend on the macroscale deformation. As we will discuss, a successful outcome to this undertaking depends on the resolution of three subproblems: determining cell deformation in a tissue, evaluating cell response to deformation, and averaging tissue production at the microscale to produce a bulk growth field. We investigate the feasibility of these tasks and possible avenues for further research.

2. Tissue Biology. An understanding of the properties of biological tissues is important before beginning the modeling process. This section is an overview of the mechanical properties of tissues, beginning at the microscopic level—the cell. We will examine its structure, its mechanical properties, and the cell cycle—which describes the process of cell division (and hence tissue growth). These cell properties will be important for the cell-based modeling of section 4. Following this we look briefly at the structure of muscle tissue before examining the adhesion between cells in an aggregate; this again is important in modeling cell ensembles, which is discussed in section 4. Finally we consider the bulk mechanical properties of cell ensembles. These are measured directly; how they arise from the microscopic adhesion and mechanical properties is an open problem that is discussed in section 5.

Living organisms are perhaps best visualized as hierarchical structures. Large-scale structures such as muscles, bones, and lungs are composed of smaller structures such as muscle tissue, blood vessels, and cartilage. In turn these are compositions of cells and extracellular matrix (ECM). The mechanical properties of biological tissues are strongly dependent on the exact nature of this hierarchy, and thus on the microstructure of these tissues. Of interest to us, given the discussion on residual stress (or prestress) in the Introduction, is the concept of tensegrity, which provides a fundamental structural basis for the existence of prestress.

A tensegrity ("tensional integrity") structure is one which can conceptually be regarded as a collection of struts undergoing compressive stress, connected by strings which are under tension [149, 150, 151]. The compressive and tensile elements are in mechanical equilibrium, which provides the structure with a high degree of stability. The entire human body can be regarded as a tensegrity structure, with each subelement being a tensegrity structure itself [152]. For instance, in the musculoskeletal system the muscles apply a tensile force to the bones and their associated cartilaginous tissue, which are under compression. In turn, the cartilage is composed of collagen, which is under tension, and a proteoglycan matrix which applies a compressive force to the collagen. This differential stress in the various components of the tissue is the ultimate origin of macroscopic residual stress, and has to be taken into account in any comprehensive model of tissue mechanics and growth.

In vertebrates, four major tissue types can be identified, namely, muscle, epithelial, connective, and nerve tissues [60]. Of these, the first three are of primary interest from a tissue mechanics point of view. Tissues can usually be viewed as comprising

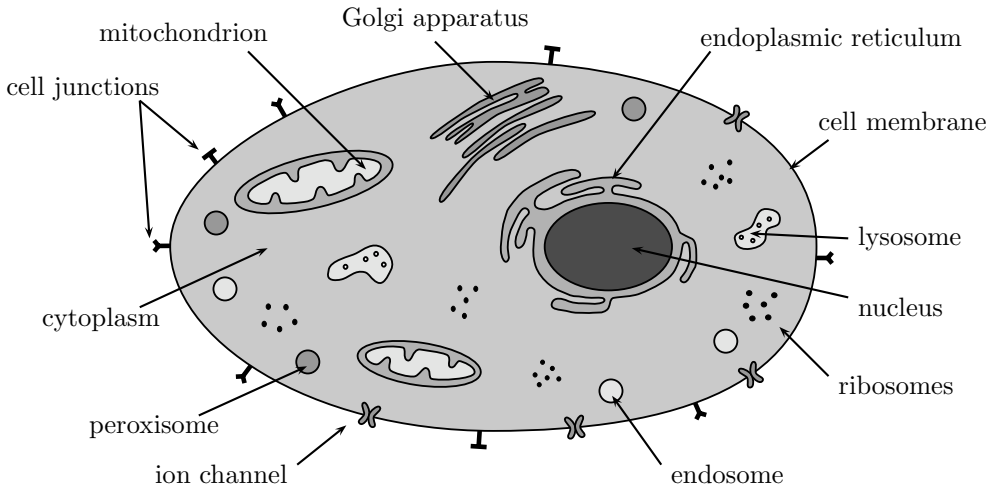

Fig. 2.1 *A diagram of a typical animal cell, displaying various organelles and other features. The cytoskeleton is omitted for clarity.*

two ingredients, namely the cells and the extracellular matrix. Epithelial tissues are layers in which the cells are bound together, with little ECM in between. On the other hand, connective tissues such as cartilage, bone matrix, adipose tissue, and ligaments are mainly composed of matrix with relatively few cells dispersed throughout the material.[1]

Clearly, tissue growth can occur either by the production of new cells (mitosis), or the production of ECM, or both. Which of these components is most important will depend on the tissue type. In epithelial tissues, mitotic effects make the greatest contribution to tissue growth. Additionally, due to the fact that most of the cell proliferation in the human body occurs in epithelial tissues, this is where around 80 % of human cancers originate [2], leading to a great deal of interest and research into these malignant epithelial tumors (carcinomas), which retain the characteristics of epithelial tissues.

Images of cells in epithelial tissue show that they are often arranged in polygonal or polyhedral structures [73, 84, 187]. Further experiments have also shown that the cells are not always confined to their position in the lattice but can move around relative to other cells [136]. This motivates much of the work attempting to abstractly model tissues as moving polygonal or polyhedral lattices [134], which we will discuss in sections 4.2 and 4.3.

2.1. Cell Mechanics. A typical animal cell has a complicated structure, as depicted in Figure 2.1 [2]. A simplified picture is of a cell membrane which surrounds a deformable cytoplasm. Embedded in the cytoplasm is the nucleus, which houses most of the cell's genetic material. The nucleus is but one of many *organelles* of the cell which have specific duties. Others include the *mitochondria*, which generate the ATP molecules that provide the energy for many reactions in the cell; the *endoplasmic reticulum*, in which proteins are synthesized by *ribosomes* attached to its surface; the *Golgi apparatus*, which collects these proteins and (usually) modifies them before

[1] Thus, for instance, blood is generally regarded as a connective tissue, with a matrix that is fluid.

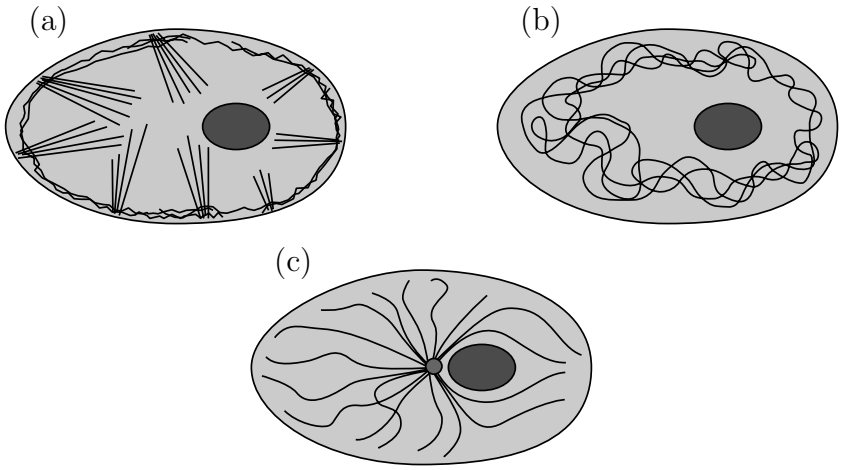

Fig. 2.2 *A sketch of the three classes of protein filament forming the cytoskeleton:* (a) *actin filaments,* (b) *intermediate filaments,* (c) *microtubules.*

distributing them to various destinations; *endosomes*, which are used to transport molecules in and out of the cell; and the *lysosomes* and *peroxisomes*, which both play a chemical-processing role. The *cytosol* is the fluid substance which forms the main part of the cytoplasm, and is also where some proteins are synthesized by unattached ribosomes. The cell's structural integrity is largely maintained by a *cytoskeleton* which is embedded in the cytoplasm. This cytoskeleton, as shown in Figure 2.2, consists of three types of protein filaments: *actin filaments*, *intermediate filaments*, and *microtubules*. Actin filaments, with a diameter of 5–9 nm, are distributed throughout the cell, but are concentrated beneath the cell membrane, in order to give it mechanical strength. Intermediate filaments have a diameter of around 10 nm and are found throughout the cytoplasm, reinforcing the cytoskeleton. Third, microtubules are hollow cylinders with one end typically attached to the *centrosome*, an organelle found near the center of the cell. Microtubules are 25 nm in diameter and play a crucial role in cell division by pulling replicated chromosomes apart. Here we see yet another hierarchy in the context of tissue tensegrity. The cell is a tensegrity structure where the microtubules are under compression and the actin filaments are under tension. This architecture gives the cell its mechanical stability, and a residual stress.

Surrounding the cytoplasm is the *cell membrane*. This is a phospholipid bilayer, in which are embedded numerous *membrane proteins* that have various essential functions. These proteins include membrane transport proteins such as ion channels, which allow certain solutes in and out of the cell, and cell junctions, which allow cells to attach to each other or to the extracellular matrix.

Mechanical analysis of cell deformation has become much more precise in recent years with the development of techniques such as atomic force microscopy, microcompression, reflection interference contrast microscopy, micropipette, and magnetic and optical tweezers [179, 1]. Early models for cells, based on the deformation of blood cells, assumed that they were solid elastic shells surrounding a viscous interior [232]. These models, while ignoring the complexity of the cytoplasm structure, have become widespread due to their ease of application and realistic results (assuming that the

deformation is small). Treating the cells as elastic bodies may be more relevant to plant cells [266], where the rigidity of the cell wall to a large degree inhibits extensive deformation. Current mechanical models for cell deformation are of two types. The first type models the cytoskeleton directly, incorporating ideas from tensegrity theory [29, 244, 261]. The other type of model, which can be considered the direct descendent of the earlier simplistic models, models the cell as a solid with exotic rheological properties [258, 178, 160]. Cell mechanics is an active field of research and the advantages of each model are still widely debated.

2.2. The Cell Cycle. Biologically, the process of cell division is governed by the cell cycle, which is common to all eukaryotic cells.[2] This describes the sequence of events which leads to the division of a mother cell into two daughter cells. The processes involved are relatively well known [196], but in the following we will give a simple overview of the components of the cycle.

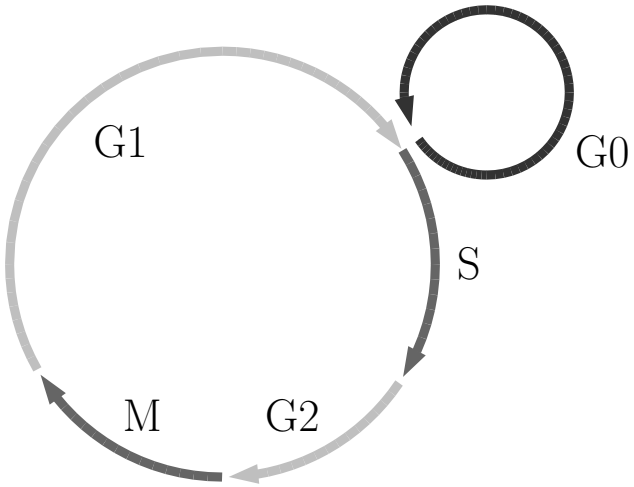

Fig. 2.3 *A schematic diagram of the cell cycle, displaying the phases in order.*

The cell cycle, as shown in Figure 2.3, may be characterized as having two states: the *mitotic phase*, or *M phase*, and the *interphase*. The interphase may be further subdivided into the *synthetic phase* or *S phase*, and two *gap phases* which lie between the M and S phases. In the S phase, the DNA in the cell is replicated in order to create two copies of the chromosomes. The M phase can typically be divided into two parts: in *mitosis*, the "sister" chromosomes are separated and the nucleus is divided into two, and in *cytokinesis* the cell itself divides, by the deposition of a new cell membrane between the two nuclei. Typically in animal cells, this deposition occurs from the existing cell wall inwards, leading to a gradual "pinching off" of the two cells from each other. Once this has occurred, the cell cycle is said to be completed. The first of the two gap phases, the *G1 phase*, occurs before the S phase, while the *G2 phase* occurs before the M phase. The most important of these is the G1 phase. It is here that the cell "decides" whether it will proceed with division. While the other stages of the cell cycle for a particular type of cell have different but fairly constant

[2]Eukaryotes include all multicellular organisms and protists.

durations, the cell may pause for a period of time in stage G1 if the conditions for division are unfavorable or inhibitory signals are received from other cells. It may also enter a state, known as G0, in which it does not divide for an extended period of time. If this is the case, the phase G1 may only be reentered with difficulty, if at all. Many of the differentiated cells in the human body are in this state. On the other hand, the purpose of phase G2 is to allow the cell to double in size. This size increase—during which the organelles of the cell are duplicated—begins in phase S, but the replication of chromosomes often takes less time than the swelling, which "catches up" during the G2 phase, before mitosis occurs.

Numerous experiments on tissues have shown that stress fields, and mechanical properties in general, can have a strong effect on cell division. The fundamental mechanism which mediates this behavior is known as mechanotransduction. This process, which is still not fully understood, is how the cells in a tissue sense the mechanical properties of their surroundings, and alter their function correspondingly through changes in biochemical pathways. Early experimental investigations into mechanotransduction examined how cell division was affected by changes in the cell's shape [91, 67]. In particular, by varying the adhesiveness of a culture medium on which cells are deposited, it was found that a greater proportion of cells entered the S phase of the cell cycle if they were flattened rather than spherical [91].

As time progressed and experimental techniques improved, the focus shifted from trying to evaluate the gross behavior of a cell being deformed to attempting to identify the actual mechanotransductive process within the cell. Beginning in the late 1980s, researchers discovered ion channels which were activated (or inactivated) by the stretching of the cell membrane (stretch-activated ion channels) [265]. Further investigations have uncovered a number of other possible mechanisms, including (but not limited to) tension in the ECM being transmitted to the cell through integrin adhesion receptors, thickness or curvature changes in the cell membrane, attachment of the cytoskeleton or ECM molecules to the ion channels themselves, and the unfolding of proteins within the cell (which could possibly expose binding sites which were previously inaccessible) [142, 278, 120, 152]. One of the key drivers of the mechanotransduction process is the tensegrity architecture of the cells and their surrounding tissue [153, 154]. A mechanical force applied to an organ is transmitted through the hierarchy of tensegrity structures to the microscopic level, thus deforming the cell. In turn, the force is transmitted to the cell's cytoskeleton, which—being a tensegrity structure itself—deforms, thus distorting key molecules within the cell, leading to a physiological response.

Much of the current investigative effort into mechanotransductive effects takes place on the tissue scale: for instance, Farge [89] showed that morphogenetically important gene pathways in *Drosophila* embryos were activated by mechanical stimulation of the whole embryo. The mechanotransductive pathways in certain tissues and pathologies are better understood than others—for example, in bone growth [46] and cardiac hypertrophy [94]—while only recently has a pathway governing the influence of ECM stiffness (and hence stress fields) on angiogenesis (capillary growth) been uncovered [184]. It is to be stressed that mechanotransduction in any two given tissues is likely to be greatly different, depending on the cells' properties and how they are attached to each other and the ECM.

These findings into the micromechanics of mechanotransduction appear to confirm the viewpoint that it is stretch, rather than any other mechanical field (e.g., stress or strain) that the cells are "truly" experiencing—given that the proposed mechanisms all essentially depend on the deformation of protein molecules. Earlier models which

attempted to correlate cell responses with stress or strain may have been using an experimentally convenient rather than physiologically justified measure of deformation, or may have been unconcerned with the precise definitions of these terms: in particular, both stress and strain are only valid at the macrolevel, arising due to averaged forces and deformations, respectively, at the microlevel [144]. Indeed, so-called baroreceptors (stress receptors) in nerves are actually activated by stretching [54].

2.3. Muscle Tissue. Skeletal muscle is a strongly hierarchical tissue, formed from bundles of *muscle fibers* bound together by connective tissue [245]. A muscle fiber is in fact a single cell which can be several centimeters long. Within each fiber are many *myofibrils* which extend the length of the cell and are in turn formed from arrays of *myofilaments*. These are arranged as a lattice of *sarcomeres*, which comprise interlocking myosin and actin myofilaments. Muscles contract due to these myofilaments sliding past each other in response to electrical stimuli. Heart muscle has a similar structure to skeletal muscle, with a number of differences, such as a branching fiber structure and a significant collagen matrix.

There has been much investigation into the micromechanics of muscle growth [245, 256, 217]. While muscle fibers usually stop dividing after birth, they may be regenerated in the case of injury. Moreover, fibers may grow longer in order to ensure that the muscles grow in tandem with the bones to which they are attached. As the stress level on the muscle increases, so does the diameter of the muscle fibers. Conversely, muscles which are immobilized, atrophy. The lengthening or thickening of fibers is enacted by the addition of sarcomeres to the myofibril in series or parallel, respectively. These mechanisms also play a role in cardiac hypertrophy [245].

2.4. Cell Adhesion and the Extracellular Matrix. It is imperative for the structural integrity of many tissues (in particular, epithelial tissues) that the cells are attached together. This is achieved by *cell adhesion molecules* (CAMs) which are proteins embedded in the cell membrane [2]. There are many types of CAMs, most notably *cadherins* and *integrins*, and each has a role in linking a cell to other cells or (in the case of nonepithelial tissues) to the ECM.

In mature tissues, particularly in epithelia, cells more often form tighter bonds known as cell junctions. Cell junctions can be classified as being one of three types. Occluding junctions form tight barriers between epithelial cells that prevent fluids from passing freely through that epithelium. Communicating junctions allow cells to exchange chemical or electrical signals. The third type, the *anchoring junction*, is the most important for structural integrity of a tissue. These junctions connect the cytoskeleton of a cell either to the extracellular matrix or to the cytoskeleton of a neighboring cell. The four basic types of anchoring junction are *adherens junctions*, *desmosomes*, *focal adhesions*, and *hemidesmosomes*. The first two link cells to other cells and employ cadherin proteins, while the second two link cells to the ECM and are formed of integrins. As previously mentioned, these anchoring junctions are attached to the cytoskeleton of the cell. Specifically, adherens junctions and focal adhesions are attached to the actin filaments, while desmosomes and hemidesmosomes are anchored to the intermediate filaments.

The extracellular matrix is a heterogeneous structure that, among other functions, helps to bind cells together. It can be thought of as a combination of two types of macromolecules [2]. The first of these classes includes the glycosaminoglycans, which are polysaccharide chains usually found bonded covalently to proteins, forming proteoglycans. Embedded in a fluid, these form a gel-like matrix which resists compression. The second class comprises the fibrous proteins, especially collagen, elastin

and fibronectin, which are embedded in the gel. Collagen molecules are arranged in long fibrils, which have a high tensile strength and have a characteristic arrangement depending on the function of the organ, for instance, as parallel bundles in tendons, or interwoven in perpendicular directions in skin. Elastin is a macromolecule which is crosslinked to form *elastic fibers*. These fibers have a structure which mimics the polymer chains in rubber and give tissues their elastic properties. Fibronectin is one of many molecules that link cells to the fibrous proteins embedded in the matrix. All these macromolecules are largely created by fibroblasts, specialized cells which reside in the ECM. These cells also assist with the alignment of the collagen fibrils in the matrix.

2.5. Mechanics of Cell Ensembles. In embryonic tissues, cells may not have managed to form advanced cell junctions (see above), and the coherence of the tissue is due almost entirely to cell adhesion molecules. This allows the cells to rearrange quite readily. As such the tissue can, on the long timescales associated with growth, be more realistically modeled as a fluid rather than as a solid.

The nature of the adhesion between cells can further justify this idea. In any drop of liquid, the constituent molecules form weak bonds between themselves, such as hydrogen bonds or van der Waals forces, which are largely in balance. At the interface between two different fluids, such as oil and water, this balance breaks down due to the difference in bonding strength between dissimilar molecules. This manifests itself at the large scale as a surface tension on the fluid interface. The effect of this tension is to minimize the surface area of the interface (subject to the mechanical properties of the fluids) leading to a separation of the two fluids into two phases, as is commonly seen in kitchen-table experiments with oil and water.

The same aggregation of a mixture into immiscible regions is seen in cell populations. Experiments show that on dissociating an embryonic tissue made up of two types of cells—and reforming the tissue in a random configuration—the two populations of cells gradually rearrange into the original two phases [31]. The accepted reason for this behavior is the differential adhesion hypothesis, which posits that the binding energy between cells of the same type is distinct from that between cells of different types [240, 175]. While experiments have verified this assumption, recent studies have shown that cell–cell adhesion is not the only factor in this rearrangement of cells; tensile forces in the cortical cytoskeleton can also play a role [165].

In the next section we will examine the continuum mechanical models that have been used to describe the behavior of biological tissues, from viscous fluid models to mixture theories and elasticity. Following this we will describe how growth effects are accounted for in nonlinear elastic models, before considering a number of examples of growth in other continuum models.

3. Modeling Tissue at the Macroscale. In this section we will review the continuum models for growth in biological tissues. However, we first need to outline the continuum models that are employed to describe tissue deformation. In general these can be divided into fluid and solid models. While blood, for example, is obviously modeled as a viscous fluid, this is also the case for cell aggregates over a long timescale, justified by the evidence of section 2.5. Over shorter timescales, the aggregate behavior would become more complicated: as long as the deformation remains sufficiently small, a tissue under loading would behave elastically as the cells will not have time to rearrange before the loading is removed. Over intermediate timescales one would therefore expect the aggregate to deform viscoelastically, retaining the characteristics of each type of model.

This bulk behavior is true of most tissues in the body, as chemical bonds will rearrange and cells will migrate over a long timescale, while remaining attached but stretched over short timescales. To further complicate matters, one must include the possibility of plastic deformation if the strains get too large (as bonds break), and nonlinear constitutive models (both fluid and solid), taking into account the complex microstructure of the tissue. A review of various rheological models for living tissue can be found in [258].

The mechanical models described above are all single-phase models, in that all parts of the tissue respond in the same way to applied stimuli. True tissues, however, have a much more complicated structure and behavior, being composed (as discussed in section 2) of different materials which obey different constitutive relations. Many researchers have thus disregarded the single-phase model of tissue and instead considered multiple-phase or *mixture* models. These models work on the principle that the material being studied is formed of n different phases, each of which may be modeled by some continuum constitutive law.[3] For instance, one type of mixture model is the poroelastic model, which incorporates an elastic phase and a fluid phase. The key assumption behind the mixture approach is that at any point in the body, all phases exist simultaneously. This is, in a sense, a "smearing out" of the more realistic situation whereby any small region of the tissue contains a certain proportion of each phase. Mathematically one may state that the mixture model is the result of homogenizing the aforementioned realistic situation, although this is not, in general, how the mixture model is derived. Instead, each phase i is presumed to have some volume fraction ϕ_i, where for tissues the phases are usually assumed to completely specify the material, i.e., $\sum_i^n \phi_i = 1$. Then, we apply conservation of mass, momentum, and energy to each of the phases in turn, noting how the quantities may be transferred from one phase to another. The conservation equations governing mixture behavior were first definitively determined by Truesdell [252].

Mixture theory has been applied to biological tissues for over thirty years [16]. A common application of mixture theory is in the modeling of tumors, where the proportion of fluid in any region of the tumor (and hence its porosity) is important, especially in determining the spatial distribution of the nutrients and drugs which, respectively, aid and hinder the tumor's growth. In these models two phases are typically considered, namely the cells and the interstitial fluid in which they are embedded. Not all models treat the cell phase as a solid skeleton. For instance, Byrne and Preziosi [40] make a number of assumptions about the movement of tumor cells as the tumor as a whole undergoes a growth process; they deduce that the cell phase can be treated as a "fluid-like material" in that it responds to the velocity gradient rather than the strain. This theory echoes the modeling of tissues as viscous fluids, as explained earlier.

Single-phase models for growth using nonelastic constitutive laws have also been formulated and can produce useful results; for example, see the paper by Basan et al. [18], who modeled a growing population of tumor cells under pressure using a compressive viscous fluid model. However, we will concentrate in this section on models of elastic growth (with discussion of inelastic effects where appropriate). In part this is because elastic behavior is necessary for the intriguing phenomenon of residual stress. We will begin by recounting a short history of mathematically based tissue growth models.

[3] As such, single-species models such as elastic or fluid models are subsumed into the multiple-phase approach.

3.1. A Short History of Macroscale Growth Models. Perhaps the first widely recognized investigation into growth in biology was made by D'Arcy Thompson in 1917, when he published *On Growth and Form* [250]. This treatise contained many original ideas, most notably Thompson's realization that the connection between animals which were closely related but physiologically different could be elucidated by superimposing a Cartesian grid on the body of the first animal, and applying a simple mapping which would transform the image to a form closely resembling the second animal. This method could also be applied to differences between juvenile and adult shapes of the same animal. He consequently realized that the differences could be explained by growth occurring at different rates in different parts of the body, causing a noticeable change in the morphology of the animal during development. Huxley [148] extended this work and placed it in a more mathematical setting by introducing the concepts of "growth gradients" and "differential growth." In particular, consider the relative growth of an organ compared to the whole of the body in which it is contained. If y is the length scale of the organ, and x is the length scale of the body, they can often be related by a power law of the form $y = ax^b$, for constant a and b. This *allometric* theory of growth was later expanded upon by Skalak et al. [234]. A surprising result of this type of modeling is that the mass of an organism during its growth process can be predicted based on metabolic processes in its cells. West et al. [269] showed that the mass of a wide variety of animal species grew according to the equation

$$\frac{\mathrm{d}m}{\mathrm{d}t} = am^{3/4} - bm, \tag{3.1}$$

where a, b are constants (different for each species), which are dependent on the metabolic characteristics of the cells. The key assumption here is that the metabolic rate B depends on the total body mass m through the power law relation $B \propto m^{3/4}$, which is true for a wide range of biological organisms and can be shown to derive from a consideration of the fractal nature of internal transport systems such as blood vessels [270].

The work of Thompson was the first of many that provided a kinematic description of growth [186, 230, 66]. However, it wasn't until 1968 that *continuum mechanics* were applied to tissue growth, when Hsu [141] investigated homogeneous growth in a class of linear viscoelastic materials. Cowin and Hegedus [62] formulated the equations in finite elasticity for growth by densification, which were later applied to the problem of bone growth.

The next contribution to biological growth using finite elasticity was made by Skalak and coworkers [233, 234]. In contrast to the densification theory, Skalak [233] considered more general volumetric growth which could give rise to incompatible deformations, i.e., where growth would cause the structure to lose its continuity, were it not held together. To maintain this continuity, the body in its final state must experience internal stresses, which are the residual stresses seen in experiments. Skalak's contribution was to note that this implied that the deformation under growth could be considered to be the superposition of two deformations: a growth, after which the structure would have a nonzero *compatibility tensor*, and an additional deformation that would cause the overall compatibility tensor to become zero. This is exactly analogous to the case of distributed dislocations in a crystal, where the density of dislocations is specified and an elastic response is caused such that the crystal remains continuous.

This work led to an important paper by Rodriguez et al. [218], on which much of the current research into growth in tissues is ultimately based. The concept of a

deformation gradient decomposition was introduced, so that growth and the elastic response to that growth could be considered separately. This theory was further enhanced by Klisch et al. [164] and by Lubarda and Hoger [182]. (Before proceeding it must be noted that the genesis of residual stress may be separate from incompatible bulk growth [105] by explicitly accounting for the different rates of growth between various components of the tissue. This will be covered in more detail in section 3.5.)

In this section we will present a basic overview of finite elasticity theory before explaining the deformation gradient decomposition method, including discussion of the resulting incompatibility of the growth, extensions to the theory, applications, and a simple example. Other theories have been proposed to study growth and remodeling in biological tissues, and we will mention in brief some other growth laws in finite and infinitesimal elasticity, together with an overview of bone remodeling theories. Finally we will describe the inclusion of growth in mixture theory.

3.2. Modeling Tissue Using Finite Elasticity. The most notable feature of elastic materials is that when they undergo some loading, due to body forces such as gravity or to tractions applied to their surfaces, they deform in such a way that the deformation disappears when the loading is removed. The most commonly known type of elastic law is linear elasticity, which is governed by Hooke's law: the displacement in a solid is proportional to the stress field.[4] However, we will consider more general types of elastic material, namely finite (or nonlinear) elastic materials, where the stress–strain behavior is not in general linear.

Continuum mechanics, in essence, is a combination of *kinematics* (the description of the deformation, including density changes according to local conservation of mass), *mechanics* (the stress field in the material, governed by the conservation of momentum, or Newton's laws), and a *constitutive law* which links the two. In particular, for finite elasticity, the kinematics are described by the deformation gradient (and through this the strain field), and the constitutive law is defined using a strain energy function, through which we know the elastic energy in the material, given a particular deformation.

In this section we will outline these concepts in more detail,[5] in preparation for a discussion of the deformation gradient decomposition method of Rodriguez et al. [218], which incorporates growth effects.

Consider an elastic body $\mathcal{B}_0$ which is in an unstressed (or *reference*) state. This body is then subjected to a deformation process which takes it to a new (*spatial* or *current*) state $\mathcal{B}_t$. We define a spatial variable $\boldsymbol{X}$ (the Lagrangian coordinate) in $\mathcal{B}_0$, and similarly we define the Eulerian coordinates to be given by the spatial variable $\boldsymbol{x}$ in $\mathcal{B}_t$. The mapping between the two states—which describes the deformation—is given by $\boldsymbol{x} = \boldsymbol{\chi}(\boldsymbol{X}, t)$.

This formulation leads us to consider the deformation gradient

$$\boldsymbol{F} = \frac{\partial \boldsymbol{\chi}}{\partial \boldsymbol{X}}. \tag{3.2}$$

This is a second-order tensor which must satisfy $J := \det \boldsymbol{F} > 0$ so that the described deformation process is invertible. The deformation gradient may be used to define an important symmetric deformation measure known as the right Cauchy–Green tensor,

[4] Compare with a linear spring, where the extension is proportional to the loading.

[5] This exposition is by necessity rather elementary; for a fuller explanation of the principles involved in nonlinear solid mechanics we refer the reader to [132] or, from a tissue mechanics perspective, to [60].

$\boldsymbol{C} = \boldsymbol{F}^{\mathrm{T}}\boldsymbol{F}$. In turn this may be used to define the most common strain measure, the Green–Lagrange strain tensor $\boldsymbol{E} = \frac{1}{2}(\boldsymbol{C} - \boldsymbol{I})$.

We assume that the density of the body $\mathcal{B}_t$ is given by a function $\rho(\boldsymbol{x}, t)$. For a body not undergoing growth, the rate of increase of mass is zero, so that the principle of conservation of mass for an element $V(t) \subseteq \mathcal{B}_t$ reads

$$\frac{\mathrm{d}}{\mathrm{d}t}\int_{V(t)} \rho \,\mathrm{d}^3\boldsymbol{x} = 0, \tag{3.3}$$

and, on using Reynolds' transport theorem, we obtain the equation for mass conservation,

$$\frac{\partial \rho}{\partial t} + \nabla \cdot (\rho \boldsymbol{v}) = 0, \tag{3.4}$$

where $\boldsymbol{v} = \partial \boldsymbol{\chi}/\partial t$ is the velocity field of the body and the divergence is that calculated using the current coordinates of the body, or $\nabla = \partial/\partial \boldsymbol{x}$. Note that on changing variables from $\boldsymbol{x}$ to $\boldsymbol{X}$, using $\mathrm{d}^3\boldsymbol{x} = J\mathrm{d}^3\boldsymbol{X}$, the equation of mass conservation may be written

$$\frac{\mathrm{d}(J\rho)}{\mathrm{d}t} = 0 \tag{3.5}$$

in the reference configuration.

Conservation of momentum gives

$$\nabla \cdot \boldsymbol{\sigma} + \rho \boldsymbol{b} = \rho \frac{\mathrm{d}\boldsymbol{v}}{\mathrm{d}t}, \tag{3.6}$$

where $\boldsymbol{\sigma}(\boldsymbol{x}, t)$ is the Cauchy stress field and $\boldsymbol{b}(\boldsymbol{x}, t)$ is the body force, both defined on the current configuration $\mathcal{B}_t$. In particular $\boldsymbol{\sigma}$ is defined so that $\boldsymbol{t} = \boldsymbol{\sigma}\boldsymbol{n}$ is the force (referred to current axes) per unit area (defined in the current configuration) acting on a surface with normal $\boldsymbol{n}$. For problems of tissue deformation the body forces can often be neglected, and the deformation process can be considered to be quasistatic, resulting in the simplified equation $\nabla \cdot \boldsymbol{\sigma} = \boldsymbol{0}$. Sometimes it's easier to map this to the (known) reference configuration. A useful measure in this respect is the first Piola–Kirchhoff stress tensor, which may be given in terms of the Cauchy stress tensor by the expression

$$\boldsymbol{P} = J\boldsymbol{\sigma}\boldsymbol{F}^{-\mathrm{T}}; \tag{3.7}$$

this is defined for points in the reference configuration $\mathcal{B}_0$.[6] In contrast to $\boldsymbol{\sigma}$, $\boldsymbol{P}$ is defined so that $\boldsymbol{P}\boldsymbol{N}$ is the force (referred to *current* axes) per unit *reference* area, acting on a surface (in the reference configuration) with normal $\boldsymbol{N}$. This may appear to be a complicated definition, but using $\boldsymbol{P}$ often leads to simpler equations as it is based on the reference configuration. The equilibrium equation for $\boldsymbol{P}$ in the absence of body forces and inertial terms is

$$\nabla_0 \cdot \boldsymbol{P} = \boldsymbol{0}, \tag{3.8}$$

[6] We follow the same convention as Holzapfel [132]; equivalent formulations exist in which $\boldsymbol{P} = J\boldsymbol{F}^{-1}\boldsymbol{\sigma}$, such as Ogden's nominal stress tensor [206]. Clearly, in any application the definitions should not be interchanged.

where $\nabla_0 = \partial/\partial \boldsymbol{X}$ is the gradient operator with respect to Lagrangian coordinates. Other common measures of stress are often used, notably the second Piola–Kirchhoff stress tensor $\boldsymbol{S} = \boldsymbol{F}^{-1}\boldsymbol{P}$. This does not have a physical interpretation [132] but is useful computationally as it is symmetric and defined solely with respect to the reference configuration.

The final component to this theory, at least for our purposes, is a constitutive relation which links the stress in a body to the deformation that it experiences. This relationship is characterized by the *strain energy function* $W = W(\boldsymbol{F})$, which may be written—due to objectivity assumptions, where the stored energy of a body is assumed to remain constant under rigid body motions—as a function of $\boldsymbol{C}$, viz. $W = W(\boldsymbol{F}) = \widehat{W}(\boldsymbol{C})$. We can also write $\widehat{W}(\boldsymbol{C}) = \widetilde{W}(\boldsymbol{E})$. The first Piola–Kirchhoff stress $\boldsymbol{P}$ may be given in terms of W by the relation

$$\boldsymbol{P} = \frac{\partial W}{\partial \boldsymbol{F}}, \tag{3.9}$$

with the expression for $\boldsymbol{\sigma}$ following from (3.7). Equivalently one may obtain the second Piola–Kirchhoff stress by the expression

$$\boldsymbol{S} = 2\frac{\partial \widehat{W}}{\partial \boldsymbol{C}} = \frac{\partial \widetilde{W}}{\partial \boldsymbol{E}}. \tag{3.10}$$

Different forms of the strain energy function can be used to model different types of material, from rubber to foam to biological tissue. If the material is incompressible, a hydrostatic pressure is added to the expression for $\boldsymbol{\sigma}$ as a Lagrange multiplier for the constraint $\det \boldsymbol{F} = 1$. One example of an incompressible material is the neo-Hookean material, for which $\widehat{W} = \frac{\mu}{2}(\mathrm{tr}\boldsymbol{C} - 3)$; in the limit of infinitesimally small deformations the constant μ is the shear modulus of the material. A number of strain energy functions that have been applied to tissues, including Fung's exponential strain energy function, are described in [60].

The equilibrium equation, the constitutive relation (3.9) or (3.10), and boundary conditions on the body that specify either the displacement or the traction, form a closed system for the deformation $\boldsymbol{\chi}(\boldsymbol{X}, t)$ of the body.

3.3. Growth in Finite Elastic Models. The preceding equations are well established and completely describe the deformation of a nonlinearly elastic solid. However, several complicating factors come into play if the deformation of the body includes a component due to growth of tissue. To begin with, the right-hand side of the conservation of mass equation (3.3) is nonzero. If the rate of increase of mass per unit current volume is given by a function $\gamma(\boldsymbol{x}, t)$, then

$$\frac{\mathrm{d}}{\mathrm{d}t}\int_{V(t)} \rho \,\mathrm{d}^3\boldsymbol{x} = \int_{V(t)} \gamma \,\mathrm{d}^3\boldsymbol{x}, \tag{3.11}$$

leading to

$$\frac{\partial \rho}{\partial t} + \nabla \cdot (\rho \boldsymbol{v}) = \gamma, \tag{3.12}$$

in the current configuration, or

$$\frac{\mathrm{d}(J\rho)}{\mathrm{d}t} = J\gamma \tag{3.13}$$

in the reference configuration. Note that since we have a volumetric source of mass in (3.12) the model is implicitly multiphase. Overall, mass must of course be conserved; the source term represents transfer of mass from a phase not explicitly treated (which could be thought of as the extracellular fluid), and which occupies a small volume and does not contribute to the momentum balance. In most applications of this theory, the equation for the conservation of linear momentum remains the same (see, for example, [182]). However, in the most general formulation this is not actually the case, and the growth process may introduce sources of momentum other than the mere convection of mass. This is discussed further by Epstein and Maugin [88] (for single-species materials), by Kuhl and Steinmann [171] (in a more abstract setting), and by Garikipati et al. [106] (for mixture models).

Simply prescribing the rate of mass increase γ is not enough to capture the full effect of the tissue growth, however, especially when the growth occurs anisotropically or inhomogeneously, for reasons which will become clear shortly. Instead, we introduce the idea of Rodriguez et al. [218], namely the deformation gradient decomposition. In this formulation, the deformation from $\mathcal{B}_0$ to $\mathcal{B}_t$ is decomposed into two steps. The first deformation identifies with each point in $\mathcal{B}_0$ an arbitrarily small neighborhood of that point, and deforms that neighborhood into a new, grown, stress-free state. The collection of these grown states is denoted $\mathcal{B}_\mathrm{g}$ and is not necessarily compatible—i.e., parts of the tissue may intersect. The second step applies an elastic deformation to the incompatible state $\mathcal{B}_\mathrm{g}$, obtaining the state $\mathcal{B}_t$—which may now contain residual stresses due to the restoring of compatibility to the body.

The overall effect is a *multiplicative decomposition* of the deformation gradient $\boldsymbol{F}$ into two parts:

$$\boldsymbol{F} = \boldsymbol{F}_\mathrm{e}\boldsymbol{F}_\mathrm{g}. \tag{3.14}$$

Here $\boldsymbol{F}_\mathrm{g}$ is known as the growth tensor and takes $\mathcal{B}_0$ to $\mathcal{B}_\mathrm{g}$, while $\boldsymbol{F}_\mathrm{e}$ is referred to as the accommodation tensor or the elastic part of the deformation gradient, taking $\mathcal{B}_\mathrm{g}$ to $\mathcal{B}_t$, as shown in Figure 3.1. This idea is a mathematical formulation of the cutting experiments on (for instance) arteries or rhubarb, recounted in section 1. The deformation $\boldsymbol{F}_\mathrm{e}^{-1}$ from $\mathcal{B}_t$ to $\mathcal{B}_\mathrm{g}$ is the "cutting" process which takes a grown, residually stressed configuration ($\mathcal{B}_t$) and results in a (possibly infinite) collection of grown, unstressed bodies ($\mathcal{B}_\mathrm{g}$). Thus the decomposition physically corresponds to a cutting of the body into infinitely many sections which are then grown ($\boldsymbol{F}_\mathrm{g}$) followed by a gluing of the sections back together ($\boldsymbol{F}_\mathrm{e}$), resulting in a stress field.

The exposition that we will give here does not fully capture the theory behind this method, but will serve to give a flavor of the mechanisms involved. A much more comprehensive presentation can be found in Lubarda and Hoger's work [182].

The decomposition of the deformation gradient was originally seen in theories of plastic deformation. The first researchers to write down the decomposition were Kröner and Seeger [166] and Bilby et al. [23]. However, Lee [176] often gets the credit for the discovery. As such the decomposition is sometimes known as the Kröner–Lee decomposition, or the unwieldy Bilby–Gardner–Stroh–Kröner–Lee decomposition [185]. For an overview of the early history of the decomposition we refer the reader to [185], and to [181] for an application to thermoelasticity.

There are of course limitations to the types of tissue growth that can be modeled by multiplicative decomposition. First, the tissue undergoing growth must behave elastically on the timescale of growth, with insignificant relaxation of stresses. Now, most tissues undergo a certain amount of relaxation, but this is either small com-

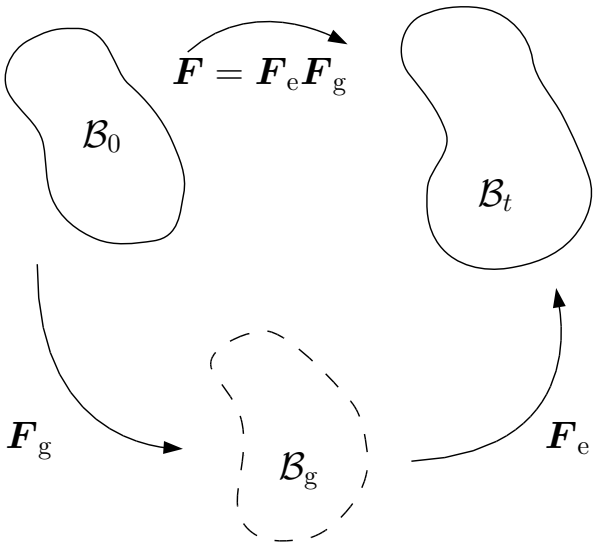

Fig. 3.1 *An illustration of the deformation gradient decomposition* $\boldsymbol{F} = \boldsymbol{F}_{\mathrm{e}}\boldsymbol{F}_{\mathrm{g}}$.

pared to the overall deformation, or is neglected in the interest of obtaining qualitative results. Also implicit in the deformation gradient decomposition is that the elastic timescale (associated with elastic wave propagation) is much shorter than the timescale associated with growth [114]. This requirement ensures that the elastic deformation due to accommodation (through $\boldsymbol{F}_{\mathrm{e}}$) occurs effectively instantaneously in response to the growth $\boldsymbol{F}_{\mathrm{g}}$. Finally, the growth process being modeled must be able to be written as a deformation gradient. This is not always possible; for instance, growth due to accretion on a surface is not a bulk process but rather one which is only valid on the domain boundaries.

Thus there are some types of growth which cannot be modeled using this decomposition, but it remains valid for a wide range of applications, especially for those exhibiting a degree of residual stress. The advantage of the multiplicative decomposition is that growth and elastic response may be treated separately. The growth tensor $\boldsymbol{F}_{\mathrm{g}}$ can be specified as a function of stress, position, density, nutrient concentration, or any number of other quantities that may have an effect on the growth rate of the tissue. Then the elastic response tensor $\boldsymbol{F}_{\mathrm{e}}$ is chosen so as to make the overall deformation compatible. How this is achieved in practice will be summarized later.

To see how this decomposition can simplify the equations describing the growth process, take the equation (3.13) for conservation of mass. We have

$$J = \det \boldsymbol{F} = \det \boldsymbol{F}_{\mathrm{e}} \det \boldsymbol{F}_{\mathrm{g}} = J_{\mathrm{e}} J_{\mathrm{g}}, \tag{3.15}$$

where J_{g} and J_{e} are, respectively, the determinants of the growth and accommodation tensors. Then (3.13) becomes

$$\frac{\mathrm{d}}{\mathrm{d}t}(J_{\mathrm{e}} J_{\mathrm{g}} \rho) = J_{\mathrm{e}} J_{\mathrm{g}} \gamma. \tag{3.16}$$

Consider a small region $\mathrm{d}V_0$ of $\mathcal{B}_0$, with mass $\mathrm{d}m_0 = \rho_0 \mathrm{d}V_0$. Under the transformation

$\boldsymbol{F}$, this region will have mass $\mathrm{d}m = \rho \mathrm{d}V$ in $\mathcal{B}_t$. If we apply the assumption that all the mass production takes place from $\mathcal{B}_0$ to $\mathcal{B}_\mathrm{g}$ only, then the aforementioned small region will have the same mass in $\mathcal{B}_\mathrm{g}$ and $\mathcal{B}_t$, i.e., $\mathrm{d}m = \rho_\mathrm{g}\mathrm{d}V_\mathrm{g} = \rho \mathrm{d}V$, where ρ_g is the density with respect to $\mathcal{B}_\mathrm{g}$. Since $\mathrm{d}V = J_\mathrm{e}\mathrm{d}V_\mathrm{g}$, we have $\rho_\mathrm{g} = J_\mathrm{e}\rho$. Then, from (3.16),

$$\frac{\mathrm{d}\rho_\mathrm{g}}{\mathrm{d}t} + \frac{\rho_\mathrm{g}}{J_\mathrm{g}}\frac{\mathrm{d}J_\mathrm{g}}{\mathrm{d}t} = J_\mathrm{e}\gamma. \tag{3.17}$$

However,

$$\frac{\mathrm{d}J_\mathrm{g}}{\mathrm{d}t} = \frac{\mathrm{d}}{\mathrm{d}t}\det \boldsymbol{F}_\mathrm{g} = (\det \boldsymbol{F}_\mathrm{g})\boldsymbol{F}_\mathrm{g}^{-\mathrm{T}} : \dot{\boldsymbol{F}}_\mathrm{g} = J_\mathrm{g}\mathrm{tr}(\boldsymbol{F}_\mathrm{g}^{-1}\dot{\boldsymbol{F}}_\mathrm{g}). \tag{3.18}$$

Using this identity and (3.17) gives us

$$\frac{\mathrm{d}\rho_\mathrm{g}}{\mathrm{d}t} + \rho_\mathrm{g}\mathrm{tr}(\boldsymbol{F}_\mathrm{g}^{-1}\dot{\boldsymbol{F}}_\mathrm{g}) = J_\mathrm{e}\gamma. \tag{3.19}$$

In applications, this expression is often simplified by introducing assumptions on the nature of the growth. In particular, the two assumptions most commonly applied are of constant-density growth and constant-volume growth. In the former, we suppose that the density is unchanged by the growth process, so that $\rho_\mathrm{g} = \rho_0$ and hence $\mathrm{d}\rho_\mathrm{g}/\mathrm{d}t = 0$. Then (3.19) becomes

$$\gamma = \rho\ \mathrm{tr}(\boldsymbol{F}_\mathrm{g}^{-1}\dot{\boldsymbol{F}}_\mathrm{g}). \tag{3.20}$$

This can now be treated as a *definition* for γ; in other words the rate of mass increase can be determined if $\boldsymbol{F}_\mathrm{g}$ is specified. In this case the equation for conservation of mass (3.17) is

$$\rho\,\frac{\mathrm{d}J_\mathrm{g}}{\mathrm{d}t} = J_\mathrm{g}\gamma. \tag{3.21}$$

Note also that $\mathrm{d}\rho_\mathrm{g}/\mathrm{d}t = 0$ can be rewritten

$$\frac{\mathrm{d}\rho}{\mathrm{d}t} + \rho\ \mathrm{tr}(\boldsymbol{F}_\mathrm{e}^{-1}\dot{\boldsymbol{F}}_\mathrm{e}) = 0. \tag{3.22}$$

Constant-density growth is usually coupled with the assumption of an incompressible tissue, so that additionally $J_\mathrm{e} = 1$ and hence $\rho = \rho_\mathrm{g} = \rho_0 = \text{constant}$. For constant-volume growth, the change in volume from $\mathcal{B}_0$ to $\mathcal{B}_\mathrm{g}$ is assumed to be zero, so that $\mathrm{d}V_0 = \mathrm{d}V_\mathrm{g}$, or $J_\mathrm{g} = 1$. Then the tissue growth occurs by densification only, with

$$\frac{\mathrm{d}\rho_\mathrm{g}}{\mathrm{d}t} = \frac{\mathrm{d}}{\mathrm{d}t}\left(\rho J_\mathrm{e}\right) = J_\mathrm{e}\gamma. \tag{3.23}$$

This is an approach which is valid for tissues such as bone, where little volume change accompanies mass growth; an implementation is briefly discussed in section 3.4.

While the mass production is assumed to occur only between the states $\mathcal{B}_0$ and $\mathcal{B}_\mathrm{g}$, the elastic response occurs only between $\mathcal{B}_\mathrm{g}$ and $\mathcal{B}_t$, as the state $\mathcal{B}_\mathrm{g}$ is assumed to be unstressed. Thus, if the strain energy function W is assumed to be the elastic strain energy per unit grown unstressed volume, (i.e., in state $\mathcal{B}_\mathrm{g}$), then the second Piola–Kirchhoff stress tensor referred to the state $\mathcal{B}_\mathrm{g}$ is given, with reference to (3.10), by

$$\boldsymbol{S}_\mathrm{e} = \frac{\partial \widetilde{W}}{\partial \boldsymbol{E}_\mathrm{e}}, \tag{3.24}$$

where the subscript "e" refers to the fact that the quantity is formed using the elastic deformation gradient $\boldsymbol{F}_{\mathrm{e}}$ rather than $\boldsymbol{F}$. We can then form the Cauchy stress tensor by using the expression $\boldsymbol{\sigma} = J_{\mathrm{e}}^{-1}\boldsymbol{F}_{\mathrm{e}}\boldsymbol{S}_{\mathrm{e}}\boldsymbol{F}_{\mathrm{e}}^{\mathrm{T}}$.

3.3.1. Incompatible Deformations. We have stated that if the deformation $\boldsymbol{F}_{\mathrm{g}}$ related to growth creates an incompatible deformation, then the tissue generates a residual stress by enforcing the compatibility of the deformation. But how do we know, simply by analyzing the growth tensor, whether a deformation is incompatible?

This was a question discussed by Skalak et al. [235], who looked at the problem by analogy with the situation in linearly elastic materials. For simply connected materials experiencing an infinitesimal strain field e_{ij}, the compatibility condition can be written $\boldsymbol{\eta} = \boldsymbol{0}$, where $\boldsymbol{\eta} = \nabla \wedge \nabla \wedge \boldsymbol{e}$, i.e., $\varepsilon_{ilm}\varepsilon_{jkn}e_{mn,lk} = 0$, where ε_{ijk} is the Levi-Civita tensor.[7] On the other hand, for multiply connected domains, an additional condition must be satisfied, namely,

$$\oint_C \left(e_{ij} + (x_k^0 - x_k)(e_{ij,k} + e_{kj,i})\right) \mathrm{d}x_j = 0 \tag{3.25}$$

for each closed curve C in the body, where x_k^0 is a point on C. An (incompatible) elastic deformation satisfying $\boldsymbol{\eta} = \boldsymbol{0}$ but not (3.25) is termed a Volterra dislocation.

Thus we may identify two possible sources for an incompatible deformation: a local incompatibility, where for any point in the material such that $\boldsymbol{\eta} \neq \boldsymbol{0}$, an arbitrary region around that point is taken to an incompatible configuration by the deformation; and second, a geometric incompatibility where any subregion of the material is transformed to a compatible state under the growth, but the geometry of the body as a whole causes the overall deformation to be incompatible.

Analogous compatibility conditions may be found for finite deformations. Naturally, they are much more complicated. For instance, in Cartesian coordinates if the Cauchy–Green tensor is given by C_{ij}, then the local compatibility condition is the requirement that the Riemann–Christoffel tensor is zero, or $R_{ijkl} = 0$, where

$$R_{ijkl} = \Gamma_{jli,k} - \Gamma_{jki,l} + C_{pq}^{-1}(\Gamma_{jkp}\Gamma_{ilq} - \Gamma_{jlp}\Gamma_{ikq}) \tag{3.26}$$

and $\Gamma_{ijk} = \frac{1}{2}(C_{jk,i} + C_{ik,j} - C_{ij,k})$ are Christoffel symbols. Less is known about Volterra dislocations (geometric incompatibility) in finitely deformed elastic materials, but Casey [42] has made a recent investigation into these. Thus, for any residually stressed biological material, the nature of the incompatibility is determined by calculating the Riemann–Christoffel tensor of the deformation between the reference state and the stress-free state: if this tensor is zero, then the residual stress in the body can be relieved by some cutting and unloading; otherwise the body needs to be divided into infinitesimally small parts to relieve the stress.

Further analysis of the Riemann–Christoffel tensor with application to residual stress in tissues can be found in [249, 161, 103].

3.3.2. Further Extensions of the Theory. In the deformation gradient decomposition method, one of the key issues is to determine the elastic part of the defor-

[7] The Levi-Civita tensor is given by

$$\varepsilon_{ijk} = \begin{cases} +1 & \text{if } (ijk) = (123) \text{ or } (231) \text{ or } (312), \\ -1 & \text{if } (ijk) = (132) \text{ or } (213) \text{ or } (321), \\ 0 & \text{otherwise.} \end{cases}$$

mation gradient $\boldsymbol{F}_{\mathrm{e}}$. The definition given was to choose $\boldsymbol{F}_{\mathrm{e}}$ so that the overall deformation described by $\boldsymbol{F}_{\mathrm{e}}\boldsymbol{F}_{\mathrm{g}}$ was compatible. Thus we could identify the Riemann–Christoffel tensor R_{ijkl} associated with this deformation, and solve $R_{ijkl} = 0$ (together with mass and momentum conservation and the constitutive relation (3.24)) for $\boldsymbol{F}_{\mathrm{e}}$. However, even with a simplified geometry the equations are certainly nontrivial [103], and solving them would seem to be an impractical approach.

This is not, however, how the system of equations is solved in practice. If $\boldsymbol{F}_{\mathrm{g}}$ is given, then the accommodation tensor is given by $\boldsymbol{F}_{\mathrm{e}} = \boldsymbol{F}\boldsymbol{F}_{\mathrm{g}}^{-1}$ from (3.14). Thus, the stress field $\boldsymbol{S}_{\mathrm{e}} = \boldsymbol{S}_{\mathrm{e}}(\boldsymbol{F}_{\mathrm{e}})$ in the material, given by (3.24), can be found as a function of the overall deformation gradient, i.e., $\boldsymbol{S}_{\mathrm{e}} = \boldsymbol{S}_{\mathrm{e}}(\boldsymbol{F}\boldsymbol{F}_{\mathrm{g}}^{-1})$, and the system of equations can be solved for the overall deformation gradient $\boldsymbol{F}$. The same process can be followed if the tissue growth is to be solved for numerically as a time-dependent problem, using incremental elasticity embedded in standard finite element codes. The elastic tensor C_{ijkl} is found from the strain energy function and the accommodation tensor $\boldsymbol{F}\boldsymbol{F}_{\mathrm{g}}^{-1}$, and is used to update the overall deformation according to standard procedures, giving the overall deformation gradient $\boldsymbol{F}$ at the next time step. More details and a specific application of this approach can be found in [128].

As an example of another situation in which the deformation gradient decomposition could be used, Garikipati et al. [107] set up a model for a nongrowing tissue in which the deformation gradient was multiplicatively decomposed into a configurational change modeling the underlying deformation of the microstructure, and a mechanical response (or accommodation). In this formulation the intermediate configuration (corresponding to $\mathcal{B}_{\mathrm{g}}$) was compatible. Equilibrium equations were found by appealing to a variational formulation and extracting the Euler–Lagrange equations.

Chen and Hoger [47] realized that the deformation gradient decomposition was somewhat speculative, and endeavored to place it on a sound kinematic footing. This was achieved by treating the *current* (Eulerian) configuration as the reference configuration, thus sidestepping the issue that certain points in the body $\mathcal{B}_t$ did not exist in $\mathcal{B}_0$. Other researchers have tried to make the model more physical, such as Ambrosi and Guillou [5], who took the thermodynamical inequalities underlying the theory and incorporated the effect of chemical transport, which is important when considering nutrient uptake by growing tissues such as tumors.

It should be noted that there are still open questions regarding the modeling of growth [105]. Apart from the obvious matter of the choice of growth tensor (some examples of which are noted below), a comprehensive understanding of the thermodynamical aspects of growth is still elusive [105]. However, in simulations of growing tumor spheroids, Narayanan et al. [199] have investigated the effects of cell proliferation on the rates of change of free energy, providing a basis for further study in this area.

3.3.3. Applications. Due to the nonlinear nature of the governing equations, the applications of this theory have largely been limited to simple geometries such as spheres and cylinders. These include investigations into the residual stress in tumor spheroids [6, 7] and arteries [248, 246], the latter studies motivated by the cutting experiments of Fung and others, as mentioned in the introduction. Other situations where this theory has been used include a study into the buckling of spherical shells that are undergoing growth [113, 20], a finite element model of a skin growth experiment [238], and the growth of atherosclerotic plaque in arteries [169].

While the geometries in the investigations above may be simplified, a wide variety of growth tensors $\boldsymbol{F}_{\mathrm{g}}$ has been proposed. Clearly, the simplest form of growth tensor that can be imposed is a constant tensor. This was one of the examples proposed

by Rodriguez et al. [218], which we will summarize in the next section. However, the growth tensor may be prescribed to be functions of other physical quantities. Ambrosi and Mollica [6] took their growth tensor—as an illustration of residual stress genesis—to be isotropic and a certain function of Lagrangian position. Goriely and Ben Amar [114] compare the results of defining the growth tensor to be functions of either Lagrangian position or Eulerian position. A significant difference was found between the two formulations, whereby the growth was exponential in the Lagrangian case but quadratic or linear in the Eulerian case.

Alternatively, it may be preferable to formulate an equation for the rate of growth $\dot{\boldsymbol{F}}_{\mathrm{g}}$. In their theory of stress-modulated growth of the aorta, Taber and Eggers [248] took the principal stretches $\lambda_{\mathrm{g}i}$ associated with $\boldsymbol{F}_{\mathrm{g}}$ and proposed that the $\dot{\lambda}_{\mathrm{g}i}$ were proportional to the Cauchy stress field in the artery wall. Later [246], this theory was adapted so that the $\dot{\lambda}_{\mathrm{g}i}$ were proportional to the difference between the stress field and a reference stress state; this had the effect that the artery grew in order to maintain a stress field which was at this reference state. Shear stresses due to fluid flow were also considered in this model. A comparable model was proposed by Rodríguez et al. [219], which incorporated the anisotropy of the arterial wall. Socci et al. [238] applied a similar law in their finite element study of skin growth, although the state to which the tissue tended to grow was defined by a given deformation gradient rather than a stress field.

Following up on their original model of tumor growth, Ambrosi and Mollica [7] modified their growth theory, choosing an isotropic growth tensor $\boldsymbol{F}_{\mathrm{g}} = g\boldsymbol{I}$, where the rate of growth was given by

$$\dot{g} \propto \mathrm{e}^{-(s/s_0)^2}(n - n_0)g; \tag{3.27}$$

here $s = \mathrm{tr}\boldsymbol{P}$ and n is the nutrient concentration. Lubarda and Hoger [182] posited an isotropic stress–growth law which had a different behavior depending on whether the stress was tensile or compressive; if $\boldsymbol{F}_{\mathrm{g}} = g\boldsymbol{I}$, then $\dot{g} = k(g)\mathrm{tr}\boldsymbol{S}_{\mathrm{e}}$, where

$$k(g) = \begin{cases} k_0^+ \left(\dfrac{g^+ - g}{g^+ - 1}\right)^{m^+}, & \mathrm{tr}\boldsymbol{S}_{\mathrm{e}} > 0, \\ k_0^- \left(\dfrac{g - g^-}{1 - g^-}\right)^{m^-}, & \mathrm{tr}\boldsymbol{S}_{\mathrm{e}} < 0, \end{cases} \tag{3.28}$$

where $k_0^{\pm}$, $m^{\pm}$ are constants, and $g^{\pm}$ are, respectively, the highest and lowest values of the growth tensor that can be achieved through the mass addition (or removal) process. This form was chosen in order to avoid runaway growth or resorption in the model, and was applied to arterial mechanics by Menzel and coworkers [129, 188, 169, 189], including analysis not only of growth but also of remodeling, i.e., the stress-induced changing of the direction of anisotropy in the artery wall.

Ambrosi and Guana [4] applied a result of DiCarlo and Quiligotti [71] which showed by thermodynamical arguments that if the growth process is governed by some external forces, and that the work done by these forces supplies the energy which drives the growth process, then the growth law for $\boldsymbol{F}_{\mathrm{g}}$ can be derived as a rate equation involving those external forces. It was shown [4] that, under certain assumptions, the growth law of Taber [246] described previously is a simplification of this thermodynamically derived rate equation.

We should note that all these growth theories are phenomenological in that they are not derived from the microscopic behavior of the tissue but rather by the plausible

tissue behavior that results from their adoption. The lack of such biologically derived growth laws is a deficiency of the current theories [105], although ensuring consistency with thermodynamic principles would go some way towards furnishing us with realistic behavior.

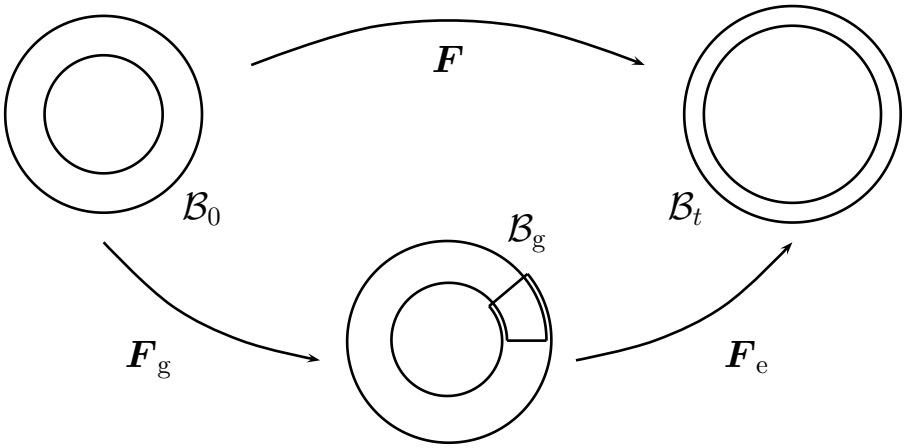

Fig. 3.2 *A simple example of the deformation gradient decomposition method.*

3.3.4. A Simple Example. To illustrate the process described above and to show that residual stresses can arise from anisotropic growth, we will present a simple example, one which was originally discussed by Rodriguez et al. [218]. We take an incompressible tissue formed from a cylindrical tube, and assume that growth occurs in the circumferential direction only, as depicted in Figure 3.2. So if the state $\mathcal{B}_0$ has coordinates (R, Θ, Z), the intermediate state $\mathcal{B}_g$ has the coordinates (R^*, Θ^*, Z^*), and the final state $\mathcal{B}_t$ has the coordinates (r, θ, z), then we have a growth field of

$$R^* = R, \qquad \Theta^* = K\Theta, \qquad Z^* = Z, \tag{3.29}$$

which gives rise to a growth tensor

$$\boldsymbol{F}_g = \begin{pmatrix} 1 & 0 & 0 \\ 0 & K & 0 \\ 0 & 0 & 1 \end{pmatrix} \tag{3.30}$$

with respect to cylindrical coordinates. We then specify a displacement from $\mathcal{B}_g$ to $\mathcal{B}_t$, which by symmetry arguments—and restricting any deformation in the z-direction—can be given by

$$r = r(R^*), \qquad \theta = \eta\Theta^*, \qquad z = Z^*. \tag{3.31}$$

This gives us an accommodation tensor in the form

$$\boldsymbol{F}_e = \begin{pmatrix} \dfrac{\mathrm{d}r}{\mathrm{d}R^*} & 0 & 0 \\ 0 & \dfrac{r\eta}{R^*} & 0 \\ 0 & 0 & 1 \end{pmatrix}. \tag{3.32}$$

The deformation $\boldsymbol{F}_{\mathrm{g}}$, as shown in Figure 3.2, is incompatible. One way of ensuring that the overall deformation is compatible is to set $\Theta = \theta$, or $\eta = 1/K$.[8] Furthermore, the incompressibility constraint gives us the form of $r(R^*) = r(R)$:

$$\det \boldsymbol{F}_{\mathrm{e}} = 1 \qquad \Rightarrow \qquad \frac{\mathrm{d}r}{\mathrm{d}R}\frac{r}{R} = K \qquad \Rightarrow \qquad r = \sqrt{KR^2 + \alpha} \tag{3.33}$$

since $R = R^*$, and for some arbitrary constant α. For incompressible materials, the first Piola–Kirchhoff stress tensor is given by (3.9), modified by the addition of a hydrostatic pressure term p:

$$\boldsymbol{P} = \frac{\partial W}{\partial \boldsymbol{F}_{\mathrm{e}}} - p\boldsymbol{F}_{\mathrm{e}}^{-\mathrm{T}}, \tag{3.34}$$

where as before the stress field arises due to the deformation between $\mathcal{B}_{\mathrm{g}}$ and $\mathcal{B}_t$. The equilibrium equation (3.8) gives us a first-order differential equation to solve for $p(R)$ and the constant α, which must be solved numerically with appropriate traction conditions on the inner and outer boundaries of the annulus.

3.4. Other Growth Models in Elasticity. Prior to the formulation of the deformation gradient decomposition, the adaptive elasticity model of Cowin and Hegedus [62] was an alternative description in a finite elasticity framework of growth in a tissue, in this case bone. The main assumption made in this theory was that for any unstrained region of the body, an increase in mass does not change the volume or strain field, corresponding to a densification of the tissue. This theory was later extended by Kuhl and Steinmann [171], and implemented in numerical investigations of bone densification [170, 173] and wound healing [172]. In this constant-volume growth theory, following the reasoning of section 3.3 leads to (3.23) and $\det \boldsymbol{F}_{\mathrm{g}} = 1$. In fact, we may set $\boldsymbol{F}_{\mathrm{g}} = \boldsymbol{I}$ and then $\mathcal{B}_{\mathrm{g}}$ becomes the reference configuration, with $\boldsymbol{F} = \boldsymbol{F}_{\mathrm{e}}$. The form of γ chosen in these models is based on the work of Harrigan and Hamilton [121], and is given by

$$\gamma \propto \left(\frac{\rho_{\mathrm{g}}}{\rho_{\mathrm{g}}^*}\right)^{-m} W - W^*, \tag{3.35}$$

where W^* and ρ_{g}^* are reference values, and m is a positive real number. Thus, for instance, if $W = W^*$ and $\rho_{\mathrm{g}} < \rho_{\mathrm{g}}^*$, then the mass will increase, thus increasing the density until it reaches the reference value ρ_{g}^*. The theory also includes in (3.23) a mass flux term which is neglected in most other models. The form chosen for W allows the material to become stiffer as it densifies; i.e., $W = (\rho_{\mathrm{g}}/\rho_{\mathrm{g}}^*)^n W^{\mathrm{elast}}$, where W^{elast} is a standard elastic strain energy, in this case a (compressible) neo-Hookean model. Changes in density are thus coupled to the elastic deformation problem.

A different type of growth considered by Skalak and coworkers [233, 234] was surface growth, where the surface on which growth occurs is not necessarily the boundary of the structure, but could be an internal surface which splits the growing body into two parts which grow away from the surface. Later, Tözeren and Skalak [251] proposed a theory of growth in fibrous tissues such as muscle and skin, and suggested a number of phenomenological relationships between the state of stress and fiber growth.

[8] We note that the incompatibility in this particular case is due to the geometry of the body rather than a local incompatibility; the latter generally arises due to different rates of growth in different parts of the body, as discussed in section 3.3.1.

Other authors have developed models for growth in tissues described by nonlinear constitutive laws. Drozdov and Khanina [81] modeled isotropic growth in a viscoelastic material which is characterized by a system of parallel (nonlinear) elastic springs. On the other hand Volokh [260] compared a tissue to a toy model where cells were represented by an array of balls. By introducing a source of new material to the toy model, a number of principles are noted, which are incorporated into a model of volumetric growth in a solid tumor. Kuhl and coworkers [167, 168] have examined the related problem of remodeling in soft tissues under the influence of an applied stress field. The microstructure of the tissue is represented by a characteristic cell (not a biological cell) in which the collagen fibers are modeled by "worm-like" chains. The orientation of the characteristic cell is gradually brought into alignment with the direction of principal strain in the tissue under the influence of applied stress fields.

A survey of theories of growth in elastic materials would not be complete without a discussion of theories based on linear constitutive models. The description of growth in such infinitesimal-strain theories may be derived from the deformation gradient decomposition described in section 3.3. Consider the displacement gradient $\boldsymbol{W} = \boldsymbol{F} - \boldsymbol{I}$. The infinitesimal theory assumes that $\|\boldsymbol{W}\| \ll 1$. Thus the strain tensor $\boldsymbol{E} = \frac{1}{2}(\boldsymbol{F}^{\mathrm{T}}\boldsymbol{F} - \boldsymbol{I})$ can be approximated by the linear strain tensor $\boldsymbol{e} = \frac{1}{2}(\boldsymbol{W} + \boldsymbol{W}^{\mathrm{T}})$. One can describe growth and accommodation displacement gradients $\boldsymbol{W}_{\mathrm{g}} = \boldsymbol{F}_{\mathrm{g}} - \boldsymbol{I}$, $\boldsymbol{W}_{\mathrm{e}} = \boldsymbol{F}_{\mathrm{e}} - \boldsymbol{I}$. From (3.14) we have

$$\boldsymbol{F} = \boldsymbol{F}_{\mathrm{e}}\boldsymbol{F}_{\mathrm{g}} = (\boldsymbol{W}_{\mathrm{e}} + \boldsymbol{I})(\boldsymbol{W}_{\mathrm{g}} + \boldsymbol{I}), \tag{3.36}$$

and thus we may form the strain tensor

$$\boldsymbol{E} = \frac{1}{2}(\boldsymbol{F}^{\mathrm{T}}\boldsymbol{F} - \boldsymbol{I}) \approx \frac{1}{2}(\boldsymbol{W}_{\mathrm{g}} + \boldsymbol{W}_{\mathrm{g}}^{\mathrm{T}} + \boldsymbol{W}_{\mathrm{e}} + \boldsymbol{W}_{\mathrm{e}}^{\mathrm{T}}) + o(\|\boldsymbol{W}\|), \tag{3.37}$$

so that $\boldsymbol{e} = \boldsymbol{e}_{\mathrm{g}} + \boldsymbol{e}_{\mathrm{e}}$, and thus in infinitesimal elasticity the multiplicative decomposition of the deformation is represented by an *additive* decomposition of the strain tensor. The constitutive relation in infinitesimal elasticity is Hooke's law, which may be written $\boldsymbol{e}_{\mathrm{e}} = \boldsymbol{K}\boldsymbol{\sigma}$, where $\boldsymbol{K}$ is the compliance tensor. By performing the decomposition into growth and elastic parts the total deformation experienced by the tissue is governed by the equation

$$\boldsymbol{e} = \boldsymbol{e}_{\mathrm{g}} + \boldsymbol{K}\boldsymbol{\sigma}. \tag{3.38}$$

This equation has recently been used to analyze the genesis of residual stresses in tumors, where the growth strain was assumed to be isotropic [157] and—to allow steady-state stress distributions—anisotropic [9]. This latter theory was applied to the study of blood vessel collapse in tumors [10] and to elucidate the effect of the surrounding tissue [13].

An additive decomposition also emerges naturally from the multiplicative decomposition if the thickness of the tissue is small, i.e., for membranes, plates, and shells [69]. Here both the strain measures (change of metric and change of curvature) are decomposed additively into growth and elastic components.

The reader may be familiar with equations of the form of (3.38) from extensions of linear elasticity to include thermoelastic, plastic, and viscoelastic effects [140]. In linear thermoelasticity the thermal expansion is assumed to vary linearly with temperature T, i.e., $e_{ij} = \frac{\alpha}{3}(T - T_0)\delta_{ij}$, where α is a constant of proportionality. This expression plays the same role as the growth strain $\boldsymbol{e}_{\mathrm{g}}$ in (3.38), giving us the

well-known constitutive law for thermoelasticity,

$$\boldsymbol{\sigma} = \boldsymbol{K}^{-1}\left(\boldsymbol{e} - \frac{\alpha}{3}(T - T_0)\boldsymbol{I}\right) \tag{3.39}$$

$$= \boldsymbol{A}\boldsymbol{e} - \alpha\left(\lambda + \frac{2\mu}{3}\right)(T - T_0)\boldsymbol{I}, \tag{3.40}$$

where $\boldsymbol{A} = \boldsymbol{K}^{-1}$ is the elasticity tensor and $\lambda + 2\mu/3$ is the bulk modulus. We can see that, kinematically speaking, thermal expansion and isotropic biological growth are equivalent, even if the constitutive form of $\boldsymbol{e}_{\mathrm{g}}$ and the effects on the material density are very different.

While thermoelasticity is the most analogous theory to growth, we note that linear elastoplasticity also admits an additive strain decomposition, $\boldsymbol{e} = \boldsymbol{e}_{\mathrm{e}} + \boldsymbol{e}_{\mathrm{p}}$. Here $\boldsymbol{e}_{\mathrm{e}} = \boldsymbol{K}\boldsymbol{\sigma}$ as before and the plastic component is chosen to satisfy a flow rule such as the Levy–von Mises flow rule [140], which states that $\partial \boldsymbol{e}_{\mathrm{p}}/\partial t$ is proportional to the deviatoric part of $\boldsymbol{\sigma}$. Similarly, in Maxwell viscoelasticity one sets $\boldsymbol{e} = \boldsymbol{e}_{\mathrm{e}} + \boldsymbol{e}_{\mathrm{v}}$, where $\dot{\boldsymbol{e}}_{\mathrm{v}} = \boldsymbol{L}\boldsymbol{\sigma}$ and $\boldsymbol{L}$ is the inverse of the viscosity tensor. This gives rise to the constitutive relation

$$\dot{\boldsymbol{e}} = \boldsymbol{K}\frac{\mathrm{d}\boldsymbol{\sigma}}{\mathrm{d}t} + \boldsymbol{L}\boldsymbol{\sigma}. \tag{3.41}$$

One may include growth in this relation by setting $\boldsymbol{e} = \boldsymbol{e}_{\mathrm{g}} + \boldsymbol{e}_{\mathrm{e}} + \boldsymbol{e}_{\mathrm{v}}$, leading to

$$\dot{\boldsymbol{e}} = \dot{\boldsymbol{e}}_{\mathrm{g}} + \boldsymbol{K}\frac{\mathrm{d}\boldsymbol{\sigma}}{\mathrm{d}t} + \boldsymbol{L}\boldsymbol{\sigma}. \tag{3.42}$$

This was the model used by Hsu [141] to analyze volumetric growth in a viscoelastic body, which was later extended by Strauss [242] and Nowinski [205]. However, for the most part the examples covered in these papers were limited to cuboids of the material, the exception being Nowinski's treatment of a pressurized circular tube. Another class of models to consider the growth law encapsulated in (3.42) apply the law to a growing rod [87, 239]. Applications of this theory range from growing plant stalks to human spine development; the use of buckling theory in the latter application may provide an insight into the onset of scoliosis, or abnormal curvature of the spine. Models with a growth law similar to (3.42) have also been applied to tumor growth [183].

3.4.1. Bone Remodeling. The earliest attempts to explain the remodeling process in bone are recounted in a comprehensive review by Roesler [220]. Beginning in the nineteenth century, researchers such as Meyer [191] examined the structure of cancellous bone, and discovered that a pattern could be discerned in the network of trabeculae which form the fabric of this part of the bone, as depicted in Figure 3.3. Meyer related an encounter with the engineer Culmann, who noted the similarity between the patterns of trabeculae in the upper femur and the stress trajectories (that indicate the directions of principal stress) in a crane that he was designing, as depicted in the now-famous drawing reproduced in Figure 3.4. Later, Wolff [274, 275] took this resemblance and formulated what has become known as *Wolff's law*: that there exists a mathematical correspondence between the stress trajectories in Culmann's crane and the trabecular structure in the femur, and that the density of bone is directly related to the density of the trajectories, corresponding to thicker bone where the stress is greatest. The existence of such a mathematical law has been questioned, however [28, 57], and today the term "Wolff's law" usually refers to a

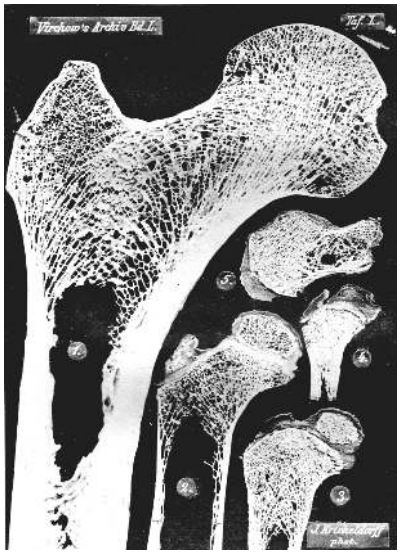

Fig. 3.3 *A photograph of trabeculae in the upper femur, reproduced from Wolff's* 1870 *paper* [274].

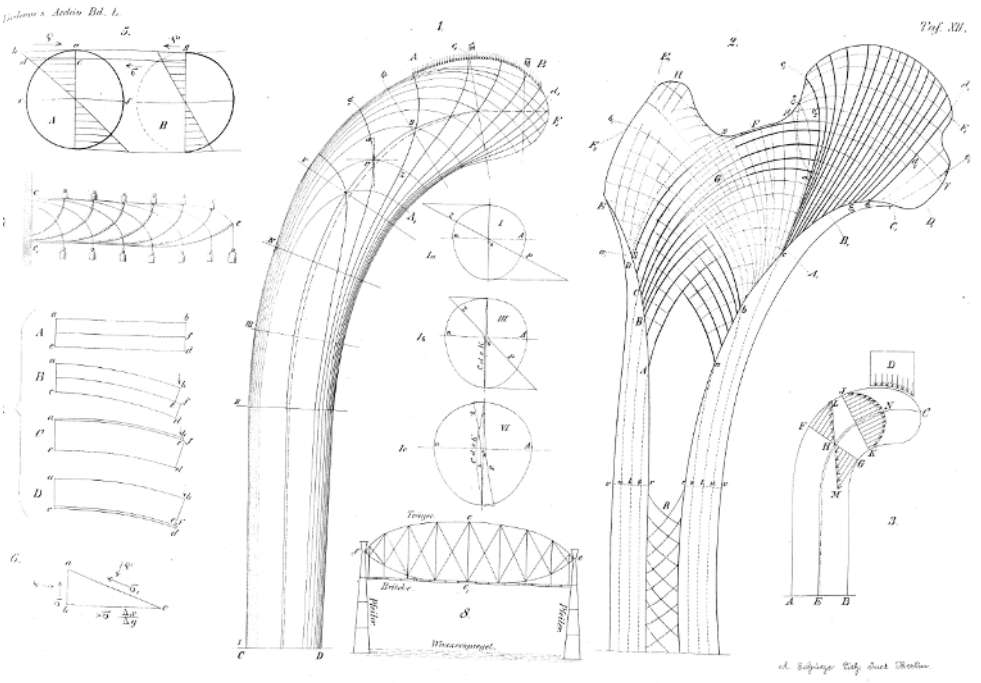

Fig. 3.4 *A drawing comparing stress trajectories in Culmann's crane (left) with the pattern of trabeculae in a human femur (right), as reproduced in Wolff's* 1870 *paper* [274].

general correspondence between the bone structure and past loading. While Wolff apparently thought originally that the bone structure had evolved such that it was strongest at the regions of higher stress [57], a different approach (which Wolff later adopted) was to assume that the bone tissue itself stiffened in response to loading, namely the *functional adaptation* principle promulgated by Roux [222]. This idea has now become part of Wolff's law.

Research into bone remodeling had been largely dormant since the late nineteenth century, until in the 1960s, contributions by Pauwels [213], Frost [95], and later Gjelsvik [108, 109] began the search for biomechanical explanations for the remodeling process. Pauwels decided that shear stresses stimulated the growth of collagen fibers, hydrostatic pressure gave rise to cartilage production, and bone was formed on these preexisting structures. On the other hand Frost thought that the cells would respond to *strain* fields rather than stress fields. Third, Gjelsvik devised a remodeling process which was based on the piezoelectric properties of bone tissue; as the stress fields changed, this changed the direction of the electrical polarization, which was assumed to govern the direction in which bone material is deposited or resorbed.

These analyses led to the first comprehensive mathematical theory for bone remodeling, namely, the *adaptive elasticity* theory of Cowin and coworkers mentioned previously. Using rigorous thermodynamical methods, Cowin and Hegedus [62] developed a nonlinear theory of elasticity using certain constitutive assumptions that were appropriate to describe bone remodeling. In this model, the material is considered to be a porous elastic solid, with a given zero-stress reference state regardless of its porosity. Then the porosity in the reference state is governed by the equation for the conservation of mass, which assumes that the mass of bone in a representative volume of material increases (or decreases) at a given rate. These equations were later specialized to the case of small-strain elasticity [124], since bone may be regarded as a linearly elastic material. Further simplifications were made for the case of small changes in porosity, and the conditions for stable solutions were identified; this led to simple solutions to the remodeling problem in a material of this type when the (homogeneous) stress or strain fields are changed instantaneously and kept at their new values. This theory was later adapted to the problem of how bone remodels in response to the insertion of a metallic pin into the medullary cavity of a bone [64].

Later—with the same application in mind—Cowin and Van Buskirk introduced a new theory of *surface* remodeling [65], where in contrast to the *internal* remodeling described previously, the remodeling process results in a change of shape of the bone. The theory is essentially an extension of linear elasticity in which the external surfaces of a body have a velocity which is proportional to the strain tensor. This work was later extended in order to investigate the change in thickness of the shaft of a long bone, modeled as a cylinder of the proposed material [61]. While Cowin and Van Buskirk's work was phenomenological and did not consider observed cell behavior, it was shown by Hart [122] that a simple constant cellular activity law was consistent with the model proposed by Cowin and Van Buskirk.

The preceding theories can be considered to be theories for *growth of bone* in the sense that mass is added to (or removed from) the system. Models for predicting the change in anisotropy of bone due to mechanical loads—which are in one sense a modern reformulation of Wolff's ideas—have been put forward, beginning with work by Cowin and coworkers [55, 63], who proposed a measure of the microstructure known as the *fabric tensor* and suggested an evolution equation for it that depended on the state of strain in the material. Further research into remodeling theories, including

some phenomenological models which consider other measures of loading than the strain and stress fields, is documented by Cowin [56] and by Hart [122].

3.5. Mixture Theory. In the introduction to this section we introduced mixture models, which enhanced the material modeling to include the effect of several phases: one notable example is the poroelastic model, which includes an elastic phase and a viscous fluid phase. Such models are also able to incorporate the effects of growth. In fact the concept of growth in these models is more intuitive, with the growth term which was so important in the open elastic systems described in section 3.3 becoming a term which describes the transfer of mass from (for instance) the fluid phase to the solid phase. We note that in order for residual stress to arise from the theory, an elastic component must form at least one of the phases in the mixture. In this section, we will not describe the derivations of the equations for mixture theory, since the details become quite technical, especially when applying thermodynamical principles. For this we refer the reader to, for example, [180, 11].

One of the first studies into the addition of growth effects into mixture theory was that of Humphrey and Rajagopal [147]. Their approach was based on the theory of evolving natural configurations, which models the apparent phenomenon that different components of the tissue will have different natural configurations (i.e., the state of the tissue once all stresses are relieved; the natural configuration in Figure 3.1 would be the state $\mathcal{B}_{\mathrm{g}}$). The physiological evidence for this is that newly produced tissue components may be stressed, but that their stress state may not match that of the existing surrounding tissue. Thus Humphrey and Rajagopal suggest that residual stress is due more to the differences between these "deposition stresses" than to incompatible growth patterns. In the model this assumption manifests itself by giving each phase in the mixture its own natural configuration.

However, determining these natural configurations is as much an open question as choosing the growth tensor $\boldsymbol{F}_{\mathrm{g}}$ in the single-species approach. Humphrey and Rajagopal postulate that each constituent would have a "preferred state" (not necessarily stress free), and also speculate that thermodynamical considerations would place limits on the permitted natural configurations. As is usual in mixture models, several simplifying assumptions need to be made to make the equations tractable; these notably include not allowing the elastic phases to move relative to the mixture as a whole.

As an example of this approach, Baek et al. [17] applied the theory to the development of brain aneurysms. Simplifying the geometry of the blood vessel to a cylindrical two-dimensional structure, they considered the tissue to have only two components, namely, collagen fibers aligned in two different directions. By specifying an initial local decrease in the mass of the tissue, the evolution of the vessel shape was determined (assuming a linear dependence between the constituent growth rate and the current stress field). Physiologically relevant results of aneurysm growth were obtained; however, the authors cautioned that further experimental data are required in order to validate the model.

Another way of simplifying the governing equations of a mixture model is by choosing simple constitutive relations for each phase. Araujo and McElwain [11, 12] take a two-phase model of a growing tumor, and choose the cell and fluid phases to be linearly elastic and inviscid, respectively. Furthermore, the growth and elastic parts of the deformation are separated, which in linear elasticity (as shown in section 3.4) corresponds to an additive decomposition of the infinitesimal strain tensor. The growth is chosen to be anisotropic; cells in the (spherical) tumor are conjectured

to divide in such a way that growth occurs in the direction of least stress. This anisotropic and inhomogeneous growth law gives rise to a residual stress field.

The aim of Loret and Simões [180] was to formulate the growth law for a growing tissue that was thermodynamically consistent. They reasoned that mixture theory would account for the mass increase of the tissue in terms of a transfer from the fluid phase. However, unlike the infinitesimal-strain theory of Araujo and McElwain, the authors used finite elasticity for the solid phase, and performed a decomposition of the deformation gradient, as described in section 3.3. This decomposition allowed them to separate the contributions of growth and mechanical deformation to the thermodynamically derived Clausius–Duhem inequality, thus motivating physically consistent growth laws. Garikipati et al. [106] developed a similar model with application to engineered tendons.

Klisch and coworkers [162, 163] applied mixture theory to cartilage, which is a tissue composed mostly of extracellular matrix. As described in section 2.4, the main components of this tissue are a fluid matrix, in which are distributed proteoglycan molecules, and collagen fibers. The authors treat these three constituents as the three phases of a mixture model for cartilage. The deformation gradients of the two solid phases (proteoglycans and collagen) are assumed to be the same, but their decomposition into growth and elastic parts (according to the theory of section 3.3) are, in general, different. This is philosophically equivalent to the "natural configurations" approach of Humphrey and Rajagopal described above. Thus a growth process in which only proteoglycan is produced can be analyzed separately to a collagen-production process (setting the growth tensor of the nongrowing component to be the identity tensor). Representative but phenomenological constitutive relations are chosen, and in the second paper the theory is specialized to infinitesimal strains in order to produce numerical results for canonical cartilage-growth examples.

Finally we mention the more recent work of Ateshian [16]. This study included a consideration of electrical charge distribution within the mixture, allowing an evaluation of how osmotic pressures (due to the inhomogeneous distribution of proteoglycan molecules) contribute to the overall residual stress field in the mixture. Additionally, if the mixture contains interfaces over which certain field variables (e.g., void fraction) were discontinuous, then interface conditions would be needed, which are derived from the basic conservation laws in the mixture. Such interface conditions are included in Ateshian's model, and can account for surface growth as described briefly in section 3.4.

3.6. Postscript. In section 3 we have examined various continuum models for growth in tissues. We have concentrated on elastic models, as an elastic component is essential for residual stress to appear. This elastic component may be a single-species model, like the elastic theories of section 3.3, or may appear in a multicomponent model such as the mixture theories of section 3.5.

The mixture approach may be seen as a generalization of the single-species models, and also as more biologically relevant due to the explicit consideration of the different components of biological tissues. In a sense, mixture theory is a form of homogenization, which forms a macroscopic continuum theory from the material's behavior at the microscopic level. Traditionally, homogenization (or upscaling, or averaging) develops a continuum model by explicitly solving the microscopic equations and averaging the result to form a macroscopic theory. This is in contrast to the mixture approach, where the microscopic equations tend not to be solved.

In the next section we will look at growth models at the microscopic level, considering specifically tissues which are mostly ensembles of cells.

4. Modeling Growth at the Cell Level. In section 3 we have studied a number of models which treat the tissue (largely) as a continuum. For certain types of tissue this is an acceptable hypothesis. For instance, in connective tissues (see section 2) the mechanical properties of the material are largely those of the ECM of which the tissue is comprised, the cells being dilutely dispersed throughout the tissue. However, in epithelial tissues and other instances in which the cells are packed closely together, the properties of the material emerge from the interactions between neighboring cells in the tissue, and are much harder to elucidate. In such circumstances an *agent-based* model is often much better suited to the task of analyzing the overall deformation of the tissue.

In such models, individual cells are modeled separately, and their properties (e.g., shape, chemical, kinematic) are governed by interactions with other cells in the model. The large-scale behavior of the tissue is analyzed by aggregating the responses of each of the cells, giving rise to characteristic properties of the tissue that would be hard to predict when setting up a continuum model. For instance, cell rearrangement is very simple to incorporate into an agent-based model, but the result of this rearrangement on a large scale is much more complicated: most likely a combination of viscous and plastic effects.

Such cell-based models have been used widely to model the behavior of cell ensembles. These include two-dimensional epithelial monolayers (for instance, in embryos [35] and in the colon [187]), multicell spheroids (i.e., early stage tumors) [227], and the slug stage of the slime mould *Dictyostelium discoideum* [68]. One particular achievement is the validation of the differential adhesion hypothesis in cell sorting: the separation of a mixture of two types of cell discussed in section 2.5. Agent-based modeling has helped to verify the hypothesis that the differing strengths of adhesion molecules on the surface of each cell is a contributing factor [240]. Such a result would be hard to obtain using a continuum model due to the inherently cell-based nature of the hypothesis.

Ease of model validation is another strength of cell-based models. Continuum models do not provide any information about the behavior of individual cells in the tissue, so comparison with experimental data is quite difficult. In comparison, agent-based models specifically model the cells and as such it is a simple matter to compare the results of a simulation to real data from in vivo and in vitro experiments. Due to the simplicity of modifying behavioral rules for individual cells, it is also easy to use agent-based models to test hypotheses on a population of cells [101].

However, agent-based models do have their drawbacks. Simulations must be performed using computational methods [237], and as such the results obtained are often limited by the available computational power. In spite of the vast growth in computing power over the last few decades, some simplification of the problem is inevitable: one may limit the number of cells in a simulation and consider more complex interactions, or take a larger cell ensemble and simplify the interaction rules; in either case the effort required to simulate the model is reduced.

Additionally, one of the key advantages of the continuum models of section 3 is that they are (largely) equation based and, as such, key parameters of the problem can often be identified using analytical mathematical techniques. This is much harder to achieve using cell-based models, as the key parameters are "hidden" inside the multitude of interaction rules between individual cells.

Nevertheless, the advantages of cell-based modeling outweigh the disadvantages for small cell ensembles. This section will review the three main classes of models that have appeared in the literature. The first of these, the class of *cellular automaton*

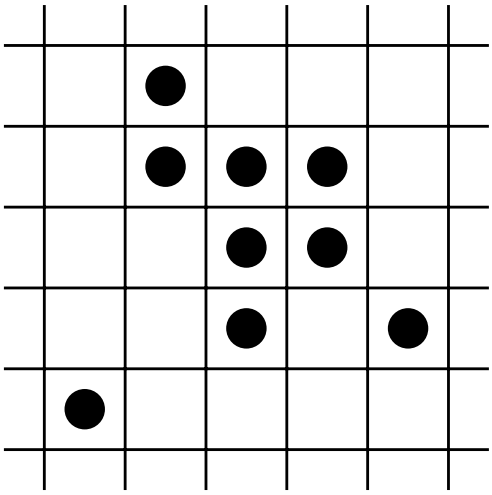

Fig. 4.1 *A simple cellular automaton model. Some lattice sites are occupied by a cell (denoted by a black dot); others are sites that cells can move into at a subsequent time step.*

models, is the simplest, and has been employed for many years on biological problems. Models in this class usually assume that cells are arranged in a grid pattern.

The second class of models which we will consider are known as *off-lattice* models. These do not confine the cells to be arranged in any pattern, but allow them to take any position in a predefined domain. We can subdivide this class into two subclasses. The first of these can be named *overlapping sphere* models, since in this setup cells are modeled as spheres (or ellipsoids in some cases), which are allowed to overlap, which is a simplification of their deformation on contact. The second off-lattice class of models that we consider consists of those known as the *center dynamics tessellation* models. In this formulation cell centers are defined as points in space. The configuration of points sets up a unique Voronoi tessellation, and the cells are identified with the polygons (or polyhedra) in the tessellation. The common property of these two subclasses is that the motion of the cells is determined by interactions between neighboring cells, often given in terms of the distance between the cell centers.

The third class of models which we will present are the *vertex dynamics tessellation* models. In these models the tissue is a polygonal tessellation, but in contrast to the center dynamics models, the emphasis in these models is on how the vertices in the tessellation move, rather than the cell centers themselves.

Finally in section 4.4 we will evaluate these cell models and how well suited they are to model growth in cell ensembles.

4.1. Cellular Automata. As stated above, perhaps the simplest models that can be used to simulate biological processes at the cell level are *cellular automaton* models. In these models the region of space being modeled is subdivided into a number of *lattice sites*, whose properties are tracked as the simulated time progresses. For models of cell population, the main property to be tracked is whether the lattice site is occupied by a cell or not. A square lattice is shown in Figure 4.1 as an example.

Cellular automata were introduced by von Neumann and Ulam (see von Neumann [262]) in order to examine self-reproduction in discrete systems, and have since become commonplace in many other disciplines. A well-known example of a cellular

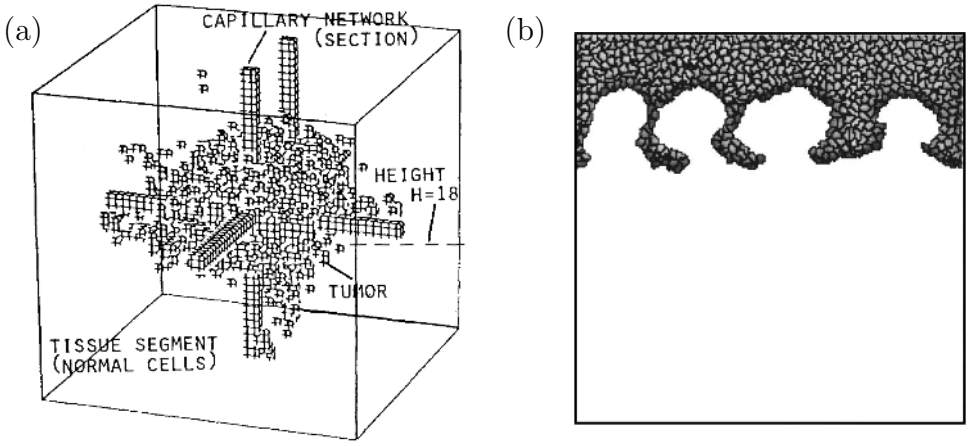

Fig. 4.2 *Two examples of cellular automaton models.* (a) *From Düchting and Vogelsaenger* [85], *growth of tumor cells around a capillary network.* (b) *From Turner and Sherratt* [254], *invasion of "fingers" of tumor cells into the ECM, using the extended Potts model. Both images reproduced with permission.*

automaton model is Conway's *Game of Life* [104], which entered the public consciousness due to its ability to exhibit complex behavior from a few simple rules. One of the main biological applications of cellular automata is in models of tumor growth [194] such as the early model of Düchting and Vogelsaenger [85], which will serve as our archetypal cellular automaton model. In this model (depicted in Figure 4.2(a)) the two types of cells which may occupy a lattice site are normal cells and tumor cells. Each cell is assigned a position within the cell cycle (see section 2.2), which will vary as the simulated time increases. At each discrete time step, a cell will undergo mitosis in stage M if the conditions are favorable. In mitosis of a normal cell, the cell looks in the six directions comprising the (three-dimensional) Cartesian basis of the lattice, and determines whether a free space exists in any of these directions. If so, all the cells in the chosen direction are shifted outwards by one cell and a daughter cell is placed in the freed space. If not, the cell enters the resting stage G0. Tumor cells do not obey this rule, and undergo unrestricted growth, unless they are placed more than a certain number of cells from a nutrient source, in which case they enter a necrotic state.

This simple cellular automaton model has a number of shortcomings, apart from the small space that was simulated (due to the computational facilities available at the time). First, the imposition of a cubic lattice can introduce symmetries into the solution which are not justified physically. Second, cells are restricted to a particular lattice site: changes of shape and size are assumed to be irrelevant. Finally, the mechanical properties of each cell are completely ignored.

Despite these shortcomings such models remain popular and have been extended to include numerous biological effects. The basic structure is always to allow each cell to make a decision on how it will behave at each time step. These decisions include whether to proliferate, die, move, or mutate. The decision may be deterministic or stochastic, and may depend on external cues such as the number of neighbors or the concentration of messenger chemicals. The ability to study mutation and natural

selection (for example due to acidosis [236]) is one of the attractions of such models. However, despite the biological complexity of these models, the physical or mechanical aspects of them are still rudimentary.

Some of the more recent models have attempted to address aspects of this problem while still adhering to a cellular automaton framework. Hawboldt et al. [123], in their model of cell growth on the surface of a sphere (a *microcarrier*), dispense with the Cartesian grid by considering an irregular lattice where each cell site is assumed to have five neighbors. The topology of the lattice is determined by a neighbor table, where all sites are numbered and the neighbors of each site are tallied. This allows for an algorithmic approach to determining which sites are occupied by cells, with the exact structure of the lattice unimportant. This unstructured lattice removes the artificial anisotropy due to the Cartesian lattice, but the lattice is still fixed in space, with sites either occupied or free, and there is no treatment of mechanics.

Some attempts have been made to include the effects of mechanics on cellular automaton models by including an ad hoc measure of the pressure, and inhibiting cell division if this pressure is too great. Sometimes, as in Kansal et al. [159], pressure is simply taken to be a known function of position within a tumor (increasing towards the center). In other models the local value of the cell density is taken as an indirect measure of the local pressure [215, 72].

While in most cellular automaton models each lattice point consists of one (or more) biological cells, in the (extended) Potts model approach [116] each biological cell is made up of several lattice points and the movement of each cell is determined by some form of energy minimization. This allows changes in cell shape and size to be modeled, and effects such as cell-membrane tension, cell–cell and cell–matrix adhesion, chemotaxis, etc., to be included in a rudimentary way. The Potts model was originally developed in order to simulate cell sorting by minimizing the total surface energy of an aggregate of cells, but has since been used by Turner and Sherratt [254] to model the invasion of a tumor through a region of extracellular matrix (see Figure 4.2(b)). Some of the mechanical properties of cells can be modeled in the extended Potts model by including an additional ad hoc mechanical term in the expression for the total energy, which has the effect of prescribing to each cell a target volume to which it would relax in the absence of external forces.

While the preceding examples have shown that it is possible to resolve some of the difficulties of cellular automaton models while keeping their basic simplicity, none have satisfactorily dealt with all of the issues, and in particular the implementation of stress effects is a major difficulty and has not been achieved in a systematic or theoretically satisfactory way. Many researchers have therefore chosen to look at other forms of agent-based models, such as the off-lattice models described below.

4.2. Off-Lattice Models. In off-lattice models, the requirement that cells are restricted to a predetermined lattice is removed. As such, the state of the cell ensemble is entirely determined by the position of the cells. Interactions between cells give rise to forces which alter the cells' positions, thus deforming the tissue. In this manner the limitations of the cellular automaton models (described above) are dispensed with and a more realistic model should result. Some applications of this method include intestinal epithelia [187], stratified epithelia [195], tumor spheroids [227], and slime mould migration [68]. Figure 4.3 shows four examples of off-lattice models in action.

We will now describe a canonical center dynamics model for a cell ensemble. This will contain most of the salient features of the models appearing in the literature; we will describe the important differences in detail later.

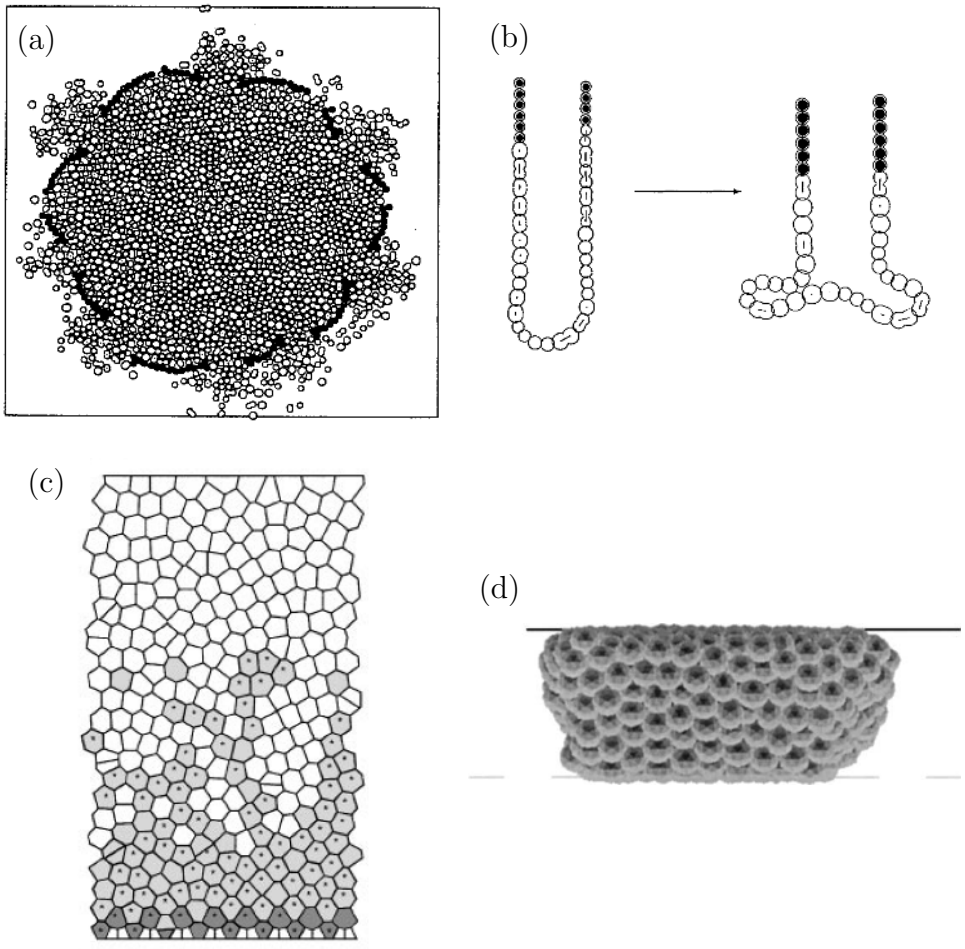

Fig. 4.3 *Examples of off-lattice models in the literature.* (a) *A growing population of tumor cells (white) overcomes an epithelial barrier (black), from Drasdo et al.* [79]. (b) *Cell division in a growing colonic crypt leads to buckling of the structure, from Drasdo and Loeffler* [80]. (c) *A population of proliferating colonic crypt cells, from the Voronoi tessellation model of Meineke et al.* [187]. (d) *A population of slime mold cells is compressed between two plates, from Palsson* [209]. *All images reproduced with permission.*

Our canonical model describes a collection of cells distributed on a three-dimensional domain. The model characterizes these cells as spheres that are allowed to overlap, and as such (if the radii of the cells are kept constant) the only parameters characterizing the cell ensemble are the positions of the cell centers. Cells that are overlapping are assumed to be in contact, and as such they experience a repulsive force. The degree of repulsion is governed by the amount of overlap, and thus the force can be written as a function of the cells' positions. The aggregation of all the forces on a particle will result in a differential equation of motion for the particle (see section 4.2.1) with the force dependent on the positions of its neighbors. A system of equations for each particle can thus be established. This system may be solved

numerically by discretizing the time domain, with the result that at each time step the state of the system, governed by the cell positions, is updated. The cell ensemble's deformation may therefore be analyzed as a function of time.

We will review the minor differences between incarnations of this theory in section 4.2.1, but we will first mention a closely related approach, which treats the cells not as overlapping spheres but as a Voronoi tessellation. This latter approach was developed to take advantage of the fact (as noted in section 2) that epithelial tissues may be visualized as tessellations of polygons. Once again the tissue is characterized purely by the positions of the cell centers (justifying the model's classification as a center dynamics model), but in the Voronoi model the cells are the polyhedra formed from the cell centers in a Voronoi tessellation of the domain.[9] In the Voronoi model the forces on a cell are again determined by the distance between neighboring cell centers, and may also depend on the size of the Voronoi cell. Figure 4.4 depicts the same collection of cells as they would be modeled in both the overlapping spheres model (assuming a constant cell radius), and the center dynamics tessellation model. This comparison shows that a common property of both models is that the positions of the cells are primarily determined by the cell centers.

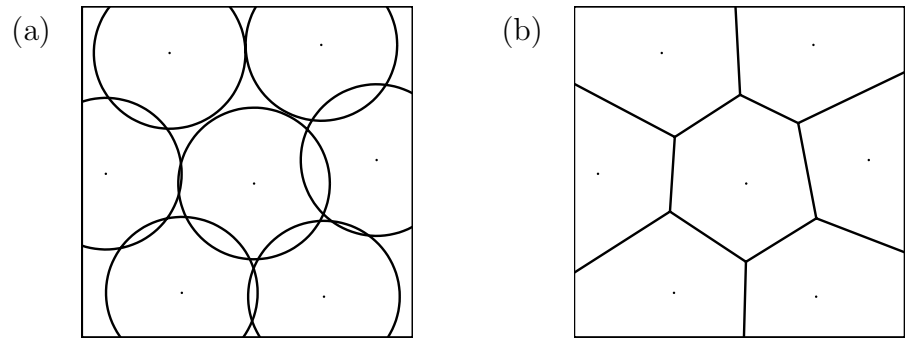

Fig. 4.4 *A depiction of the same configuration of cells in* (a) *the overlapping spheres model, and* (b) *the center dynamics tessellation model.*

Although the Voronoi model is more computationally expensive it has the attraction that the pictures look more like real tissues. For these reasons the results of even the overlapping spheres models are sometimes visualized as a Voronoi tessellation. As a further move towards realism, a recent study extended the Voronoi model to account for curved cell boundaries [24].

In section 4.2.1 we will review the various interaction rules that have been used in center dynamics models. Following this, in section 4.2.2 we will analyze how growth (i.e., mitosis) may be incorporated into the model. Finally we will evaluate the various aspects of off-lattice models and determine their effectiveness in modeling collections of cells.

[9] A two-dimensional Voronoi tessellation takes a collection of points on a plane and tessellates the plane with polygons; each polygon is the set of all points that are closer to a particular cell center than any other. This also holds for three dimensions where a tessellation of polyhedra is formed.

4.2.1. Cell Interactions. The key aspect of off-lattice modeling for our purposes is the interaction between cells, because it is through these interactions that the mechanical property of the tissue manifests itself.

Some models of cells' influence on each other are rather simplistic. For example, cell interactions are sometimes described as collisions [224, 264]. Bodenstein's model [25] (later enhanced and released as the proprietary package *Nudge++* [26]) formulated an algorithm for the motion of cells where, at each time step, if a (circular) cell was moved such that it overlapped with a second cell, the latter was displaced at the next time step by an amount proportional to the degree of overlap. This is also the behavior of Grabe and Neuber's model [115], which also included an attractive displacement if the separation between cells was positive but small. While the behavior of these models can be realistic, it is not based on mechanical principles and thus has less physical relevance.

Most other models approach the problem from a more mechanistic point of view. In this formulation, if the position of the center of cell i is given by $\boldsymbol{r}_i(t)$, the equation of motion of the center is given by

$$m_i \frac{\mathrm{d}^2 \boldsymbol{r}_i}{\mathrm{d}t^2} = \boldsymbol{F}_i - \gamma_i \frac{\mathrm{d}\boldsymbol{r}_i}{\mathrm{d}t} - \sum_j \gamma_{ij} \left(\frac{\mathrm{d}\boldsymbol{r}_i}{\mathrm{d}t} - \frac{\mathrm{d}\boldsymbol{r}_j}{\mathrm{d}t} \right), \tag{4.1}$$

where m_i is the mass of the cell, γ_i is the drag coefficient between the cell and the intercellular medium, γ_{ij} is the drag coefficient between cells i and j, and $\boldsymbol{F}_i$ is the net (nondrag) force on the cell. In most applications, the γ_{ij} are chosen to be zero (but not always; see [130]) and γ_i is presumed to be a scalar quantity (theoretically the drag could be nonisotropic, in which case γ_i is a second-rank tensor). A common expression for γ_i is the Stokes relation for the drag on a sphere of radius R_i in a medium of viscosity η [227], given by

$$\gamma_i = 6\pi\eta R_i. \tag{4.2}$$

Usually the overdamped limit is taken in which the inertia of the cells is neglected, to leave

$$\gamma_i \frac{\mathrm{d}\boldsymbol{r}_i}{\mathrm{d}t} = \boldsymbol{F}_i. \tag{4.3}$$

Solutions to this system can be found by discretizing time with a time step Δt:

$$\gamma_i \frac{\boldsymbol{r}_i(t_{n+1}) - \boldsymbol{r}_i(t_n)}{\Delta t} = \boldsymbol{F}_i(t_n). \tag{4.4}$$

The forces are calculated at each time step t_n, and the equation will then give us the positions at time t_{n+1}.

The main difference between the models that we will consider in this section is the form they choose for the force $\boldsymbol{F}_i$. We will concentrate on the forces that arise due to interactions between cells, although other factors have been included by many authors in the definition of the force.[10] Consider cell i, and let $j_1, j_2, \ldots, j_k$ be its nearest neighbors. Whether two cells are designated as neighbors depends on the model: for the center dynamics tessellation models, two cells are considered neighbors

[10] These include the influence of a substrate on which the collection of cells are placed [80], and chemical gradients in the tissue causing the cells to move in one particular direction [241].

if they share a boundary; in the overlapping spheres models it is generally the case that two cells are neighbors if they either overlap or are separated by less than a given distance. Then the total interaction force is given by

$$\boldsymbol{F}_i = \sum_{n=1}^{k} \boldsymbol{F}_{i,j_n}, \tag{4.5}$$

where $\boldsymbol{F}_{i,j}$ is the interaction force between cells i and j. In the cell models this force is always directed along a line linking the two cell centers, so that if $r_{i,j} = |\boldsymbol{r}_i - \boldsymbol{r}_j|$ is the distance between cell centers and

$$\boldsymbol{n}_{i,j} = \frac{\boldsymbol{r}_j - \boldsymbol{r}_i}{r_{i,j}} \tag{4.6}$$

is the unit vector in the direction from cell i to cell j, we can write

$$\boldsymbol{F}_i = \sum_{n=1}^{k} F_{i,j_n} \boldsymbol{n}_{i,j_n}. \tag{4.7}$$

It is in developing an expression for the scalar interaction force $F_{i,j}$ that most off-lattice models differ.

Some authors, especially Drasdo and coworkers [79, 78, 102], prefer to consider an interaction *potential* $W_{i,j}$. This is related to the force $F_{i,j}$ by the relation

$$F_{i,j} = \frac{\partial W_{i,j}}{\partial r_{i,j}}. \tag{4.8}$$

This approach comes into its own when the equation of motion (4.3) is modified by the addition of a stochastic term on the right-hand side. This models the observed behavior of isolated cells undergoing a random walk. The system of equations, thus modified (in which case they are often referred to as Langevin-type equations), can be solved by discretization as before, but if we have a formulation in terms of potentials, the Metropolis algorithm can be used. This is a Monte Carlo approach which was originally applied to a system of interacting molecules [190]. At each time step we choose a cell and make a trial displacement. If this trial displacement causes the total energy (or potential) of the system to decrease, the trial is accepted and we proceed to the next time step. If the energy is increased by an amount $\Delta W > 0$, the trial is accepted with probability $\mathrm{e}^{-\Delta W/f}$. In this expression, f is an effective energy and may be viewed as equivalent to the expression $k_{\mathrm{B}}T$ which is encountered in fluids[11] [22]. If D is a diffusion coefficient for the cells, then f may be related to γ_i by $f = \gamma_i D$. Drasdo et al. [76] compared the results of a Metropolis simulation with the numerical solution of the Langevin system of equations and found them to be in agreement, thus justifying the use of the method for this application.[12]

The interaction forces or potentials between cells are usually characterized by two quantities, namely, the difference between the separation of the cell centers and the equilibrium spacing (which in the case of overlapping spheres is the separation between the cells' surfaces), and the contact area between cells. In the overlapping

[11] Here k_{B} is the Boltzmann constant and T is the absolute temperature of the fluid.

[12] The Potts model, mentioned earlier in connection with cellular automaton methods, is also a Monte Carlo method of this type, and is widely used in cell-based simulations [116, 226].

spheres case, the separation and contact area are depicted in Figure 4.5. Note that the separation is negative when the spheres are overlapping, and that the contact area is a circle in the three-dimensional case where cells are spheres. Where cells are represented by tessellated polyhedra, the contact area is simply the area of the polyhedron face which lies between the cells.

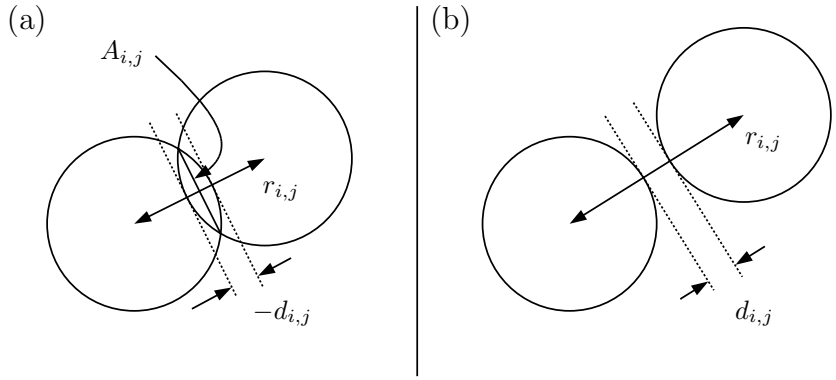

Fig. 4.5 *The characteristic properties of neighboring cells:* (a) *overlapping cells,* (b) *nonoverlapping cells. The quantities are the separation of cell centers, $r_{i,j}$; the separation of cell surfaces, $d_{i,j}$ (negative in the overlapping case); and the contact area, $A_{i,j}$ (only in the overlapping case).*

The two physical properties of cells that are modeled by the interaction forces are *adhesion*, caused by adhesion molecules on the cell's outer surface, and *repulsion*, caused by the cell's resistance to deformation. All models include an element of repulsion, while the influence of adhesion in the models vary. Some models assume that adhesion only occurs if the cells are in contact (or have negative separation) while the other models prescribe an attractive force between cells which are not in contact. While this may sound strange we must remember that by "not in contact" we mean simply that the cells are separated by a distance greater than their equilibrium separation.

We will now describe the interaction forces that different authors have employed previously. Many of these are summarized in Table 4.1. The diagrams are illustrative only; in particular, where the contact area is used, we have supposed that the cells are of equal size for the purposes of these plots.

The simplest type of interaction between cells is a linear spring, and this is the assumption of Drasdo and Loeffler [80] in their model of intestinal crypts (see Figure 4.3(b)). The same interaction between individual cells was used in the Voronoi polygon-based model of Meineke et al. [187] (see Figure 4.3(c)) and the overlapping spheres model of Walker et al. [263]. In the latter two papers only cells which are bonded to each other experience an adhesive force. In some ways this corresponds to a "cutoff" for attraction, as shown in Table 4.1. A slightly more detailed interaction force was employed by Stekel et al. [241]. Their repulsive force was proportional to the contact area, while the attractive force was again linear until some critical separation, when it reduced to zero.

Palsson and Othmer [210, 209], in their model of an aggregation of slime mold cells (see Figure 4.3(d)), also preferred a nonlinear force acting between the (ellipsoidal)

Table 4.1 *Force separation and potential separation diagrams for some off-lattice models.*

Model	Force separation	Potential separation
Linear spring [80, 187, 263]	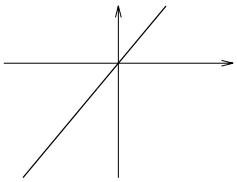	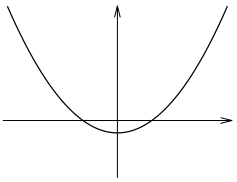
Linear spring with cutoff	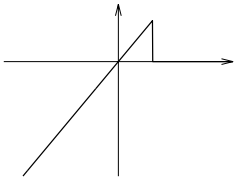	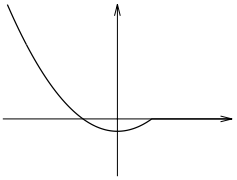
Repulsion $\propto$ contact area [241]	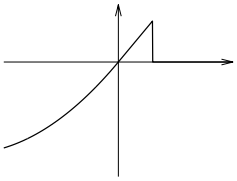	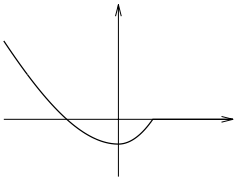
Palsson's model [209]	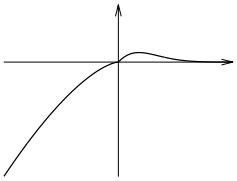	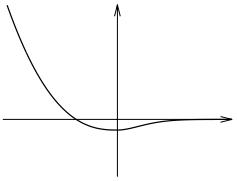
Drasdo's model [79, 74, 75]	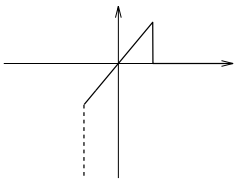	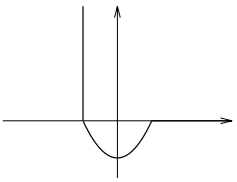
Adhesion and Hertz repulsion [227]	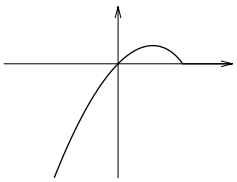	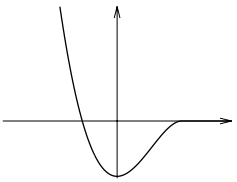

cells. This force was such that touching cells had no interaction force; overlapping cells repelled each other and neighboring cells exerted an empirical attractive force on each other that had a maximum at some critical separation distance, and decreased to zero as the separation decreased to zero or increased to infinity. This model also assumed that the ellipsoids could deform viscoelastically, the three axes being modeled as spring–dashpot systems. A more complicated model for this cell aggregate was given by Dallon and Othmer [68], using the same basic principles, but where the repulsive force emerged by considering the deformation of the viscoelastic ellipsoid axes.

As mentioned previously, Drasdo and coworkers [79, 74, 75, 77] solved their equations of motion by considering a Monte Carlo approach which was based on the interaction potential. Apart from the advantages in terms of computation, this approach also allows for cells to be rigid, which is difficult to prescribe if the force approach is used. The rigidity is encoded in the method by prescribing the interaction potential to be infinite if the overlap becomes too great. Apart from this simplistic repulsion mechanism, their model only accounted for the attraction due to cell adhesion molecules on the cells' surfaces. This was achieved by prescribing the interaction potential to be zero for a separation greater than some critical parameter. The remaining section of the potential was given by some function, which was usually taken to be (a negative) constant, although a parabolic well was also chosen, which is depicted in Table 4.1. Corresponding models for epithelial sheets (or strings) of cells replace the zero potential for far-apart cells by infinity, which is an artificial mechanism of keeping the cells in contact.[13] More recently, Drasdo and Höhme [78] employed a more physically realistic interaction potential, known as the Johnson–Kendall–Roberts (JKR) model [49]. This describes the interaction between two elastic adhesive spheres and includes an element of hysteresis due to the adhesive properties of the cell.

Finally there are those models in which there is only an interaction force when cells are in contact. Galle et al. [102], in their model of an aggregate of cells, assumed that the interaction potential was given by combining three potentials, namely, an adhesion potential which was proportional to the contact area, a compression potential which modeled the resistance of cells to compression, and a repulsion potential which modeled the resistance of cells to deformation by Hertz's theory of elastic contact. Schaller and Meyer-Hermann [227], while writing the interaction in terms of forces rather than potentials, also assume that repulsion is given by Hertz's theory. However, they model adhesion by assuming the *force* is proportional to the contact area, rather than the potential, as was proposed by Galle et al. In a potential-based formulation, Drasdo et al. [76] assumed that cells had a rigid core, together with an interaction potential whose attractive part was proportional to the contact area and a repulsion part that was quadratic in the separation. Höhme et al. [130] used a similar interaction potential but where the repulsion was Hertzian, without a rigid core.

Clearly, researchers have used a wide variety of different approaches to model interactions between cells in off-lattice models. However, do the various interaction laws have a noticeable effect on the macroscale behavior of the tissue? This is the key question regarding these models, and one which we will analyze in section 4.2.3, following a discussion on growth in off-lattice models.

[13] This assumption is often made in one-dimensional atomistic models, where the role of the cells is taken by atoms and the potential is an interatomic potential well such as the Lennard–Jones potential. The modified potential tends to infinity as the separation increases so that the line of atoms remains continuous. This assumption can be justified: see [208], which derives a one-dimensional model from a two-dimensional lattice undergoing shear.

4.2.2. Cell Division and Growth. Recall from section 2.2 that there are two main features of the cell division process. The first of these is the growth of a cell from a given volume to twice that volume, and the second is the actual division of an enlarged cell into two cells of the original volume. We can categorize cell division models according to how these two phenomena are modeled. In particular we consider two basic types of mitotic steps (the second phenomenon described above). Of these two types, the first, which we denote mechanism 1, involves a daughter cell being placed instantaneously next to the mother cell. Mechanism 2 was introduced by Drasdo et al. and is a more faithful model for cell division as observed experimentally. We will now investigate in more detail the models which employ each division mechanism.

Mechanism 1 is perhaps the simplest model of cell division, and involves a daughter cell being placed at a certain distance from the mother cell instantaneously. This mechanism was employed by Bodenstein [25]. In this model the position of the daughter cell was assigned randomly, with subsequent cell–cell interactions due to overlapping determining whether this position was reasonable. This model also assumed that both mother and daughter cells would be of the same size, with no expansion of the mother cell occurring before division. Stekel et al. [241] also assumed this model of division, but the angle of placement was biased so that cells divided away from the stem cells that were considered in the model. The later model of Bodenstein and Stern [26] allowed a cell to double in size by fixed volume increments during the G1 phase, and formed two daughter cells instantaneously, both half the size of the mother cell.

Introduced by Drasdo et al. [79], mechanism 2 is a more physically realistic model for cell division, and can be seen in practice in Figure 4.3(a),(b). This model considered the cell cycle as consisting only of the mitotic phase (M) and interphase (I). The reason for this is that the three phases comprising the interphase are indistinguishable from the point of view of the mechanics of cell division, the difference being internal to the cell. The modeling of the process, as depicted in Figure 4.6, assumed that during the interphase, the volume of the cell increased from a given initial value (corresponding to a radius R_0) to twice the value (corresponding to a radius $R_{\max} = 2^{1/3}R_0$ in three dimensions). Then, during the mitotic phase, the cell forms a dumbbell shape as shown in Figure 4.6(c); the centers of the spheres forming the dumbbell move apart, while the radii R of the spheres decrease to keep the overall volume constant. When the spheres are finally separated with $d = 2R_0$, the mitotic phase is finished and the cells reenter state I. This model is not wholly faithful to the cell cycle, because as mentioned previously this model proceeds by *trials* (small increases in cell volume, or separation d) which succeed if the energy is reduced (or succeed with a certain probability if the energy is increased by a little). The growth phase in I and the parting phase in M are both structured as these trials, whereas physically one would expect that once a cell has left phase G1, growth and cytokinesis are certain to occur. Nevertheless, this mechanism remains one of the most realistic yet relatively simple in the literature. It is also to be noted that the direction of cell division is not specified; however, all cells have a chance of undergoing a rotation trial, which again will succeed if the energy of the system is lowered.

The division mechanism used in Schaller and Meyer-Hermann's analysis [227] is a hybrid of mechanisms 1 and 2. Cell expansion occurs in the G1 phase, with an amalgamated S/G2 phase inserted before division occurs in the M phase. In this stage cell centers are instantaneously placed a certain distance apart, with a corresponding decrease in cell radius to keep the partly divided cell at the same volume. Further parting of the cell centers is achieved by now considering the cells as separate, while

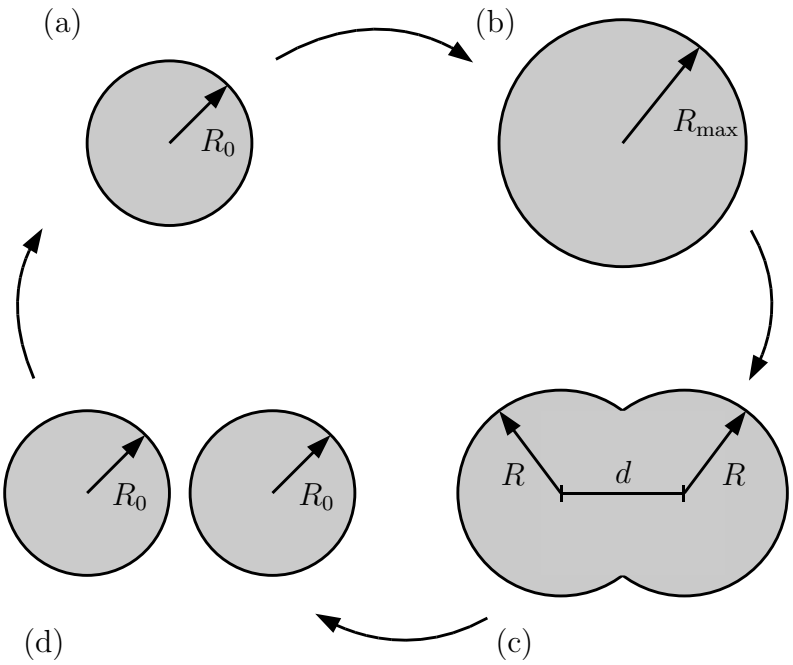

Fig. 4.6 *The mitosis process as portrayed in the model of Drasdo et al.*

the radii are decreased correspondingly until the cells are far enough apart to be treated independently.

In general, cell division in the center dynamics tessellation models can be considered as a specialization of mechanism 1. By splitting the cell center instantaneously into two centers and placing them at a certain distance from each other, a new membrane between the cell centers is automatically introduced as part of the Voronoi tessellation process. In the model of Meineke et al. [187], cells divide according to their position in the cell cycle, with the cell center being displaced in a random direction. The daughter cells rearrange later if the chosen direction turns out to be energetically unfavorable. This is in contrast to Honda et al. [138], where the direction of the cell center's division is chosen parallel to the long axis of the cell, which is found by analyzing the shape of the cell and identifying the direction in which the cell is longest.

In section 4.2.3 we will evaluate the various aspects of off-lattice modeling, including the question of whether using the more realistic cell division mechanism (mechanism 2) has a noticeable effect on the large-scale dynamics of the cell population.

4.2.3. Evaluation. The preceding sections have given an overview of the wide range of problems that have been studied using off-lattice models, and the variations in their implementation. What is less clear is the importance of these various modifications of the underlying theory, and which variation should be used for a given biological problem. We hope that this section will at least partly answer these issues.

Perhaps the most obvious question to ask regarding the different off-lattice models is whether the form of the cell–cell interaction, as depicted in Table 4.1, is of any

importance. After all, the profiles are all qualitatively similar, with a repulsive profile if cells are too close and an attractive profile for detached but neighboring cells. Thus we should not expect the qualitative large-scale behavior of the cell ensemble to change on varying the exact form of the interaction law. Indeed, recent simulations comparing these models indicate that the bulk behavior is broadly similar for all these force laws, although there can be problems with stability if the repulsion is not strong enough as cells approach each other [212] (for example, with a linear law, the attraction from next-nearest neighbors can overcome the repulsion from nearest neighbors leading to an "implosion"; see Figure 4.7).

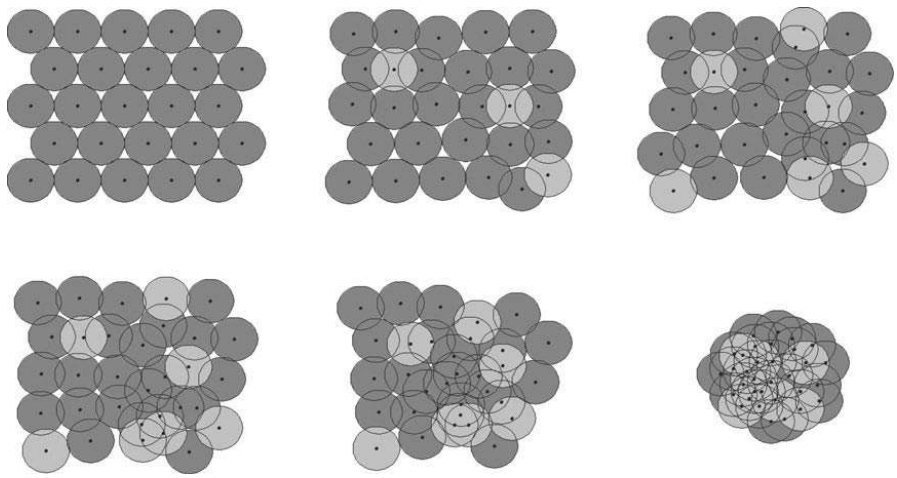

Fig. 4.7 *A simulation of a growing population of cells modeled by the overlapping sphere method. The birth of cells (light gray) leads to a nonphysical "implosion" solution as attractions from next-nearest neighbors overcome repulsion from nearest neighbors. Figure reproduced from Pathmanathan et al.* [212] *with permission.*

However, accurate models of cell–cell interactions do have their place: on the cell scale. Different amounts of overlap correspond to different degrees of cell deformation, and this may become important if cell mechanotransduction (the influence of cell deformation on intracellular signaling) is taken into account, as this could play a key role in the mitotic rate of a particular cell. Thus the overall growth rate of a growing cell colony may be affected by a different interaction law, even if the bulk mechanical response remains largely unaffected. We should note here that only simple mechanotransductive effects are incorporated in the cited models. For instance, the Metropolis simulations of Drasdo et al. assert that cells only undergo a division trial if the cells are sufficiently separated. As biological understanding increases, we believe that there is scope to expand this mechanotransduction modeling within the off-lattice framework.

In a similar manner to the different interaction laws, one could ask whether the various cell division mechanisms have an effect on the bulk growth properties. This is a question that has not received much interest in the literature. Drasdo et al. [76] compared mechanism 2 as depicted in Figure 4.6 to a slightly modified version, where no expansion occurred before division, and where the dividing cells were considered

as two completely overlapping spheres whose center-to-center distance increased from zero until they were fully separated. No great qualitative difference was observed between the large-scale simulations of cells employing these two mechanisms for mitosis. However, to our knowledge no one has critically compared mechanisms 1 and 2. We hypothesize that allowing a gradual separation of cell centers, as in mechanism 2, would provide a smoother response, as the orientation of the dividing "dumbbells" would be allowed to vary during the process, whereas in mechanism 1 the instantaneous placement of the daughter cell may not be in an energetically favorable position, leading to a sudden rearrangement of the cells soon after mitosis.

Some of the off-lattice models studied are modeled using Monte Carlo simulations, which implicitly include a stochastic component for the cells' displacement. Is the inclusion of stochasticity relevant here? Experiments show that isolated cells are affected by Brownian motion [193]. However, we would expect that in closely packed cell ensembles, the magnitude of the interaction forces would outweigh the stochastic component. Thus, for practical purposes, whether or not to incorporate stochastic terms should depend on the type of tissue being modeled.

Finally we consider the deformability of the cells modeled in this framework. For many of the models the shape of the cells remains unchanged during their motion, deformation being simulated only through the repulsion component of cell interactions. We note that the models of Othmer and coworkers [210, 209, 68] allow the cells to deform, and this gives rise to a more realistic repulsion profile. Some models, however, have gone further and dispensed with the center dynamics assumption in order to directly model the changing shape of the cells. We mention here in brief a paper by Rejniak [216], who considered the growth of cells in a two-dimensional tumor by the *immersed boundary method*, essentially modeling the cell walls computationally as deformable elastic membranes and the cell cytoplasm and surrounding medium as incompressible viscous fluids. Cell division is accomplished in the theory by placing fluid sources in each cell, allowing the cells to double in size before dividing as the nuclei separate and the cell membrane contracts normally to the line connecting the separating nuclei. Adhesion is modeled by positing an attractive force between elements of the cell membrane, which is linear in the separation distance.

We should also note the contribution of Newman [203], who adopted the idea that cells could be modeled as a collection of interacting subcellular elements, each of which behaves as a cell center would in the canonical off-lattice model. If there were N cells, with each cell being composed of M subcellular elements, then we obtain a system of size $M \times N$ for the centers of the subcellular elements. This would allow the cell's mechanical properties to be determined by interaction potentials between the subcellular elements, while another potential would exist between subcellular elements belonging to different cells, reflecting the cell membrane properties and the influence of the ECM.

For the tightly packed cell ensembles which are modeled using Voronoi tessellation, while the configuration of the system (and hence the deformation of the cells) is exactly defined by the positions of the cell centers, many of the interaction profiles use components related to cell shape, such as the area of contact between two cells. However, many authors have taken the view that it is more realistic to model such cell packings by recording the *vertex* positions rather than the cell center positions, which have no biological relevance. This would also have the advantage of recording more information about the cells' deformation, yielding more physiologically accurate cell deformations. Such an approach gives rise to the vertex dynamics model, which is reviewed next.

4.3. Vertex Dynamics Models. As the name suggests, vertex dynamics models are a form of agent-based modeling where, rather than the cell centers, it is the vertices of a polygonal tessellation of the cells that are allowed to move during a simulation. Clearly they are suitable for modeling tightly packed cell ensembles, where the intercellular space is negligible. In order to give an overview of this method, we will describe the vertex dynamics model of Weliky, Oster, and coworkers [268, 267].

The model sets up equations of motion for the vertices of a lattice formed from the edges of each polygonal cell. The equation of motion for a vertex is the same as (4.3) for the center dynamics models, but in this case the forces are tension and pressure terms, as depicted in Figure 4.8(a). Each cell has a tension directed along its edges, proportional to the cell perimeter, and a pressure term, inversely proportional to the cell area/volume, and directed such that it bisects the internal angle at the vertex. Now, at any vertex in the lattice, three cells meet and as such we have six tension terms and three pressure terms at each vertex. The resultant force is calculated and substituted into the equation of motion (4.3). Thus a system of equations is built up and solved in the same manner as for the center dynamics models. The results can be seen in Figure 4.9(a).

Much as for off-lattice models, researchers have proposed many variations of this paradigm vertex dynamics model. Some of the earliest (two-dimensional) investigations into this model were made by Honda and coworkers [135, 136, 134, 139] investigating how cells undergoing rearrangement, i.e., changing neighbors, might minimize their surface area while retaining a constant volume: this was termed the *boundary shortening method*. Rudge and Haseloff [223] applied the vertex dynamics approach to model a problem of mitosis in plant cells, which are also generally polygonal in shape and thus perfectly suited to analysis of this type. In this model the cell walls are modeled as linear springs with a given stiffness and natural length (which increases with time to model cell growth). The mechanics of the system are modeled quasi-statically: the mechanical response to a cell growth event is assumed to be instantaneous.

In the models of Brodland and coworkers [45, 33, 34, 32], the only forces acting on each node were assumed to be directed along the cell wall. (Thus, with reference to Figure 4.8, in these models the force P is absent.) This force was assumed to be

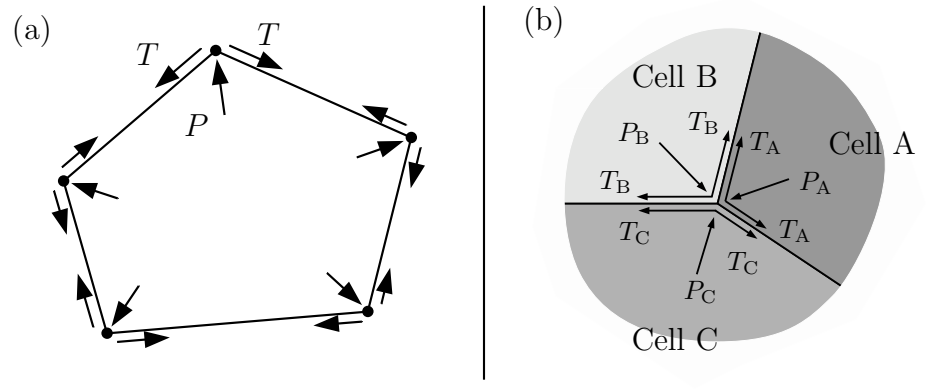

Fig. 4.8 (a) *The forces acting at each node of a cell according to the theory of Weliky et al. In the model the forces in a given cell have the same magnitude at each node.* (b) *The forces acting at each node of the mesh, indicating the contributions from each cell.*

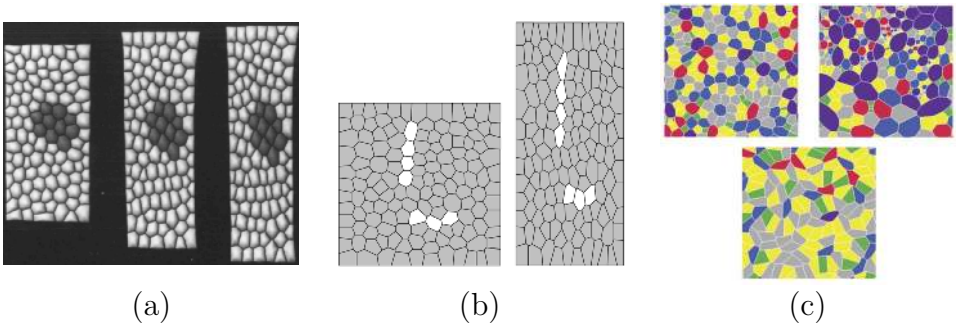

Fig. 4.9 *Examples of vertex dynamics models.* (a) *Cells rearrange as a sheet of epithelial tissue extends, from Weliky et al.* [267]. (b) *A similar situation from Brodland et al.* [32]*, with different forces assumed to act on the vertices compared with image* (a). (c) *Steady-state configurations of cells using an energy-based model, with different parameter values, taken from Farhadifar et al.* [90]. *All images reproduced with permission.*

constant, although a number of possible contributions were identified, including the influence of the cytoskeleton, tension in the cell membrane, and cell–cell adhesion.[14] Figure 4.9(b) depicts the results of a numerical experiment using this hypothesis. This model was adapted [33] to account for the phenomenon of cell sorting, by considering the value of the force connecting two vertices to be dependent on the types of cell on either side of the connecting line.

Another difference between these models and those of Weliky et al. is the connection between the forces acting on each vertex and the vertex displacements. The motion in Brodland et al.'s models was calculated using a finite-element-based formulation. The centroid of the cell was identified, and a triangular mesh was formed by linking the vertices of each cell with the corresponding centroids. The velocities of the nodes of each triangular element were determined by using a finite-element implementation of overdamped motion of the element. The elements were not assumed to be incompressible; the cell's incompressibility was accounted for by a separate constraint on the area of each polygonal cell. Later work by Brodland et al. [35] modified the model so that the viscosity of the cytoplasm—accounted for by the damping term in the equation of motion for each node—was replaced by a system of dashpots in each cell, which better reflected the cell's eccentricity. This work was extended to three dimensions [259].

The previous models have all been force based in their descriptions of the mechanics of the vertices. A more mechanically relevant approach which has emerged in more recent models is the approach based on energy minimization. The advantage of this method is that it avoids having to determine the force on a vertex corresponding to a mechanical principle. For instance, in the model of Weliky et al. the response to cell compression is encoded in the pressure terms P, and the response to cell stretching in the tension term T. A more mechanically correct method would be to evaluate the stored energy in both the cell body and cell membrane, and sum this over all cells. This total stored energy $W(r_k)$ is a function of all the vertex positions, and then the

[14] Cell adhesion molecules would cause two isolated cells, in the absence of other mechanical effects, to maximize their contact area. In this formulation, therefore, cell–cell adhesion can be regarded as a force which pushes vertices further apart.

force term F_i in the equation of motion (4.3) for vertex positions will be given by $F_i = -\partial W/\partial r_i$.

One of the more comprehensive energy functionals is that of Farhadifar et al. [90]:

$$W = \sum_{\alpha} \frac{K_\alpha}{2}(A_\alpha - A_\alpha^{(0)})^2 + \sum_{i,j} \Lambda_{ij} l_{ij} + \sum_{\alpha} \frac{\Gamma_\alpha}{2} L_\alpha^2. \tag{4.9}$$

In this expression α indexes the cells and (i, j) the nodes. The first term represents the energy associated with cell compression, A_α being the area of the cell, $A_\alpha^{(0)}$ being a "target" area, and K_α being a bulk modulus equivalent. The second term represents the energy associated with line tension in an interface between cells. Λ_{ij} is the "tension" in the interface linking vertices i and j, and l_{ij} is the length of that interface. Increased cell adhesion may be modeled by decreasing Λ_{ij}. The third term embodies the energy stored by the cell boundary. The perimeter of cell α is L_α and Γ_α is an associated elastic constant. Example calculations are shown in Figure 4.9(c).

In order to model the geometric properties of cone cells in *Drosophila* eyes, Hilgenfeldt et al. [127] chose a vertex dynamics model mediated by an energy functional consisting only of the perimeter term (modeling cell membrane stiffness) and cell–cell adhesion, which—similarly to the cell sorting model of Brodland and Chen described previously—incorporated a different cell adhesion strength between cells of different type. Honda et al. [137] formulated a three-dimensional energy-based version of the vertex dynamics model in order to model multicellular aggregates. In this case the potential comprised two parts, representing compression energy and surface energy—the first two terms of (4.9).

All of the vertex dynamics models that we have studied above must be solved computationally, in the same way as for off-lattice models. Recall that in that case the models could be solved either by discretizing the system of differential equations or by using a Monte Carlo method. In the vertex dynamics case the former approach appears to be dominant, which is in agreement with our conclusion from the previous section that in closely packed cell aggregates the stochastic motion of cells is mitigated by the strong interactions between cells.

In the computational solution of the system of equations for vertex motion, it must be noted that cell rearrangement implies that the topological state of the vertex network changes over time. The canonical example of vertex rearrangement in two dimensions is shown in Figure 4.10 and is called a T1 process in the literature [90]. The computational scheme must be carefully configured so that such rearrangements are accounted for properly.

Finally we consider cell division. The mechanisms for mitosis in the vertex dynamics models are similar to those of the off-lattice models. Honda et al. [139] incorporate cell division by identifying the "long axis" of the cell and introducing a new membrane normal to this axis, splitting the cell in two. This method was also used by Brodland and Veldhuis [34]. None of these three models used the cell cycle to identify when cells divided; in particular, Brodland and Veldhuis assumed a constant rate of cell division. Additionally, most models of cell division assumed that cells halved in size when divided, then grew back to their original size. However, Rudge and Haseloff included in their model the growth of a cell before mitosis, by allowing the natural length of the springs in their cell-wall model to increase until the cell volume had doubled, at which point the cell was made to divide.

Of the many variations of vertex dynamics model in the literature, which ones best capture the behavior of cell aggregates? A key question is whether to prescribe

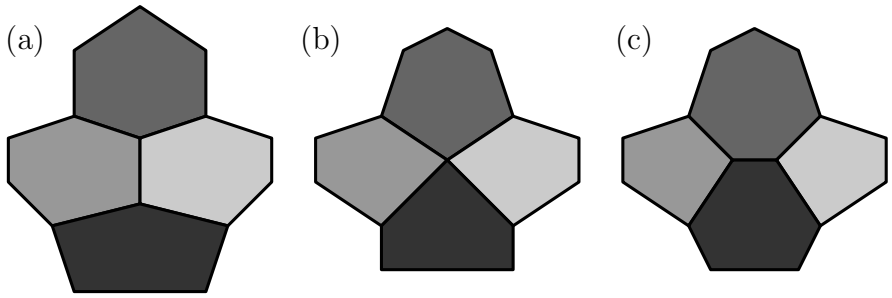

Fig. 4.10 *Rearrangement of cells in a two-dimensional vertex dynamics model.*

forces at a vertex or to follow the energy-based approach. Our instinct would be to opt for the latter approach. While the energy terms can easily be made to depend on physical parameters such as the cell area, perimeter, or boundary length (and, indeed, it is the energy that one would expect to depend on these physical attributes), setting up a force term from cell wide attributes such as cell area is difficult. Compare the simplicity of the compression energy term in (4.9) to the ad hoc way in which the pressure term P is introduced in the model of Weliky et al. (Figure 4.8).

The other issue to be debated here is which mechanical processes to include. Should one opt for a comprehensive approach—as in (4.9)—or opt for the simpler option as did Brodland and co-workers, who only consider cell adhesion? Partly this is a question of computational complexity—one can model a larger cell ensemble or more experiments if the interaction laws are simplified. However, the mechanics of cell deformation are still a little mysterious, and so more complicated behavior such as that described by the energy functional (4.9) is rather speculative: describing how we expect a cell should behave. Such an approach can still yield useful results: by performing several numerical experiments using (4.9) with varying parameters, Farhadifar et al. [90] could analyze the resulting cell configurations and find a region of parameter space which would result in realistic tissue behavior. Three example configurations are shown in Figure 4.9(c).

4.4. Evaluation of Cell-Level Models. We have now reviewed a number of cell-based models that describe the deformation of ensembles of cells. In this section we will evaluate these models, and in particular establish which models are best suited to modeling growing ensembles.

We begin by examining cellular automaton models. The chief advantage of these simulations is their simplicity. If one is only looking for the qualitative effect of some biological principle, cellular automata are the simplest to set up and computationally the least intensive. Placed against this is the realization that the model may not uncover subtle results due to its simplistic approach, and in particular mechanical effects are unsatisfactorily incorporated.

Mechanical effects are included by design in the other two models, the off-lattice and vertex dynamics simulations. As such they are a more realistic approach to modeling cell ensembles. However, one must still make a choice between the two methods. Our instinct would be to model more dilute cell ensembles by using the off-lattice model, and tightly packed ensembles using the vertex dynamics model. The justification for this is that in dilute collections of cells, the interactions between cells can realistically be regarded as normal forces acting at the region of contact between

the cells. In the more tightly packed cell ensembles, other mechanical principles come into play, notably the resistance of cells to compression, which is difficult to prescribe satisfactorily in an off-lattice model, yet is routinely included in the overall energy in vertex dynamics models.

Thus, for more dilute cell ensembles, where the cells retain a more rounded character, we believe that the overlapping sphere method is the most appropriate, whereas if the cells are tightly attached together, the vertex dynamics approach is better suited to incorporate the more complicated mechanical interactions between cells. For tissues which lie between these two extremes—such as tumors—one may choose either approach and so the mechanical interactions need to be carefully examined before settling on a simulation framework.

Growth in such cell ensembles occurs by cell division, and can be modeled in the cell-based approach either as the instantaneous appearance of a new cell (corresponding to mechanism 1 of the off-lattice models) or as a gradual process, involving a slow doubling of the cell's size before gradually separating (as in mechanism 2). Simulating the second mechanism involves more computational complexity, so is it really required? We suspect that it depends on the size of the cell ensemble under consideration. If we have a comparatively small cell collection, the instantaneous appearance of new cells would result in a noticeable jump in the deformation of the cell ensemble. Conversely in a large cell ensemble the addition of a new cell would barely make any difference to the overall deformation, the jumps being smoothed out in the same way that Brownian motion on a molecular scale will give rise to a smooth diffusion rate on the macroscale. The choice of cell division model will therefore depend on the scale of tissue being modeled.

In the next section we will elaborate further on the notion of smoothing out the microscopic (cell-scale) solution to see how one may develop a tissue-scale model from cell-based interaction rules.

5. Connecting Tissue-Level and Cell-Level Models. In the two previous sections, we have looked at different models for growth in tissues, from both a macroscale (tissue) and a microscopic (cell-based) viewpoint. However, few of the theories have attempted either to reconcile the macroscopic equations with the mechanics at the cell level, or indeed to determine how, for instance, mitotic activity would depend on the overall state of stress in the tissue. Such relationships may be analyzed by the mathematical theories of homogenization and localization. Given a body composed of some heterogeneous material, where the body's characteristic length scale is much greater than the typical length scale of the variation in material properties, one may approximate the behavior of the body under external loads by that of a homogeneous body, whose properties are in some sense an average of those in the original specimen. The process of obtaining these effective properties is known as homogenization. Mathematically speaking, we define the ratio of the heterogeneity length scale to the typical body scale to be $\varepsilon \ll 1$, so that a material property of the body (for instance, elastic moduli, permeability, thermal conductivity, etc.) can be denoted by $k(\boldsymbol{x}, \boldsymbol{x}/\varepsilon)$. Homogenization gives us an effective material property $k_{\text{eff}}(\boldsymbol{x})$, which can be thought of as the quantity that emerges when the original problem is analyzed asymptotically in the limit $\varepsilon \to 0$. Conversely, localization is the theory that, given a homogenized material with a known (or presumed) microstructure, extracts a representation of the state of the material at the microscopic level.

Homogenization and localization are more easily achieved when the heterogeneous material has some regular structure, which is often true for biological materials [93].

Thus the microstructure may be replaced by a representative periodic lattice, for which homogenization is a relatively well understood process [21]. This assumption of periodicity lies behind many of the biomechanical applications of homogenization, from bone tissue [131] to heart muscle [41]. When the microstructure does not have such regularity, often the best that can be done analytically is to find variational bounds on the effective properties [192]. On the other hand one can take a computational approach and study the mechanical behavior of a tissue by averaging the deformation of the microstructure over some representative volume element (RVE). One such volume-averaging study, by Stylianopoulos and Barocas [243], in modeling the mechanics of collagenous material, took the microstructure to be a network of interconnected fibers. Note that this method, unlike homogenization, does not extract effective material properties and hence the averaging process must be carried out separately for each macroscopic deformation one might wish to consider.

There has been very little investigation into the properties of materials whose microstructure is a collection of cells, as exemplified by the models of section 4. Turner [253] modeled a collection of deformable elastic cells and, with a crude measure of the stored elastic energy due to contact, derived a fourth-order equation for the evolution of the cell density. We also note a paper by Bodnar and Velazquez [27], who take a one-dimensional collection of cells evolving according to (4.3), with and without a stochastic term, and under the influence of a number of different potentials. Taking the continuum limit, the density of particles was found to satisfy some partial differential equation, which (in the case of repulsive potentials) is a nonlinear diffusion equation. Mitotic effects were not included.

In an effort to discover the large-scale behavior of a collection of cells behaving according to the center dynamics approach, Pathmanathan et al. [212] found that a two-dimensional aggregate under compression would behave elastically up to some critical point, at which cell rearrangements would kick in, causing a permanent plastic deformation. Under unloading, the tissue again behaves elastically. In tension and in simple shear, however, the behavior is more akin to a brittle elastic material, with elastic deformations interrupted by sudden jumps, where collections of cells break from each other.

Considering the vertex dynamics models for epithelial cells, Brodland et al. [32] set out to obtain a model in the continuum limit which would have the same properties as the collection of cells. Given a cell tessellation, the average shape of a cell can be represented by an ellipse, parametrized by the three properties of size, elongation, and orientation. Knowing these three parameters allows the stresses in the material to be found [36], which in turn gives rise to a strain rate by the assumption of a linear viscous constitutive law for the material. Thus the motion of the material under growth may be found by a timestepping routine, where the stresses at each time step give rise to the strain rate, thus giving the new average cell properties and therefore the new stresses. Mitosis and cell annealing (reducing the elongation) may also be incorporated into the model. On a different note, Fozard et al. [92] recently derived a homogenized equation for the behavior of a one-dimensional vertex dynamics cell model. The properties of the cells were allowed to vary, but mitosis was not included.

These investigations indicate that particle rearrangement in the cell-based models leads to fluid-like behavior at the coarse-scale continuum level, with cell rearrangements leading to plastic flow. In this respect it may be useful to take some ideas from granular medium theory, where the aggregate response of many interacting particles (cf. cells) gives rise to a continuum law which contains elements of plastic flow, among others. However, the granular flow models tend to assume no cohesion between parti-

cles, in contrast to cellular aggregates. Tissues which aren't primarily cell aggregates behave much more elastically, due to the absence of large-scale tissue rearrangement.

The difficulty in obtaining constitutive mechanical models for tissues by homogenization is obvious. However, one can create models for tissue which are inspired by, rather than derived from, the microstructural characteristics. For instance, Kuhl and Holzapfel [168] used a representation of collagenous tissue which assumed that the collagen fiber phase could be represented by a "worm-like chain model." Another notable model [133] accounted for the anisotropy of arteries—characterized by helical fibers embedded in the vessel walls—by a strain energy function whose principal directions were aligned with the fibers.

Obtaining the effective material properties of tissues by homogenization—especially mechanical properties such as the strain energy function—would be a breakthrough in biomechanics. However, in this section we ask whether it is possible for growth phenomena to be homogenized without solving the full homogenization problem for the tissue. Essentially, we investigate the feasibility of obtaining from microscopic processes an effective growth tensor $\boldsymbol{F}_{\mathrm{g}}$ (in the language of section 3.3) while *assuming* that the strain energy function which gives rise to $\boldsymbol{F}_{\mathrm{e}}$ is the correct effective function for the tissue under consideration. This question is motivated by the need to uncover the biological basis for the form of $\boldsymbol{F}_{\mathrm{g}}$, which—as we have argued previously—requires an analysis based on the behavior of the cells themselves. To this end, we identify three challenges, whose resolution would greatly enhance our understanding of tissue growth mechanics:

1. *Deformation localization*: Given a deformation field in a tissue, what can we say about the deformation or forces experienced by a cell embedded in that tissue?
2. *Mechanotransduction*: Given that a cell is deformed in a certain way, how does this affect the cell cycle or the rate of ECM production?
3. *Growth averaging*: How does the rate of mitosis or ECM production at the microlevel correspond to the growth tensor $\boldsymbol{F}_{\mathrm{g}}$ in the overall tissue?

The satisfactory resolution of 1–3 would give rise to a dependence between stress and growth, as depicted schematically in Figure 5.1. Other factors which affect growth rates, such as morphogen concentration, can also be incorporated into this framework: the morphogen concentration field will be determined at the macroscale, and will affect microscopic (cell-level) behavior such as mitotic rate. For the remainder of this section we will review the progress which has been made in meeting the three challenges enumerated above.

5.1. Deformation Localization. This concept is important in connecting the growth field to the tissue deformation, since the cells embedded in the tissue are likely to experience a substantially different deformation from the tissue as a whole. As noted previously, localization is the theory that predicts microstructural properties from the equivalent quantities at the macroscale. Clearly the configuration of the microstructure is crucial, so the deformation experienced by the cell for a given tissue deformation will be different depending on the type of tissue in which it is embedded.

There have been few investigations which examine this issue directly. We note in particular work by Breuls et al. [30]. In this study the deformation of cells in an engineered tissue construct was considered, where the microstructure was assumed to be periodic. Both the matrix phase and the cells were assumed to be neo-Hookean materials. The periodicity allowed the (nonlinearly elastic) deformation of the tissue at the macroscale to be determined by a standard homogenization method. This

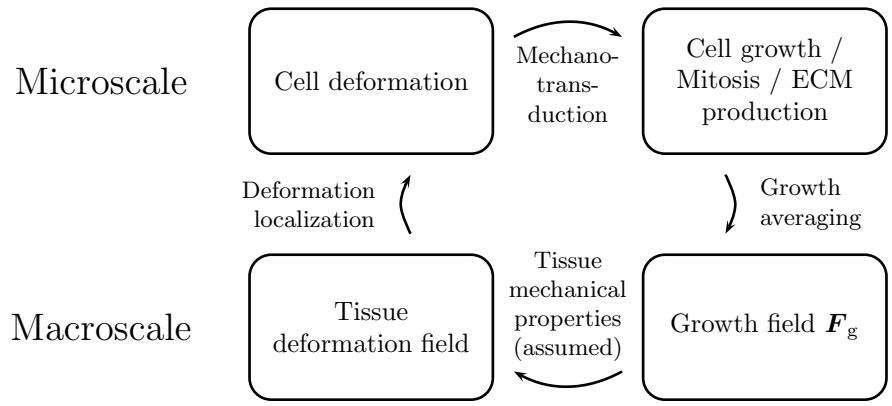

Fig. 5.1 *Schematic diagram illustrating the steps required to characterize a stress–growth relationship in a tissue.*

involved solving a microstructural *cell problem*, so the deformation of a cell in the tissue was found as a by-product of the homogenization process.

In fact, although this paper was one of the few to explicitly consider the cell deformation, any homogenization or volume-averaging theory that involves solving a microstructural problem as part of the macroscale calculation will produce a typical state of deformation at the microscale. Thus, for instance, the typical deformation of a network of interconnected fibers in a tissue can be found using the averaging theory of Stylianopoulos and Barocas [243]. Similarly, in the vertex dynamics model of Brodland et al. [36], the dependence of the stress in the tissue on the average shape of the cells could conceivably be inverted in order to produce the cell deformations as a function of the tissue stress.

Thus, we observe that deformation localization is intimately linked with the homogenization or volume averaging of tissues. Further progress in localization must therefore go hand in hand with efforts to apply ever more realistic models of the microstructure to tissue deformation problems.

5.2. Mechanotransduction. The concept of mechanotransduction, in which the cell changes its behavior in response to a mechanical stimulus, was introduced in section 2.2. Models for this process should form a key part of any theory of tissue growth. Such models have so far concentrated on mechanical aspects. For instance, Shafrir and Forgacs [228] considered the cell cytoskeleton to be an interconnected network of rods, and evaluated how a force on the membrane of a model cell would be transmitted through this network towards the cell nucleus. With an application to bone growth in mind, Cowin [59] reviewed models for evaluating the deformation due to fluid motion of fibers connecting osteocytes (bone cells) to the bone matrix.

These examples illustrate a key requirement for models of mechanotransduction, namely that a close collaboration between theoreticians and experimentalists is required. New discoveries are continually being presented, identifying hitherto-disregarded pathways and enhancing the understanding of the micromechanical and biochemical aspects of mechanotransduction. On the other hand, models which in-

clude every plausible mechanism may be impractical if not impossible to formulate; thus there is a need for an identification of the key components of the (often bewilderingly large) system of chemical interactions, offering a simplified model which may be subjected to meaningful analysis. Recent theoretical work into ion channels (see, for instance, [38] and references cited within) may also be incorporated into this effort.

5.3. Growth Averaging. Having ideally determined the cell response to applied deformations through localization and mechanotransduction, all that remains is to link the production of new tissue material at the cell level to a global macroscopic growth field, which may be characterized (for elastic tissues) by the growth tensor $\boldsymbol{F}_{\mathrm{g}}$, as shown in the theory of section 3.3.

Taber [245] identified four mechanisms by which new tissue could be produced. These were

- cell division (hyperplasia),
- cell growth (hypertrophy),
- production of new ECM,
- accretion of material on internal or external surfaces.

Cell division (and the associated doubling in cell volume during the cell cycle) is largely responsible for growth in epithelia and tumors. Growth in mature skeletal and cardiac muscles generally takes place by hypertrophy, through elongation or thickening of the muscle fibers. Connective tissues such as tendons are largely composed of ECM proteins, so new ECM production is the primary mechanism of growth here. Accretion of minerals on internal surfaces leads to the densification of bone.

While this classification of tissue growth is useful in distinguishing conceptually different mechanisms, the full details involved in the growth process are inevitably much more complex. Tendons, for instance, grow by production of long collagen fibers by fibroblast cells. In reality, however, the cells secrete short protein molecules which subsequently self-assemble into the hierarchical rope-like structure from which the tendon is formed [231].

We now consider how the growth process at the cell level, described by processes such as those above, may be averaged. For each point in the material, the growth field $\boldsymbol{F}_{\mathrm{g}}$, as noted in section 3.3, describes the growth-induced deformation of an infinitesimally small neighborhood Ω of that point. This motivates the following simple averaging approach. The neighborhood Ω in the macroscopic description would be identified with an RVE in the microscopic description (using the averaging terminology discussed on page 104). This RVE should be large enough that the characteristic length of the cells (or the microstructure in general) is small compared to the RVE dimensions. Simultaneously, the RVE should be small enough that the rate of growth is constant over its whole volume. This RVE would be placed in a stress-free environment and allowed to grow at the rate and in the direction indicated by the mechanotransductive step. By approximating the (stress-free) RVE by ellipsoids pre- and post-growth, one may then characterize the growth tensor $\boldsymbol{F}_{\mathrm{g}}$.

If it is clear that the growth is isotropic and does not change the tissue's density, all that is required for the averaging process is the rate of mass increase per unit volume, γ. Then, since $\boldsymbol{F}_{\mathrm{g}} = g\boldsymbol{I}$, we have from (3.20) that $\gamma = 3\rho\dot{g}g^{-1}$, which gives us an evolution equation for the growth function g. However, one must be wary of imposing isotropic growth without justification. For instance, while the mitosis rules for some of the off-lattice or vertex dynamics models of section 4 are indeed isotropic, others impose a directionality based on the state of deformation of the tissue.

Ultimately, of course, whether the growth tensor is a faithful representation of the tissue growth will depend mainly on the microscopic model of growth, or how exactly

material is added to the tissue. To this end, we again stress that collaboration with experimentalists is needed in order to obtain realistic models which accurately capture the tissue behavior.

6. Conclusion. In this review article, we hope that we have managed to convey an overview of the research that has been carried out into modeling tissue growth, while stressing the distance yet to be traveled before the mechanisms involved can be fully understood. Nevertheless, the prize is great: as noted in the introduction, the interplay between stress and tissue growth has a strong bearing on many pathologies; being able to play a part in reducing their burden on humanity is a laudable task.

Clouding this vision of the future is the realization that the human body is no simple machine. With each new insight into the workings of cellular processes, an extra layer of complexity is added to the picture. This has been the motivation for experimental biologists and physiologists to collaborate with applied mathematicians, an approach which has borne many important results, as discussed in this article. This collaboration should continue, with theories being based on the best current knowledge of the physiology, motivating new experiments to confirm or refute the theoretical predictions.

Of course, while there may be similarities between the methods used to analyze growth in different tissues, and while their biophysical properties may be superficially similar, each tissue is likely to be significantly different in how growth interacts with stress.[15] Nevertheless, with improved experimental and theoretical techniques, we are convinced that research into the biomechanics of growth will maintain its current pace, with exciting consequences for the fields of mathematics, engineering, physiology, and medicine.

Acknowledgment. The authors would like to thank the reviewers for their helpful and insightful comments.

REFERENCES

[1] K.A. Addae-Mensah and J.P. Wikswo, *Measurement techniques for cellular biomechanics* in vitro, Exp. Biol. Med., 233 (2008), pp. 792–809.
[2] B. Alberts, A. Johnson, J. Lewis, M. Raff, K. Roberts, and P. Walter, *Molecular Biology of the Cell*, 5th ed., Garland Science, New York, 2008.
[3] D. Ambrosi, G.A. Ateshian, E.M. Arruda, M. Ben Amar, S.C. Cowin, J. Dumais, A. Goriely, G.A. Holzapfel, J.D. Humphrey, R. Kemkemer, E. Kuhl, J. Ma, J.E. Olberding, L.A. Taber, R. Vandiver, and K. Garikipati, *Perspectives on biological growth and remodeling*, J. Mech. Phys. Solids, 59 (2011), pp. 863–883.
[4] D. Ambrosi and F. Guana, *Stress-modulated growth*, Math. Mech. Solids, 12 (2007), pp. 319–342.
[5] D. Ambrosi and A. Guillou, *Growth and dissipation in biological tissues*, Contin. Mech. Thermodyn., 19 (2007), pp. 245–251.
[6] D. Ambrosi and F. Mollica, *On the mechanics of a growing tumor*, Int. J. Eng. Sci., 40 (2002), pp. 1297–1316.
[7] D. Ambrosi and F. Mollica, *The role of stress in the growth of a multicell spheroid*, J. Math. Biol., 48 (2004), pp. 477–499.
[8] R.P. Araujo and D.L.S. McElwain, *A history of the study of solid tumour growth: The contribution of mathematical modelling*, Bull. Math. Biol., 66 (2004), pp. 1039–1091.
[9] R.P. Araujo and D.L.S. McElwain, *A linear-elastic model of anisotropic tumour growth*, European J. Appl. Math., 15 (2004), pp. 365–384.
[10] R.P. Araujo and D.L.S. McElwain, *New insights into vascular collapse and growth dynamics in solid tumors*, J. Theoret. Biol., 228 (2004), pp. 335–346.

[15] However, as we have seen, at the large scale surprisingly accurate laws such as (3.1) often arise.

[11] R.P. Araujo and D.L.S. McElwain, *A mixture theory for the genesis of residual stresses in growing tissues* I: *A general formulation*, SIAM J. Appl. Math., 65 (2005), pp. 1261–1284.
[12] R.P. Araujo and D.L.S. McElwain, *A mixture theory for the genesis of residual stresses in growing tissues* II: *Solutions to the biphasic equations for a multicell spheroid*, SIAM J. Appl. Math., 66 (2005), pp. 447–467.
[13] R.P. Araujo and D.L.S. McElwain, *The role of mechanical host–tumour interactions in the collapse of tumour blood vessels and tumour growth dynamics*, J. Theoret. Biol., 238 (2006), pp. 817–827.
[14] R.R. Archer, *Growth Stresses and Strains in Trees*, Springer, Berlin, 1987.
[15] A. Ascenzi, *Biomechanics and Galileo Galilei*, J. Biomech., 26 (1993), pp. 95–100.
[16] G.A. Ateshian, *On the theory of reactive mixtures for modeling biological growth*, Biomech. Model. Mechan., 6 (2007), pp. 423–445.
[17] S. Baek, K.R. Rajagopal, and J.D. Humphrey, *A theoretical model of enlarging intracranial fusiform aneurysms*, Trans. ASME J. Biomech. Eng., 128 (2006), pp. 142–149.
[18] M. Basan, T. Risler, J.-F. Joanny, X. Sastre-Garau, and J. Prost, *Homeostatic competition drives tumor growth and metastasis nucleation*, HFSP J., 3 (2009), pp. 265–272.
[19] L.V. Beloussov, J.G. Dorfman, and V.G. Cherdantzev, *Mechanical stresses and morphological patterns in amphibian embryos*, J. Embryol. Exp. Morphol., 34 (1975), pp. 559–574.
[20] M. Ben Amar and A. Goriely, *Growth and instability in elastic tissues*, J. Mech. Phys. Solids, 53 (2005), pp. 2284–2319.
[21] A. Bensoussan, J.-L. Lions, and G.C. Papanicolaou, *Asymptotic Analysis for Periodic Structures*, North-Holland, Amsterdam, 1978.
[22] D.A. Beysens, G. Forgacs, and J.A. Glazier, *Cell sorting is analogous to phase ordering in fluids*, Proc. Natl. Acad. Sci. USA, 97 (2000), pp. 9467–9471.
[23] B.A. Bilby, L.R.T. Gardner, and A.N. Stroh, *Continuous distributions of dislocations and the theory of plasticity*, in IX^{e} Congrès International de Mécanique Appliquée. Actes. Tome VIII, Université de Bruxelles, 1957, pp. 35–44.
[24] M. Bock, A.K. Tyagi, J.-U. Kreft, and W. Alt, *Generalized Voronoi tessellation as a model of two-dimensional cell tissue dynamics*, Bull. Math. Biol., 72 (2010), pp. 1696–1731.
[25] L. Bodenstein, *A dynamic simulation model of tissue growth and cell patterning*, Cell Differ., 19 (1986), pp. 19–33.
[26] L. Bodenstein and C.D. Stern, *Formation of the chick primitive streak as studied in computer simulations*, J. Theoret. Biol., 233 (2005), pp. 253–269.
[27] M. Bodnar and J.J.L. Velazquez, *Derivation of macroscopic equations for individual cell-based models: A formal approach*, Math. Methods Appl. Sci., 28 (2005), pp. 1757–1779.
[28] R. Brand and L. Claes, *Book review: 'The Law of Bone Remodelling,'* J. Biomech., 22 (1989), pp. 185–187.
[29] C.P. Brangwynne, F.C. MacKintosh, S. Kumar, N.A. Geisse, J. Talbot, L. Mahadevan, K.K. Parker, D.E. Ingber, and D.A. Weitz, *Microtubules can bear enhanced compressive loads in living cells because of lateral reinforcement*, J. Cell Biol., 173 (2006), pp. 733–741.
[30] R.G.M. Breuls, B.G. Sengers, C.W.J. Oomens, C.V.C. Bouten, and F.P.T. Baaijens, *Predicting local cell deformations in engineered tissue constructs: A multilevel finite element approach*, Trans. ASME J. Biomech. Eng., 124 (2002), pp. 198–207.
[31] G.W. Brodland, *Computational modeling of cell sorting, tissue engulfment, and related phenomena: A review*, Appl. Mech. Rev., 57 (2004), pp. 47–76.
[32] G.W. Brodland, D.I.-L. Chen, and J.H. Veldhuis, *A cell-based constitutive model for embryonic epithelia and other planar aggregates of biological cells*, Int. J. Plast., 22 (2006), pp. 965–995.
[33] G.W. Brodland and H.H. Chen, *The mechanics of cell sorting and envelopment*, J. Biomech., 33 (2000), pp. 845–851.
[34] G.W. Brodland and J.H. Veldhuis, *Computer simulations of mitosis and interdependencies between mitosis orientation, cell shape and epithelia reshaping*, J. Biomech., 35 (2002), pp. 673–681.
[35] G.W. Brodland, D. Viens, and J.H. Veldhuis, *A new cell-based FE model for the mechanics of embryonic epithelia*, Comput. Meth. Biomech. Biomed. Eng., 10 (2007), pp. 121–128.
[36] G.W. Brodland and C.J. Wiebe, *Mechanical effects of cell anisotropy on epithelia*, Comput. Meth. Biomech. Biomed. Eng., 7 (2004), pp. 91–99.
[37] A. Brú and D. Casero, *The effect of pressure on the growth of tumour cell colonies*, J. Theoret. Biol., 243 (2006), pp. 171–180.

[38] M. Burger, R.S. Eisenberg, and H.W. Engl, *Inverse problems related to ion channel selectivity*, SIAM J. Appl. Math., 67 (2007), pp. 960–989.
[39] H.M. Byrne, T. Alarcon, M.R. Owen, S.D. Webb, and P.K. Maini, *Modelling aspects of cancer dynamics: A review*, Philos. Trans. R. Soc. Lond. Ser. A Math. Phys. Eng. Sci., 364 (2006), pp. 1563–1578.
[40] H. Byrne and L. Preziosi, *Modelling solid tumour growth using the theory of mixtures*, Math. Med. Biol., 20 (2003), pp. 341–366.
[41] D. Caillerie, A. Mourad, and A. Raoult, *Cell-to-muscle homogenization. Application to a constitutive law for the myocardium*, ESAIM Math. Model. Numer. Anal., 37 (2003), pp. 681–698.
[42] J. Casey, *On Volterra dislocations of finitely deforming continua*, Math. Mech. Solids, 9 (2004), pp. 473–492.
[43] D.L. Cassens and J.R. Serrano, *Growth stress in hardwood timber*, in Proceedings of the 14th Central Hardwood Forest Conference, D.A. Yaussy, D.M. Hix, R.P. Long, and P.C. Goebel, eds., U.S. Dept. of Agriculture, Forest Service, Northeastern Research Station, 2004, pp. 106–115.
[44] J. Chalmers and R.D. Ray, *The growth of transplanted foetal bones in different immunological environments*, J. Bone Joint Surg. Br. Vol., 44 (1962), pp. 149–164.
[45] H.H. Chen and G.W. Brodland, *Cell-level finite element studies of viscous cells in planar aggregates*, Trans. ASME J. Biomech. Eng., 122 (2000), pp. 394–401.
[46] J.C. Chen and D.R. Carter, *Important concepts of mechanical regulation of bone formation and growth*, Curr. Opin. Orthop., 16 (2005), pp. 338–345.
[47] Y.-C. Chen and A. Hoger, *Constitutive functions of elastic materials in finite growth and deformation*, J. Elasticity, 59 (2000), pp. 175–193.
[48] E.K. Chu, J.S. Foley, J. Cheng, A.S. Patel, J.M. Drazen, and D.J. Tschumperlin, *Bronchial epithelial compression regulates epidermal growth factor receptor family ligand expression in an autocrine manner*, Am. J. Respir. Cell Mol. Biol., 32 (2005), pp. 373–380.
[49] Y.-S. Chu, S. Dufour, J.P. Thiery, E. Perez, and F. Pincet, *Johnson–Kendall–Roberts theory applied to living cells*, Phys. Rev. Lett., 94 (2005), 028102.
[50] C.J. Chuong and Y.C. Fung, *Three-dimensional stress distribution in arteries*, Trans. ASME J. Biomech. Eng., 105 (1983), pp. 268–274.
[51] A.J. Coulombre, *The role of intraocular pressure in the development of the chick eye.* I. *Control of eye size*, J. Exp. Zool., 133 (1956), pp. 211–225.
[52] A.J. Coulombre and J.L. Coulombre, *The role of intraocular pressure in the development of the chick eye.* IV. *Corneal curvature*, AMA Arch. Ophthalmol., 59 (1958), pp. 502–506.
[53] M.J. Cowan and R.G. Crystal, *Lung growth after unilateral pneumonectomy: Quantitation of collagen synthesis and content*, Am. Rev. Respir. Dis., 111 (1975), pp. 267–277.
[54] S.C. Cowin, *Mechanical modeling of the stress adaptation process in bone*, Calcif. Tissue Int., 36 (1984), pp. S98–S103.
[55] S.C. Cowin, *Wolff's law of trabecular architecture at remodeling equilibrium*, Trans. ASME J. Biomech. Eng., 108 (1986), pp. 83–88.
[56] S.C. Cowin, *Bone stress adaptation models*, Trans. ASME J. Biomech. Eng., 115 (1993), pp. 528–533.
[57] S.C. Cowin, *The false premise in Wolff's law*, in Bone Mechanics Handbook, 2nd ed., S.C. Cowin, ed., CRC Press, Boca Raton, FL, 2001, Chap. 30.
[58] S.C. Cowin, *Tissue growth and remodeling*, Annu. Rev. Biomed. Eng., 6 (2004), pp. 77–107.
[59] S.C. Cowin, *The significance of bone microstructure in mechanotransduction*, J. Biomech., 40 (2007), pp. S105–S109.
[60] S.C. Cowin and S.B. Doty, *Tissue Mechanics*, Springer, New York, 2007.
[61] S.C. Cowin and K. Firoozbakhsh, *Bone remodeling of diaphysial surfaces under constant load: Theoretical predictions*, J. Biomech., 14 (1981), pp. 471–484.
[62] S.C. Cowin and D.H. Hegedus, *Bone remodeling* I: *Theory of adaptive elasticity*, J. Elasticity, 6 (1976), pp. 313–326.
[63] S.C. Cowin, A.M. Sadegh, and G.M. Luo, *An evolutionary Wolff's law for trabecular architecture*, Trans. ASME J. Biomech. Eng., 114 (1992), pp. 129–136.
[64] S.C. Cowin and W.C. Van Buskirk, *Internal bone remodeling induced by a medullary pin*, J. Biomech., 11 (1978), pp. 269–275.
[65] S.C. Cowin and W.C. Van Buskirk, *Surface bone remodeling induced by a medullary pin*, J. Biomech., 12 (1979), pp. 269–276.
[66] R.W. Cox and M.A. Peacock, *The growth of elastic cartilage*, J. Anat., 128 (1979), pp. 207–213.
[67] A.S.G. Curtis and G.M. Seehar, *The control of cell division by tension or diffusion*, Nature, 274 (1978), pp. 52–53.

[68] J.C. Dallon and H.G. Othmer, *How cellular movement determines the collective force generated by the* Dictyostelium discoideum *slug*, J. Theoret. Biol., 231 (2004), pp. 203–222.
[69] J. Dervaux, P. Ciarletta, and M. Ben Amar, *Morphogenesis of thin hyperelastic plates: A constitutive theory of biological growth in the Föppl–von Kármán limit*, J. Mech. Phys. Solids, 57 (2009), pp. 458–471.
[70] M.E. Desmond and A.G. Jacobson, *Embryonic brain enlargement requires cerebrospinal fluid pressure*, Dev. Biol., 57 (1977), pp. 188–198.
[71] A. DiCarlo and S. Quiligotti, *Growth and balance*, Mech. Res. Comm., 29 (2002), pp. 449–456.
[72] S. Dormann and A. Deutsch, *Modeling of self-organized avascular tumor growth with a hybrid cellular automaton*, In Silico Biol., 2 (2002), pp. 393–406.
[73] K.J. Dormer, *Fundamental Tissue Geometry for Biologists*, Cambridge University Press, Cambridge, UK, 1980.
[74] D. Drasdo, *Buckling instabilities of one-layered growing tissues*, Phys. Rev. Lett., 84 (2000), pp. 4244–4247.
[75] D. Drasdo and G. Forgacs, *Modeling the interplay of generic and genetic mechanisms in cleavage, blastulation and gastrulation*, Dev. Dynam., 219 (2000), pp. 182–191.
[76] D. Drasdo, S. Hoehme, and M. Block, *On the role of physics in the growth and pattern formation of multi-cellular systems: what can we learn from individual-cell based models?*, J. Stat. Phys., 128 (2007), pp. 287–345.
[77] D. Drasdo and S. Höhme, *Individual-based approaches to birth and death in avascular tumors*, Math. Comput. Modelling, 37 (2003), pp. 1163–1175.
[78] D. Drasdo and S. Höhme, *A single-cell-based model of tumor growth* in vitro: *Monolayers and spheroids*, Phys. Biol., 2 (2005), pp. 133–147.
[79] D. Drasdo, R. Kree, and J.S. McCaskill, *Monte Carlo approach to tissue-cell populations*, Phys. Rev. E, 52 (1995), pp. 6635–6657.
[80] D. Drasdo and M. Loeffler, *Individual-based models to growth and folding in one-layered tissues: Intestinal crypts and early development*, Nonlinear Anal., 47 (2001), pp. 245–256.
[81] A.D. Drozdov and H. Khanina, *A model for the volumetric growth of a soft tissue*, Math. Comput. Modelling, 25 (1997), pp. 11–29.
[82] J.C. Drummond, *A comparative study of tumour and normal tissue growth*, Biochem. J., 11 (1917), pp. 325–377.
[83] S. Du and F. Yamamoto, *An overview of the biology of reaction wood formation*, J. Integr. Plant Biol., 49 (2007), pp. 131–143.
[84] B. Dubertret and N. Rivier, *Geometrical models of the renewal of the epidermis*, Compt. Rendus Acad. Sci. III Sci. Vie, 323 (2000), pp. 49–56.
[85] W. Düchting and T. Vogelsaenger, *Recent progress in modelling and simulation of three-dimensional tumor growth and treatment*, Biosystems, 18 (1985), pp. 79–91.
[86] G. Eaves, *The invasive growth of malignant tumours as a purely mechanical process*, J. Pathol., 109 (1973), pp. 233–237.
[87] V.M. Entov, *Mechanical model of scoliosis*, Mech. Solid., 18 (1983), pp. 199–206.
[88] M. Epstein and G.A. Maugin, *Thermomechanics of volumetric growth in uniform bodies*, Int. J. Plast., 16 (2000), pp. 951–978.
[89] E. Farge, *Mechanical induction of Twist in the* Drosophila *foregut/stomodeal primordium*, Curr. Biol., 13 (2003), pp. 1365–1377.
[90] R. Farhadifar, J.-C. Röper, B. Aigouy, S. Eaton, and F. Jülicher, *The influence of cell mechanics, cell–cell interactions, and proliferation on epithelial packing*, Curr. Biol., 17 (2007), pp. 2095–2104.
[91] J. Folkman and A. Moscona, *Role of cell shape in growth control*, Nature, 273 (1978), pp. 345–349.
[92] J.A. Fozard, H.M. Byrne, O.E. Jensen, and J.R. King, *Continuum approximations of individual-based models for epithelial monolayers*, Math. Med. Biol., 27 (2010), pp. 39–74.
[93] P. Fratzl and R. Weinkamer, *Nature's hierarchical materials*, Progr. Mater. Sci., 52 (2007), pp. 1263–1334.
[94] N. Frey and E.N. Olson, *Cardiac hypertrophy: The good, the bad, and the ugly*, Annu. Rev. Physiol., 65 (2003), pp. 45–79.
[95] H.M. Frost, *The Laws of Bone Structure*, Charles C. Thomas, Springfield, IL, 1964.
[96] Y.C. Fung, *Biomechanics: Motion, Flow, Stress, and Growth*, Springer, New York, 1990.
[97] Y.C. Fung, *What are the residual stresses doing in our blood vessels?*, Ann. Biomed. Eng., 19 (1991), pp. 237–249.

[98] Y.C. Fung, *Biomechanics: Mechanical Properties of Living Tissues*, 2nd ed., Springer, New York, 1993.
[99] Y.C. Fung, *Biomechanics: Circulation*, 2nd ed., Springer, New York, 1997.
[100] Y.C. Fung and S.Q. Liu, *Strain distribution in small blood vessels with zero-stress state taken into consideration*, Am. J. Physiol. Heart Circ. Physiol., 262 (1992), pp. H544–H552.
[101] J. Galle, G. Aust, G. Schaller, T. Beyer, and D. Drasdo, *Individual cell-based models of the spatial–temporal organization of multicellular systems—achievements and limitations*, Cytometry A, 69 (2006), pp. 704–710.
[102] J. Galle, M. Loeffler, and D. Drasdo, *Modeling the effect of deregulated proliferation and apoptosis on the growth dynamics of epithelial cell populations* in vitro, Biophys. J., 88 (2005), pp. 62–75.
[103] J.-F. Ganghoffer and B. Haussy, *Mechanical modeling of growth considering domain variation. Part* I: *Constitutive framework*, Int. J. Solid. Struct., 42 (2005), pp. 4311–4337.
[104] M. Gardner, *Mathematical games: The fantastic combinations of John Conway's new solitaire game "life,"* Sci. Am., 223 (1970), pp. 120–123.
[105] K. Garikipati, *The kinematics of biological growth*, Appl. Mech. Rev., 62 (2009), 030801.
[106] K. Garikipati, E.M. Arruda, K. Grosh, H. Narayanan, and S. Calve, *A continuum treatment of growth in biological tissue: The coupling of mass transport and mechanics*, J. Mech. Phys. Solids, 52 (2004), pp. 1595–1625.
[107] K. Garikipati, J.E. Olberding, H. Narayanan, E.M. Arruda, K. Grosh, and S. Calve, *Biological remodelling: Stationary energy, configurational change, internal variables and dissipation*, J. Mech. Phys. Solids, 54 (2006), pp. 1493–1515.
[108] A. Gjelsvik, *Bone remodeling and piezoelectricity.* I, J. Biomech., 6 (1973), pp. 69–77.
[109] A. Gjelsvik, *Bone remodeling and piezoelectricity.* II, J. Biomech., 6 (1973), pp. 187–193.
[110] A.L. Goldberg, J.D. Etlinger, D.F. Goldspink, and C. Jablecki, *Mechanism of work-induced hypertrophy of skeletal muscle*, Med. Sci. Sports Exerc., 7 (1975), pp. 248–261.
[111] A.E. Goodship and J.L. Cunningham, *Pathophysiology of functional adaptation of bone in remodeling and repair* in vivo, in Bone Mechanics Handbook, 2nd ed., S.C. Cowin, ed., CRC Press, Boca Raton, FL, 2001, Chap. 26.
[112] A.E. Goodship, J.L. Cunningham, V. Oganov, J. Darling, A.W. Miles, and G.W. Owen, *Bone loss during long term space flight is prevented by the application of a short term impulsive mechanical stimulus*, Acta Astronaut., 43 (1998), pp. 65–75.
[113] A. Goriely and M. Ben Amar, *Differential growth and instability in elastic shells*, Phys. Rev. Lett., 94 (2005), 198103.
[114] A. Goriely and M. Ben Amar, *On the definition and modeling of incremental, cumulative, and continuous growth laws in morphoelasticity*, Biomech. Model. Mechan., 6 (2007), pp. 289–296.
[115] N. Grabe and K. Neuber, *A multicellular systems biology model predicts epidermal morphology, kinetics and* Ca^{2+} *flow*, Bioinformatics, 21 (2005), pp. 3541–3547.
[116] F. Graner and J.A. Glazier, *Simulation of biological cell sorting using a two-dimensional extended Potts model*, Phys. Rev. Lett., 69 (1992), pp. 2013–2016.
[117] A.J. Grodzinsky, M.E. Levenston, M. Jin, and E.H. Frank, *Cartilage tissue remodeling in response to mechanical forces*, Annu. Rev. Biomed. Eng., 2 (2000), pp. 691–713.
[118] W. Grossman, *Cardiac hypertrophy: Useful adaptation or pathologic process?*, Am. J. Med., 69 (1980), pp. 576–584.
[119] H. Haapasalo, S. Kontulainen, H. Sievänen, P. Kannus, M. Järvinen, and I. Vuori, *Exercise-induced bone gain is due to enlargement in bone size without a change in volumetric bone density: A peripheral quantitative computed tomography study of the upper arms of male tennis players*, Bone, 27 (2000), pp. 351–357.
[120] O.P. Hamill and B. Martinac, *Molecular basis of mechanotransduction in living cells*, Physiol. Rev., 81 (2001), pp. 685–740.
[121] T.P. Harrigan and J.J. Hamilton, *Optimality conditions for finite element simulation of adaptive bone remodeling*, Int. J. Solid. Struct., 29 (1992), pp. 2897–2906.
[122] R.T. Hart, *Bone modeling and remodeling: Theories and computation*, in Bone Mechanics Handbook, 2nd ed., S.C. Cowin, ed., CRC Press, Boca Raton, FL, 2001, Chap. 31.
[123] K.A. Hawboldt, N. Kalogerakis, and L.A. Behie, *A cellular automaton model for microcarrier cultures*, Biotechnol. Bioeng., 43 (1994), pp. 90–100.
[124] D.H. Hegedus and S.C. Cowin, *Bone remodeling* II: *Small strain adaptive elasticity*, J. Elasticity, 6 (1976), pp. 337–352.
[125] G. Helmlinger, P.A. Netti, H.C. Lichtenbeld, R.J. Melder, and R.K. Jain, *Solid stress inhibits the growth of multicellular tumor spheroids*, Nat. Biotechnol., 15 (1997), pp. 778–783.

[126] G.J. Herbison and J.M. Talbot, *Muscle atrophy during space flight: Research needs and opportunities*, Physiologist, 28 (1985), pp. 520–527.
[127] S. Hilgenfeldt, S. Erisken, and R.W. Carthew, *Physical modeling of cell geometric order in an epithelial tissue*, Proc. Natl. Acad. Sci. USA, 105 (2008), pp. 907–911.
[128] G. Himpel, E. Kuhl, A. Menzel, and P. Steinmann, *Computational modelling of isotropic multiplicative growth*, Comput. Model. Eng. Sci., 8 (2005), pp. 119–134.
[129] G. Himpel, E. Kuhl, A. Menzel, and P. Steinmann, *Modelling of mass changes in anisotropic materials*, Proc. Appl. Math. Mech., 5 (2005), pp. 299–300.
[130] S. Höhme, J.G. Hengstler, M. Brulport, M. Schäfer, A. Bauer, R. Gebhardt, and D. Drasdo, *Mathematical modelling of liver regeneration after intoxication with* CCl_4, Chem. Biol. Interact., 168 (2007), pp. 74–93.
[131] S.J. Hollister, D.P. Fyhrie, K.J. Jepsen, and S.A. Goldstein, *Application of homogenization theory to the study of trabecular bone mechanics*, J. Biomech., 24 (1991), pp. 825–839.
[132] G.A. Holzapfel, *Nonlinear Solid Mechanics*, Wiley, Chichester, UK, 2000.
[133] G.A. Holzapfel, T.C. Gasser, and R.W. Ogden, *A new constitutive framework for arterial wall mechanics and a comparative study of material models*, J. Elasticity, 61 (2000), pp. 1–48.
[134] H. Honda, *Geometrical models for cells in tissues*, Int. Rev. Cytol., 81 (1983), pp. 191–248.
[135] H. Honda and G. Eguchi, *How much does the cell boundary contract in a monolayered cell sheet?*, J. Theoret. Biol., 84 (1980), pp. 575–588.
[136] H. Honda, Y. Ogita, S. Higuchi, and K. Kani, *Cell movements in a living mammalian tissue: Long-term observation of individual cells in wounded corneal endothelia of cats*, J. Morphol., 174 (1982), pp. 25–39.
[137] H. Honda, M. Tanemura, and T. Nagai, *A three-dimensional vertex dynamics cell model of space-filling polyhedra simulating cell behavior in a cell aggregate*, J. Theoret. Biol., 226 (2004), pp. 439–453.
[138] H. Honda, H. Yamanaka, and M. Dan-Sohkawa, *A computer simulation of geometrical configurations during cell division*, J. Theoret. Biol., 106 (1984), pp. 423–435.
[139] H. Honda, H. Yamanaka, and G. Eguchi, *Transformation of a polygonal cellular pattern during sexual maturation of the avian oviduct epithelium: Computer simulation*, J. Embryol. Exp. Morphol., 98 (1986), pp. 1–19.
[140] P.D. Howell, G. Kozyreff, and J.R. Ockendon, *Applied Solid Mechanics*, Cambridge University Press, Cambridge, UK, 2009.
[141] F.-H. Hsu, *The influences of mechanical loads on the form of a growing elastic body*, J. Biomech., 1 (1968), pp. 303–311.
[142] S. Huang and D.E. Ingber, *The structural and mechanical complexity of cell-growth control*, Nat. Cell Biol., 1 (1999), pp. E131–E138.
[143] S. Huang and D.E. Ingber, *Cell tension, matrix mechanics, and cancer development*, Canc. Cell, 8 (2005), pp. 175–176.
[144] J.D. Humphrey, *Stress, strain, and mechanotransduction in cells*, Trans. ASME J. Biomech. Eng., 123 (2001), pp. 638–641.
[145] J.D. Humphrey, *Continuum biomechanics of soft biological tissues*, Proc. R. Soc. Lond. Ser. A Math. Phys. Eng. Sci., 459 (2003), pp. 3–46.
[146] J.D. Humphrey and S. Na, *Elastodynamics and arterial wall stress*, Ann. Biomed. Eng., 30 (2002), pp. 509–523.
[147] J.D. Humphrey and K.R. Rajagopal, *A constrained mixture model for growth and remodeling of soft tissues*, Math. Models Methods Appl. Sci., 12 (2002), pp. 407–430.
[148] J.S. Huxley, *Problems of Relative Growth*, Methuen, London, 1932.
[149] D.E. Ingber, *Cellular tensegrity: Defining new rules of biological design that govern the cytoskeleton*, J. Cell Sci., 104 (1993), pp. 613–627.
[150] D.E. Ingber, *Tensegrity* I. *Cell structure and hierarchical systems biology*, J. Cell Sci., 116 (2003), pp. 1157–1173.
[151] D.E. Ingber, *Tensegrity* II. *How structural networks influence cellular information processing networks*, J. Cell Sci., 116 (2003), pp. 1397–1408.
[152] D.E. Ingber, *Cellular mechanotransduction: Putting all the pieces together again*, FASEB J., 20 (2006), pp. 811–827.
[153] D.E. Ingber, *From molecular cell engineering to biologically inspired engineering*, Cell. Mol. Bioeng., 1 (2008), pp. 51–57.
[154] D.E. Ingber, *Tensegrity-based mechanosensing from macro to micro*, Prog. Biophys. Mol. Biol., 97 (2008), pp. 163–179.
[155] R.K. Jain, *Determinants of tumor blood flow: A review*, Canc. Res., 48 (1988), pp. 2641–2658.

[156] Z.F.G. Jaworski, M. Liskova-Kiar, and H.K. Uhthoff, *Effect of long-term immobilisation on the pattern of bone loss in older dogs*, J. Bone Joint Surg. Br. Vol., 62 (1980), pp. 104–110.

[157] A.F. Jones, H.M. Byrne, J.S. Gibson, and J.W. Dold, *A mathematical model of the stress induced during avascular tumour growth*, J. Math. Biol., 40 (2000), pp. 473–499.

[158] S. Judex and R.F. Zernicke, *Does the mechanical milieu associated with high-speed running lead to adaptive changes in diaphyseal growing bone?*, Bone, 26 (2000), pp. 153–159.

[159] A.R. Kansal, S. Torquato, G.R. Harsh, E.A. Chiocca, and T.S. Deisboeck, *Simulated brain tumor growth dynamics using a three-dimensional cellular automaton*, J. Theoret. Biol., 203 (2000), pp. 367–382.

[160] K.E. Kasza, A.C. Rowat, J. Liu, T.E. Angelini, C.P. Brangwynne, G.H. Koenderink, and D.A. Weitz, *The cell as a material*, Curr. Opin. Cell Biol., 19 (2007), pp. 101–107.

[161] A. Klarbring and T. Olsson, *On compatible strain with reference to biomechanics of soft tissues*, ZAMM Z. Angew. Math. Mech., 85 (2005), pp. 440–448.

[162] S.M. Klisch, S.S. Chen, R.L. Sah, and A. Hoger, *A growth mixture theory for cartilage with application to growth-related experiments on cartilage explants*, Trans. ASME J. Biomech. Eng., 125 (2003), pp. 169–179.

[163] S.M. Klisch, R.L. Sah, and A. Hoger, *A cartilage growth mixture model for infinitesimal strains: Solutions of boundary-value problems related to* in vitro *growth experiments*, Biomech. Model. Mechan., 3 (2005), pp. 209–223.

[164] S.M. Klisch, T.J. Van Dyke, and A. Hoger, *A theory of volumetric growth for compressible elastic biological materials*, Math. Mech. Solids, 6 (2001), pp. 551–575.

[165] M. Krieg, Y. Arboleda-Estudillo, P.-H. Puech, J. Käfer, F. Graner, D.J. Müller, and C.-P. Heisenberg, *Tensile forces govern germ-layer organization in zebrafish*, Nat. Cell Biol., 10 (2008), pp. 429–436.

[166] E. Kröner and A. Seeger, *Nicht-lineare Elastizitätstheorie der Versetzungen und Eigenspannungen*, Arch. Ration. Mech. Anal., 3 (1959), pp. 97–119.

[167] E. Kuhl, K. Garikipati, E.M. Arruda, and K. Grosh, *Remodeling of biological tissue: Mechanically induced reorientation of a transversely isotropic chain network*, J. Mech. Phys. Solids, 53 (2005), pp. 1552–1573.

[168] E. Kuhl and G.A. Holzapfel, *A continuum model for remodeling in living structures*, J. Mater. Sci., 42 (2007), pp. 8811–8823.

[169] E. Kuhl, R. Maas, G. Himpel, and A. Menzel, *Computational modeling of arterial wall growth*, Biomech. Model. Mechan., 6 (2007), pp. 321–331.

[170] E. Kuhl, A. Menzel, and P. Steinmann, *Computational modeling of growth*, Comput. Mech., 32 (2003), pp. 71–88.

[171] E. Kuhl and P. Steinmann, *On spatial and material settings of thermo-hyperelastodynamics for open systems*, Acta Mech., 160 (2003), pp. 179–217.

[172] E. Kuhl and P. Steinmann, *Computational modeling of healing: An application of the material force method*, Biomech. Model. Mechan., 2 (2004), pp. 187–203.

[173] E. Kuhl and P. Steinmann, *Material forces in open system mechanics*, Comput. Methods Appl. Mech. Engrg., 193 (2004), pp. 2357–2381.

[174] J.M. Lawrence, *Arm loss and regeneration in Asteroidea (Echinodermata)*, in Echinoderm Research 1991: Proceedings of the Third European Conference on Echinoderms, A. A. Balkema, Rotterdam, The Netherlands, 1992, pp. 39–52.

[175] T. Lecuit and P.-F. Lenne, *Cell surface mechanics and the control of cell shape, tissue patterns and morphogenesis*, Nat. Rev. Mol. Cell. Biol., 8 (2007), pp. 633–644.

[176] E.H. Lee, *Elastic–plastic deformation at finite strains*, Trans. ASME J. Appl. Mech., 36 (1969), pp. 1–6.

[177] G.D. Leikauf and H.S. Deshmukh, *When wheeze leads to squeeze: Growth under pressure*, Am. J. Respir. Cell Mol. Biol., 32 (2005), p. 366.

[178] C.T. Lim, E.H. Zhou, and S.T. Quek, *Mechanical models for living cells—a review*, J. Biomech., 39 (2006), pp. 195–216.

[179] K.-K. Liu, *Deformation behaviour of soft particles: A review*, J. Phys. D Appl. Phys., 39 (2006), pp. R189–R199.

[180] B. Loret and F.M.F. Simões, *A framework for deformation, generalized diffusion, mass transfer and growth in multi-species multi-phase biological tissues*, Eur. J. Mech. A Solids, 24 (2005), pp. 757–781.

[181] V.A. Lubarda, *Constitutive theories based on the multiplicative decomposition of deformation gradient: Thermoelasticity, elastoplasticity, and biomechanics*, Appl. Mech. Rev., 57 (2004), pp. 95–108.

[182] V.A. Lubarda and A. Hoger, *On the mechanics of solids with a growing mass*, Int. J. Solid. Struct., 39 (2002), pp. 4627–4664.
[183] B.D. MacArthur and C.P. Please, *Residual stress generation and necrosis formation in multi-cell tumour spheroids*, J. Math. Biol., 49 (2004), pp. 537–552.
[184] A. Mammoto, K.M. Connor, T. Mammoto, C.W. Yung, D. Huh, C.M. Aderman, G. Mostoslavsky, L.E.H. Smith, and D.E. Ingber, *A mechanosensitive transcriptional mechanism that controls angiogenesis*, Nature, 457 (2009), pp. 1103–1108.
[185] G.A. Maugin, *Geometry and thermomechanics of structural rearrangements: Ekkehart Kröner's legacy*, ZAMM Z. Angew. Math. Mech., 83 (2003), pp. 75–84.
[186] T. McMahon, *Size and shape in biology*, Science, 179 (1973), pp. 1201–1204.
[187] F.A. Meineke, C.S. Potten, and M. Loeffler, *Cell migration and organization in the intestinal crypt using a lattice-free model*, Cell Prolif., 34 (2001), pp. 253–266.
[188] A. Menzel, *Anisotropic remodelling of biological tissues*, in Mechanics of Biological Tissue, G.A. Holzapfel and R.W. Ogden, eds., Springer, Berlin, Heidelberg, 2006, pp. 91–104.
[189] A. Menzel, *A fibre reorientation model for orthotropic multiplicative growth*, Biomech. Model. Mechan., 6 (2007), pp. 303–320.
[190] N. Metropolis, A.W. Rosenbluth, M.N. Rosenbluth, A.H. Teller, and E. Teller, *Equation of state calculations by fast computing machines*, J. Chem. Phys., 21 (1953), pp. 1087–1092.
[191] G.H. Meyer, *Die Architektur der Spongiosa*, Arch. Anat. Physiol. Wiss. Medicin, 34 (1867), pp. 615–628.
[192] G.W. Milton, *The Theory of Composites*, Cambridge University Press, Cambridge, UK, 2002.
[193] J.C.M. Mombach and J.A. Glazier, *Single cell motion in aggregates of embryonic cells*, Phys. Rev. Lett., 76 (1996), pp. 3032–3035.
[194] J. Moreira and A. Deutsch, *Cellular automaton models of tumor development: A critical review*, Adv. Complex Syst., 5 (2002), pp. 247–267.
[195] D. Morel, R. Marcelpoil, and G. Brugal, *A proliferation control network model: The simulation of two-dimensional epithelial homeostasis*, Acta Biotheor., 49 (2001), pp. 219–234.
[196] D.O. Morgan, *The Cell Cycle: Principles of Control*, New Science Press, London, 2007.
[197] J.D. Murray, *Mathematical Biology*, 3rd ed., Springer, New York, 2003.
[198] P.D.F. Murray, *Bones: A Study of the Development and Structure of the Vertebrate Skeleton*, revised ed., Cambridge University Press, Cambridge, UK, 1985.
[199] H. Narayanan, S.N. Verner, K.L. Mills, R. Kemkemer, and K. Garikipati, *In silico estimates of the free energy rates in growing tumor spheroids*, J. Phys. Condens. Matter, 22 (2010), 194122.
[200] C.M. Nelson, *Geometric control of tissue morphogenesis*, Biochim. Biophys. Acta Mol. Cell. Res., 1793 (2009), pp. 903–910.
[201] C.M. Nelson, R.P. Jean, J.L. Tan, W.F. Liu, N.J. Sniadecki, A.A. Spector, and C.S. Chen, *Emergent patterns of growth controlled by multicellular form and mechanics*, Proc. Natl. Acad. Sci. USA, 102 (2005), pp. 11594–11599.
[202] R.M. Nerem, *Vascular fluid mechanics, the arterial wall, and atherosclerosis*, Trans. ASME J. Biomech. Eng., 114 (1992), pp. 274–282.
[203] T.J. Newman, *Modeling multicellular systems using subcellular elements*, Math. Biosci. Eng., 2 (2005), pp. 613–624.
[204] P. Nordström, U. Pettersson, and R. Lorentzon, *Type of physical activity, muscle strength, and pubertal stage as determinants of bone mineral density and bone area in adolescent boys*, J. Bone Miner. Res., 13 (1998), pp. 1141–1148.
[205] J.L. Nowinski, *Mechanics of growing materials*, Int. J. Mech. Sci., 20 (1978), pp. 493–504.
[206] R.W. Ogden, *Non-linear Elastic Deformations*, Ellis Horwood, Chichester, UK, 1984.
[207] T.P. Padera, B.R. Stoll, J.B. Tooredman, D. Capen, E. di Tomaso, and R.K. Jain, *Cancer cells compress intratumour vessels*, Nature, 427 (2004), p. 695.
[208] S. Pagano and R. Paroni, *A simple model for phase transitions: From the discrete to the continuum problem*, Quart. Appl. Math., 61 (2003), pp. 89–109.
[209] E. Palsson, *A three-dimensional model of cell movement in multicellular systems*, Future Generat. Comput. Syst., 17 (2001), pp. 835–852.
[210] E. Palsson and H.G. Othmer, *A model for individual and collective cell movement in* Dictyostelium discoideum, Proc. Natl. Acad. Sci. USA, 97 (2000), pp. 10448–10453.
[211] M.J. Paszek, N. Zahir, K.R. Johnson, J.N. Lakins, G.I. Rozenberg, A. Gefen, C.A. Reinhart-King, S.S. Margulies, M. Dembo, D. Boettiger, D.A. Hammer, and V.M. Weaver, *Tensional homeostasis and the malignant phenotype*, Canc. Cell, 8 (2005), pp. 241–254.

[212] P. Pathmanathan, J. Cooper, A. Fletcher, G. Mirams, P. Murray, J. Osborne, J. Pitt-Francis, A. Walter, and S.J. Chapman, *A computational study of discrete mechanical tissue models*, Phys. Biol., 6 (2009), 036001.
[213] F. Pauwels, *Eine neue Theorie über den Einfluß mechanischer Reize auf die Differenzierung der Stützgewebe*, Z. Anat. Entwicklungs., 121 (1960), pp. 478–515.
[214] W.S. Peters and A.D. Tomos, *The history of tissue tension*, Ann. Bot., 77 (1996), pp. 657–665.
[215] A.-S. Qi, X. Zheng, C.-Y. Du, and B.-S. An, *A cellular automaton model of cancerous growth*, J. Theoret. Biol., 161 (1993), pp. 1–12.
[216] K.A. Rejniak, *An immersed boundary framework for modelling the growth of individual cells: An application to the early tumour development*, J. Theoret. Biol., 247 (2007), pp. 186–204.
[217] M.J. Rennie, H. Wackerhage, E.E. Spangenburg, and F.W. Booth, *Control of the size of the human muscle mass*, Annu. Rev. Physiol., 66 (2004), pp. 799–828.
[218] E.K. Rodriguez, A. Hoger, and A.D. McCulloch, *Stress-dependent finite growth in soft elastic tissues*, J. Biomech., 27 (1994), pp. 455–467.
[219] J. Rodríguez, J.M. Goicolea, J.C. García, and F. Gabaldón, *Finite element models for mechanical simulation of coronary arteries*, in Functional Imaging and Modeling of the Heart, Lecture Notes in Comput. Sci. 2674, Springer, Berlin, Heidelberg, 2003, pp. 295–305.
[220] H. Roesler, *The history of some fundamental concepts in bone biomechanics*, J. Biomech., 20 (1987), pp. 1025–1034.
[221] T. Roose, S.J. Chapman, and P.K. Maini, *Mathematical models of avascular tumor growth*, SIAM Rev., 49 (2007), pp. 179–208.
[222] W. Roux, *Der züchtende Kampf der Teile, oder die 'Teilauslese' im Organismus. (Theorie der 'funktionellen Anpassung')*, Wilhelm Engelmann, Leipzig, 1881.
[223] T. Rudge and J. Haseloff, *A computational model of cellular morphogenesis in plants*, in Advances in Artificial Life, Lecture Notes in Comput. Sci. 3630, Springer, Berlin, 2005, pp. 78–87.
[224] E.F. Ryder, L. Bullard, J. Hone, J. Olmstead, and M.O. Ward, *Graphical simulation of early development of the cerebral cortex*, Comput. Meth. Programs Biomed., 59 (1999), pp. 107–114.
[225] J. Sachs, *Text-book of Botany, Morphological and Physical*, 2nd ed., Clarendon Press, Oxford, 1882.
[226] N.J. Savill and P. Hogeweg, *Modelling morphogenesis: From single cells to crawling slugs*, J. Theoret. Biol., 184 (1997), pp. 229–235.
[227] G. Schaller and M. Meyer-Hermann, *Multicellular tumor spheroid in an off-lattice Voronoi–Delaunay cell model*, Phys. Rev. E, 71 (2005), 051910.
[228] Y. Shafrir and G. Forgacs, *Mechanotransduction through the cytoskeleton*, Am. J. Physiol. Cell Physiol., 282 (2002), pp. C479–C486.
[229] B.I. Shraiman, *Mechanical feedback as a possible regulator of tissue growth*, Proc. Natl. Acad. Sci. USA, 102 (2005), pp. 3318–3323.
[230] W.K. Silk and R.O. Erickson, *Kinematics of plant growth*, J. Theoret. Biol., 76 (1979), pp. 481–501.
[231] F.H. Silver, J.W. Freeman, and G.P. Seehra, *Collagen self-assembly and the development of tendon mechanical properties*, J. Biomech., 36 (2003), pp. 1529–1553.
[232] R. Skalak, *Modelling the mechanical behavior of red blood cells*, Biorheology, 10 (1973), pp. 229–238.
[233] R. Skalak, *Growth as a finite displacement field*, in Proceedings of the IUTAM Symposium on Finite Elasticity, D.E. Carlson and R.T. Shield, eds., Martinus Nijhoff, The Hague, The Netherlands, 1981.
[234] R. Skalak, G. Dasgupta, M. Moss, E. Otten, P. Dullemeijer, and H. Vilmann, *Analytical description of growth*, J. Theoret. Biol., 94 (1982), pp. 555–577.
[235] R. Skalak, S. Zargaryan, R.K. Jain, P.A. Netti, and A. Hoger, *Compatibility and the genesis of residual stress by volumetric growth*, J. Math. Biol., 34 (1996), pp. 889–914.
[236] K. Smallbone, R.A. Gatenby, R.J. Gillies, P.K. Maini, and D.J. Gavaghan, *Metabolic changes during carcinogenesis: Potential impact on invasiveness*, J. Theoret. Biol., 244 (2007), pp. 703–713.
[237] R.H. Smallwood, W.M.L. Holcombe, and D.C. Walker, *Development and validation of computational models of cellular interaction*, J. Mol. Histol., 35 (2004), pp. 659–665.
[238] L. Socci, G. Pennati, F. Gervaso, and P. Vena, *An axisymmetric computational model of skin expansion and growth*, Biomech. Model. Mechan., 6 (2007), pp. 177–188.

[239] A.A. Stein, *The deformation of a rod of growing biological material under longitudinal compression*, J. Appl. Math. Mech., 59 (1995), pp. 139–146.
[240] M.S. Steinberg, *Differential adhesion in morphogenesis: A modern view*, Curr. Opin. Genet. Dev., 17 (2007), pp. 281–286.
[241] D. Stekel, J. Rashbass, and E.D. Williams, *A computer graphic simulation of squamous epithelium*, J. Theoret. Biol., 175 (1995), pp. 283–293.
[242] A.M. Strauss, *Mechanics of growing materials with memory*, Publ. Inst. Math. (Beograd) (N.S.), 12 (1971), pp. 131–135.
[243] T. Stylianopoulos and V.H. Barocas, *Volume-averaging theory for the study of the mechanics of collagen networks*, Comput. Methods Appl. Mech. Engrg., 196 (2007), pp. 2981–2990.
[244] C. Sultan, D. Stamenović, and D.E. Ingber, *A computational tensegrity model predicts dynamic rheological behaviors in living cells*, Ann. Biomed. Eng., 32 (2004), pp. 520–530.
[245] L.A. Taber, *Biomechanics of growth, remodeling and morphogenesis*, Appl. Mech. Rev., 48 (1995), pp. 487–545.
[246] L.A. Taber, *A model for aortic growth based on fluid shear and fiber stresses*, Trans. ASME J. Biomech. Eng., 120 (1998), pp. 348–354.
[247] L.A. Taber, *Biophysical mechanisms of cardiac looping*, Int. J. Dev. Biol., 50 (2006), pp. 323–332.
[248] L.A. Taber and D.W. Eggers, *Theoretical study of stress-modulated growth in the aorta*, J. Theoret. Biol., 180 (1996), pp. 343–357.
[249] K. Takamizawa and T. Matsuda, *Kinematics for bodies undergoing residual stress and its applications to the left ventricle*, Trans. ASME J. Appl. Mech., 57 (1990), pp. 321–329.
[250] D.W. Thompson, *On Growth and Form*, 2nd ed., Cambridge University Press, Cambridge, UK, 1942.
[251] A. Tözeren and R. Skalak, *Interaction of stress and growth in a fibrous tissue*, J. Theoret. Biol., 130 (1988), pp. 337–350.
[252] C. Truesdell and R. Toupin, *The classical field theories*, in Handbuch der Physik, Vol. III/1, S. Flügge, ed., Springer, Heidelberg, 1960.
[253] S. Turner, *Using cell potential energy to model the dynamics of adhesive biological cells*, Phys. Rev. E, 71 (2005), 041903.
[254] S. Turner and J.A. Sherratt, *Intercellular adhesion and cancer invasion: A discrete simulation using the extended Potts model*, J. Theoret. Biol., 216 (2002), pp. 85–100.
[255] R.N. Vaishnav and J. Vossoughi, *Residual stress and strain in aortic segments*, J. Biomech., 20 (1987), pp. 235–239.
[256] H.H. Vandenburgh, S. Hatfaludy, P. Karlisch, and J. Shansky, *Mechanically induced alterations in cultured skeletal muscle growth*, J. Biomech., 24 (1991), pp. S91–S99.
[257] R. Vandiver and A. Goriely, *Tissue tension and axial growth of cylindrical structures in plants and elastic tissues*, Europhys. Lett. EPL, 84 (2008), 58004.
[258] C. Verdier, *Rheological properties of living materials. From cells to tissues*, J. Theor. Med., 5 (2003), pp. 67–91.
[259] D. Viens and G.W. Brodland, *A three-dimensional finite element model for the mechanics of cell–cell interactions*, Trans. ASME J. Biomech. Eng., 129 (2007), pp. 651–657.
[260] K.Y. Volokh, *Stresses in growing soft tissues*, Acta Biomater., 2 (2006), pp. 493–504.
[261] K.Y. Volokh, O. Vilnay, and M. Belsky, *Tensegrity architecture explains linear stiffening and predicts softening of living cells*, J. Biomech., 33 (2000), pp. 1543–1549.
[262] J. von Neumann, *Theory of Self-Reproducing Automata*, University of Illinois Press, Urbana, 1966.
[263] D.C. Walker, J. Southgate, G. Hill, M. Holcombe, D.R. Hose, S.M. Wood, S. Mac Neil, and R.H. Smallwood, *The epitheliome: Agent-based modelling of the social behaviour of cells*, Biosystems, 76 (2004), pp. 89–100.
[264] C. Warrender, S. Forrest, and F. Koster, *Modeling intercellular interactions in early* Mycobacterium *infection*, Bull. Math. Biol., 68 (2006), pp. 2233–2261.
[265] P.A. Watson, *Function follows form: Generation of intracellular signals by cell deformation*, FASEB J., 5 (1991), pp. 2013–2019.
[266] C. Wei, P.M. Lintilhac, and J.J. Tanguay, *An insight into cell elasticity and load-bearing ability. Measurement and theory*, Plant Physiol., 126 (2001), pp. 1129–1138.
[267] M. Weliky, S. Minsuk, R. Keller, and G. Oster, *Notochord morphogenesis in* Xenopus laevis*: Simulation of cell behavior underlying tissue convergence and extension*, Development, 113 (1991), pp. 1231–1244.
[268] M. Weliky and G. Oster, *The mechanical basis of cell rearrangement.* I. *Epithelial morphogenesis during* Fundulus *epiboly*, Development, 109 (1990), pp. 373–386.

[269] G.B. West, J.H. Brown, and B.J. Enquist, *A general model for ontogenetic growth*, Nature, 413 (2001), pp. 628–631.
[270] G.B. West, W.H. Woodruff, and J.H. Brown, *Allometric scaling of metabolic rate from molecules and mitochondria to cells and mammals*, Proc. Natl. Acad. Sci. USA, 99 (2002), pp. 2473–2478.
[271] J. Wiener, A.V. Loud, F. Giacomelli, and P. Anversa, *Morphometric analysis of hypertension-induced hypertrophy of rat thoracic aorta*, Am. J. Pathol., 88 (1977), pp. 619–634.
[272] B.F. Wilson and R.R. Archer, *Reaction wood: induction and mechanical action*, Annu. Rev. Plant Physiol., 28 (1977), pp. 23–43.
[273] B.F. Wilson and R.R. Archer, *Tree design: Some biological solutions to mechanical problems*, BioScience, 29 (1979), pp. 293–298.
[274] J. Wolff, *Über die innere Architectur der Knochen und ihre Bedeutung für die Frage vom Knochenwachsthum*, Virchows Arch., 50 (1870), pp. 389–450.
[275] J. Wolff, *Das Gesetz der Transformation der Knochen*, Hirschwald, Berlin, 1892. English translation by P.G.J. Maquet and R. Furlong, *The Law of Bone Remodelling*, Springer, Berlin, 1986.
[276] J.S. Young, *The invasive growth of malignant tumours: An experimental interpretation based on elastic-jelly models*, J. Pathol. Bacteriol., 77 (1959), pp. 321–339.
[277] F. Yuan, *Stress is good and bad for tumors*, Nat. Biotechnol., 15 (1997), pp. 722–723.
[278] C. Zhu, G. Bao, and N. Wang, *Cell mechanics: Mechanical response, cell adhesion, and molecular deformation*, Annu. Rev. Biomed. Eng., 2 (2000), pp. 189–226.